NOTE TO USERS

This reproduction is the best copy available.

Reproduced with permission of the copyright owner. Further reproduction prohibited without permission.

Reproduced with permission of the copyright owner. Further reproduction prohibited without permission.

B1566816

RELATIONSHIPS BETWEEN FAT CRYSTAL CHARACTERISTICS AND EMULSION STABILITY IN WATER IN OIL SYSTEMS

by

Shane Mason Hodge
B.Sc. University of Guelph, 1998

A thesis
Presented to Ryerson University

in partial fulfillment of the
requirements for the degree of
Master of Applied Science
in the Program of
Chemical Engineering

Toronto, Ontario, Canada
© Shane Mason Hodge 2004

PROPERTY OF
RYERSON UNIVERSITY LIBRARY

Reproduced with permission of the copyright owner. Further reproduction prohibited without permission.

UMI Number: EC52957

INFORMATION TO USERS

The quality of this reproduction is dependent upon the quality of the copy submitted. Broken or indistinct print, colored or poor quality illustrations and photographs, print bleed-through, substandard margins, and improper alignment can adversely affect reproduction.

In the unlikely event that the author did not send a complete manuscript and there are missing pages, these will be noted. Also, if unauthorized copyright material had to be removed, a note will indicate the deletion.

UMI®

UMI Microform EC52957

Copyright 2008 by ProQuest LLC.

All rights reserved. This microform edition is protected against unauthorized copying under Title 17, United States Code.

ProQuest LLC
789 E. Eisenhower Parkway
PO Box 1346
Ann Arbor, MI 48106-1346

Reproduced with permission of the copyright owner. Further reproduction prohibited without permission.

Reproduced with permission of the copyright owner. Further reproduction prohibited without permission.

Ryerson University requires the signatures of all persons using or photocopying this thesis.

Please sign below, and give address and date.

Reproduced with permission of the copyright owner. Further reproduction prohibited without permission.

Abstract

Relationships Between Fat Crystal Characteristics and Emulsion Stability in Water in Oil Systems

Masters of Applied Science, Chemical Engineering, 2004
Shane Mason Hodge
Department of Chemical Engineering
Ryerson University

Investigations were made into the stabilization of water in oil emulsions using crystalline particles of paraffin wax and fully hydrogenated canola and cottonseed oils. A model system was studied to develop a methodology of study and provide a benchmark for a subsequent study of a real-world system. The model system involved the use of light mineral oil, purified water, paraffin wax and glycerol monooleate emulsifier. The wax was crystallized prior to and following emulsification. Prepared emulsion samples were monitored for sedimentation and flocculation behaviour. Measurements of coalescence were obtained by pulsed field gradient NMR. Formation of the solid crystalline wax phase following emulsification resulted in emulsions more stable to flocculation and coalescence than samples containing the same amount of wax crystallized prior to emulsification. Analysis of emulsion samples with polarized light microscopy showed the wax crystals were associated with the water droplet interfaces rather than dispersed freely within the continuous oil phase. Another investigation employed similar experimental protocols but incorporated food-grade materials. Two different solid fats were used, chosen for their differing polymorphic (crystal habit) behaviour. Solid crystals of canola stearine (β-tending) and cottonseed stearine (β′-tending) were compared in their abilities to stabilize emulsions at levels of addition between 0 and 2%. Each type of fat was incorporated into the emulsion in a pre-crystallized state, or while melted and crystallized following emulsification. Cottonseed stearine was found to be

Reproduced with permission of the copyright owner. Further reproduction prohibited without permission.

in the β polymorph when quickly crystallized following emulsification from 45° to 5°C over 6 minutes. Further calorimetric and X-ray diffraction investigations revealed this crystallization behaviour was a result of a solid-state transformation via an imperfectly formed β´ intermediate. With respect to the post-crystallized emulsions, where the polymorphism of the two fats were both in the β-form, the canola stearine provided better stabilization against coalescence than the cottonseed stearine. This observation coincided with a stronger energy of interfacial attachment for crystallized canola than for cottonseed as calculated from measurements of contact angle and interfacial tension. With the pre-crystallized system, incorporation of cottonseed stearine resulted in reduced sedimentation and coalescence compared to samples containing pre-crystallized canola stearine. This difference was attributed to the presence of fine shards of β´-form crystals. The system that imparted the highest degree of overall stability incorporated the use of canola stearine crystallized following emulsification.

Reproduced with permission of the copyright owner. Further reproduction prohibited without permission.

Acknowledgements

The author would like to thank the following people for their assistance with this research and/or their support during this time: D. Rousseau, B. Craven, D. Walmsley, D. Forester, P. Scharping, R.C. and G. & J. Hodge. The author would also like to gratefully acknowledge the generous financial assistance provided by the National Science and Engineering Research Council, Ryerson University School of Graduate Studies and the Dairy Farmers of Canada.

Reproduced with permission of the copyright owner. Further reproduction prohibited without permission.

Table of Contents

Reproduced with permission of the copyright owner. Further reproduction prohibited without permission.

List of Tables

Reproduced with permission of the copyright owner. Further reproduction prohibited without permission.

List of Figures

Reproduced with permission of the copyright owner. Further reproduction prohibited without permission.

Reproduced with permission of the copyright owner. Further reproduction prohibited without permission.

List of Symbols

Symbols

γ	Interfacial tension
γ_{ow}	oil-water interfacial tension
γ_{os}	oil-solid interfacial tension
γ_{ws}	water-solid intefacial tension
ε	mechanical energy
η_c	viscosity of continuous phase
σ	standard deviation of log normal distribution
θ_Y	Young's contact angle
d_{10}	number weighted mean droplet diameter
d_{33}	volume-weighted mean droplet diameter
E_{disp}	energy of displacement
p_{in}	Pressure inside droplet
p_{out}	Pressure in continuous phase
r	Droplet radius
t	time

Acronyms

AOCS	American Oil Chemists' Society
(C)LSM	(Confocal) Laser Scanning Microscopy
CMC	Critical Micelle Concentration
CO	Canola Oil
DSC	Differential Scanning Calorimetry
GC	Gas Chromatograph
HCO	Hydrogenated Canola Oil
HCSO	Hydrogenated CottonSeed Oil
ID	Inside Diameter
IV	Iodine Value
MAG	Monoglyceride
NMR	Nuclear Magnetic Resonance
OD	Outside Diameter

O/W	Oil-in-Water
PFG	Pulsed Field Gradient
PgPr	Polyglycerol Polyricinoleate
PLM	Polarized Light Microscopy
SFC	Solid Fat Content % (w/w)
TAG	Triglyceride
W/O	Water-in-Oil
XRD	X-Ray Diffraction

Reproduced with permission of the copyright owner. Further reproduction prohibited without permission.

1 Introduction

1.1 Emulsions

Emulsions are dispersions of one liquid within another, where the two liquids are immiscible. Emulsions are encountered in foods, pharmaceuticals, cosmetics, and crude oil (Friberg *et al.*, 1997). Most often the stability of the emulsion is desired. However, in certain cases, such as with crude oils, processors seek to find ways of destabilizing the emulsion (Lee, 1999). One means by which emulsions may be stabilized is by colloidal solid particles. Pickering (1907) was the first to document the stabilization of emulsions by solids, and as a result, emulsions of this type are commonly referred to as 'Pickering Emulsions'. The study of colloidal particles in food emulsions, and in particular the role of fat crystals, is a much more recent phenomenon, being pioneered in the 1960s by Lucassen-Reynders (1962) and together with van den Tempel (1963). More recently, Johansson and her collaborators (1995a,b,c,d,e) investigated triglyceride crystals and their effect on emulsion stability. They found that for W/O emulsions, there was a destabilizing effect up to a certain critical concentration of crystals, and then further addition increased stability.

In food systems, both water-in-oil (W/O) and oil-in-water (O/W) type emulsions are encountered. These systems are inherently thermodynamically unstable. Energy is required to create emulsions as it involves generating a large increase in the interfacial area between the two immiscible phases.

Emulsions may be destabilized by a number of mechanisms. 1) Creaming (or sedimentation) is the separation of the two phases induced by differences in densities between the two phases. 2) Flocculation involves the attraction of droplets of the

same phase to near neighbours by weak colloidal interactions. When droplets flocculate, they maintain their structural integrity (McClements & Demetriades, 1998), and in some cases can even be re-dispersed. Droplets can flocculate without creaming resulting in the macroscopic observation of a non-uniformly dispersed system. 3) Coalescence is the complete merger of droplets, associated with inter-droplet film thinning and rupture. As a result of coalescence, phase inversion may occur where droplets of the dispersed phase partially coalesce and as a result entrap the once-continuous phase within it. This is the mechanism by which butter (a water-in-oil emulsion) is formed from milk (an oil-in-water emulsion) during churning (Van Boekel, 1980). 4) Ostwald ripening involves the growth of larger droplets at the expense of smaller droplets of the same phase and is driven by solubility gradients created by differences in droplet Laplace pressures. The Laplace pressure inside a droplet is an increase in pressure above that of the surrounding medium. It results from the contraction of the droplet surface due to the surface tension of the interface. The pressure inside the droplet, p_{in}, is related to the pressure outside the droplet (in the continuous phase), p_{out}, by the surface tension of the droplet interface, γ, and the radius of the droplet, r (Atkins, 1990):

$$p_{in} = p_{out} + \frac{2\gamma}{r} \qquad (1)$$

Smaller droplets will have greater internal pressures than larger droplets. When the droplet phase is partially soluble in the continuous phase this results in concentration gradients that are highest in the proximity of smaller droplets. Molecules of the droplet phase can thus migrate along these concentration gradients from smaller droplets to larger droplets.

Reproduced with permission of the copyright owner. Further reproduction prohibited without permission.

The kinetic stability of emulsions can be improved through a number of methods. One method is to initially decrease the average droplet size of the dispersed phase by mechanical means, thereby reducing the rate of creaming or settling, as is done in the homogenization of milk (Swaisgood, 1996). Surfactants may be added to emulsion systems to lower the interfacial tension between the two immiscible fluids. Surfactants act to stabilize emulsions by forming a cohesive film around the droplets that resists coalescence (Dickinson, 1992). Especially in aqueous systems (i.e. O/W emulsions), the addition of surface-active proteins can stabilize emulsions by increasing the interfacial viscosity, thereby slowing the rate of film drainage, and thus coalescence. A highly viscous and rigid interfacial film laden with particles will slow the rate of film drainage and resist rupture, resulting in improved stability (Edwards & Wasan, 1991). Polymers adsorbed to the interface will resist droplet coalescence through steric effects whereas non-adsorbed polymers may contribute to flocculation through depletion interactions (Walstra, 1996).

In W/O systems, fat crystals have been shown to stabilize emulsions (Lucassen-Reynders, 1962; Hodge & Rousseau, 2003). There are two mechanisms by which they accomplish this: 1) Fat crystals may form a network throughout the oil phase of the emulsion reducing the rate of diffusion and settling of water droplets through the continuous oil phase, and 2) Fat crystals may also be adsorbed to the surface of W/O emulsion droplets providing a solid barrier to coalescence. Stabilizing crystals may originate by way of surfactant solidification at the interface where the surfactants are lipid-based amphiphiles such as monoacylglycerols (MAGs). Alternatively, crystals formed prior to the creation of the emulsion may migrate towards the droplet interface (Friberg *et al.*, 1997). The key factors that will

determine the influence of fat crystals on water-in-oil emulsion stabilization are: the wettability of the crystals at the interface (Friberg *et al.*, 1997); interfacial film viscosity (Lucassen-Reynders, 1993); and fat crystal microstructure (polymorphism, morphology, etc.) (Ogden & Rosenthal, 1998).

1.1.1 Wettability and Contact Angle

Fat crystals influence emulsion stability primarily .epending on how they are wetted by the continuous and dispersed phases (Darling, 1982). During or after emulsification, fat crystals may be adsorbed to the interface if it is more energetically favourable than remaining in the continuous oil phase. Adsorbed fat crystals will be preferentially wetted by either the aqueous or oil phase depending on the composition of the aqueous and oil phases as well as the composition and surface properties of the fat crystal itself. The wettability of the fat crystal is described by the contact angle formed at the boundary of the three phases (Johansson & Bergenståhl, 1995c) where the contact angle is the angle the liquid-liquid interface makes to the solid phase as measured through the aqueous phase. (See Figure 1)

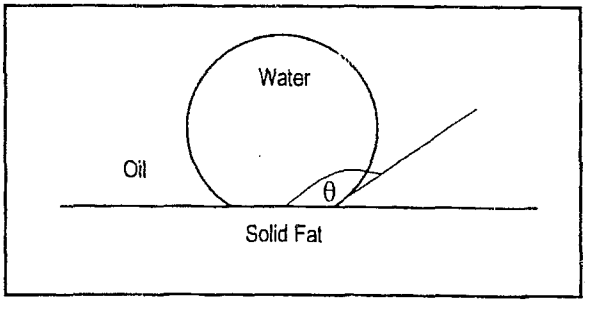

Figure 1: Schematic representation of a water droplet resting on a planar solid fat surface showing how the measurement of the contact angle is obtained. The reference line is drawn tangent to the oil water interface at the point of contact with the solid fat plane.

Reproduced with permission of the copyright owner. Further reproduction prohibited without permission.

Particles with contact angles smaller than 90° will stabilize O/W emulsions. With contact angles greater than 90° (as shown in Figure 2), the particles will stabilize a W/O emulsion (Schulman & Leja, 1954). If the particles are completely wetted by either the oil or water phase they become fully dispersed in that phase and will have no stabilizing effect.

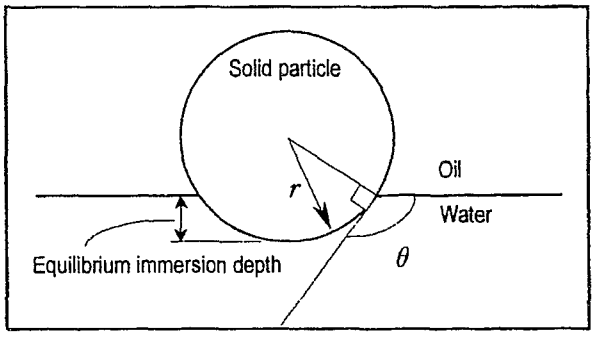

Figure 2: Relationship of positioning of a spherical particle at an oil/water interface and the contact angle as measured through the aqueous phase.

If a drop of water is placed on a hydrophobic surface, such as a slab of solidified fat, the water will not spread upon it, but rather it will bead. The contact angle of the droplet's surface to the planar crystal face helps characterize the surface's surface free energy and critical surface tension, which in turn helps to understand wetting behaviour and surface morphology.

The positioning of the solid particles is dependent on interplay between the three surface tensions present (i.e. oil/water, solid/oil and solid/water, or γ_{ow}, γ_{so} and γ_{sw}, respectively). Reinders (1913) stated that three possibilities existed:

1st case: $$\gamma_{sw} > \gamma_{ow} - \gamma_{so} \quad (2)$$

In this case, the crystal would be completely wetted by water.

2^{nd} case: $$\gamma_{os} > \gamma_{ow} - \gamma_{sw} \quad (3)$$

In this case, the crystal would be completely wetted by oil.

3^{rd} case: $$\gamma_{ow} > \gamma_{os} - \gamma_{sw} \quad (4)$$

In this case, the crystal would be wetted by both the water and oil phases. It is only under this condition that a fat crystal will locate itself at the oil and water interface. Young's equation (Young, 1855) resolves these forces present at the three phase junction:

$$\gamma_{ow}\cos\theta = \gamma_{so} - \gamma_{sw} \quad (5)$$

where θ is the contact angle measured through the water phase. The contact angle formed in any system will depend on the surface and/or interfacial properties of all of the phases. Thermodynamically, the surface/interfacial tension, hydrophobic/hydrophilic properties, presence of impurities and particle properties, such as roughness determine these properties. In foods, depending on the final application, it is possible to modify the contact angle between the aqueous and oil phases.

1.1.2 Interfacial Viscosity

In the presence of an interfacial particle film, an interface will begin to demonstrate viscoelastic behaviour. The ability of an emulsion to resist coalescence will largely depend on the properties of the interface. A highly viscous and rigid interfacial film laden with particles will slow the rate of film drainage and resist rupture, resulting in improved stability (Edwards & Wasan, 1991). Thus, by controlling the interface rheology one can control the drainage of the thin liquid films trapped between coalescing droplets. This increase in viscosity may, in turn, increase the energy required to displace interfacial crystals from between two

Reproduced with permission of the copyright owner. Further reproduction prohibited without permission.

coalescing droplets, thus contributing further to increased stability (Tambe and Sharma, 1993).

Reproduced with permission of the copyright owner. Further reproduction prohibited without permission.

2 Stabilization of Water in Mineral Oil Emulsions by Paraffin Wax Crystals

2.1 Introduction

Much has been learned regarding the role of paraffin wax crystals in the stabilization of crude oil emulsions. These W/O emulsions are formed as a result of oceanic spills, and more regularly during normal drilling and recovery operations. Wax crystals play a critical role in crude oil systems, usually imparting stability to these emulsions. Thompson *et al.* (1985) found that the presence of wax crystals did not affect the viscosity or density of the continuous crude oil phase, nor the oil/water interfacial tension, yet they did impart a substantial stabilizing effect to the emulsions. Thus, the stabilizing effect of the wax crystals was concluded to be a result of the wax crystals themselves rather than a result of their effects on the bulk properties of the system. Many of the particles found in crude are surface-active, being composed of asphaltenes - a group of chemically heterogeneous compounds with regions of stacked aromatic sheets, alkane chains, and polar moieties. This mixed composition imparts an amphiphilic nature to the asphaltenes allowing them to function as surfactants (Lee, 1999). Of note is the fact that wax particles only stabilize crude oil emulsions in the presence of these asphaltene surfactants.

Garti *et al.* (1999) examined W/O/W emulsions stabilized by α-crystals (the α-form was maintained by an α-tending emulsifier). The presence of the emulsifier was necessary for emulsion stabilization. Furthermore, crystals had to be submicron in size to stabilize emulsions with droplets in the range of 6-18 μm in size. Larger crystals were not effectively adsorbed to the interface and flocculated as free crystals in the oil phase.

The aim of the research in this section was to determine the effect that paraffin wax crystals added to the continuous phase of a water in mineral oil emulsion have on stability. We wanted to study the effect of concentration as well as the effect of crystallizing the wax before the emulsification stage and compare this to crystallizing the wax after emulsification to observe any differences in emulsion stability. Stability was assessed by evaluating sedimentation and coalescence behaviour over time.

2.2 Materials and Methods

This section details the procedures developed to create the water in mineral oil emulsions, the materials used to make them, and the means by which their stability was measured. Stability was assessed based on sedimentation behaviour over 10 days, and the degree of droplet coalescence observed over the same time period. The structural relationship between emulsion water droplets and solid wax crystals was observed by microscopy.

2.2.1 Materials

Light mineral oil was used as the continuous phase of the emulsions and was obtained from Fisher Scientic (Nepean, ON). Water was double distilled. The surfactant used was Atsurf 456K (Quest International, Hoffman Estates, IL). Atsurf 456K is a low HLB (hydrophilic-lipophilic balance) emulsifier, composed predominatly of glycerol monooleate. It will tend to a will tend to stabilize W/O emulsions as the surfactant molecule resides predominatly in the non-polar oil phase. The critical micelle concentration (CMC) of Atsurf 456K in light mineral oil at room temperature was approximately 0.1%, as measured by interfacial tensiometry. Measurements of interfacial tension were determined using a 6 cm DuNouy ring

Reproduced with permission of the copyright owner. Further reproduction prohibited without permission.

tensiometer (Fisher Tensiomat Model 21, Fisher Scientific, Nepean, ON). Correction f[illegible]were applied for the density of the water (0.997 g/cm3), density of the mineral oil (0.851 g/cm3) and the ratio of the ring radius to the wire radius (53.7488890). The wax used was IGI 1260 paraffin wax (The International Group, Inc., Agincourt, ON) with a manufacturer-specified melting point of 71°C.

2.2.2 Determination of Solubility of Wax in Mineral Oil

The solubility of the wax in mineral oil was determined by turbidometric analysis. Dilutions of wax in mineral oil at various concentrations (from 0.10% to 0.01% (w/w)) were melted by heating to 100°C, poured into 1.5 cm x 15 cm test tubes and then subsequently quench-cooled in a water bath to 5°C. Following storage for 24 hrs, samples were then poured into pre-cooled cuvettes and the absorbance at 500 nm taken using a thermostated UV/Vis Lambda 40 Spectrometer (Perkin Elmer, Woodbridge, ON).

2.2.3 Emulsion Preparation

Water-in-mineral oil emulsions of 20% (v/v) were prepared with Atsurf 456K at 0.25% (w/w) in the oil phase and various levels of paraffin wax (0%, 0.125%, 0.25%, 0.5%, 1.0% and 2.0% (w/w) in the oil phase). Emulsions were prepared via two regimes. These regimes were termed "pre-crystallization" and "post-crystallization". The pre-crystallization regime is described first. With this regime of emulsion preparation, the solid fat was crystallized prior to emulsification. To do this, 50 g of a 4% (w/w) mixture of paraffin wax in mineral oil was heated to 100°C in a 100 ml beaker then cooled by placing in a refrigerator at 5°C for 24 hours. The resulting oil and wax crystal slurry was combined with the appropriate amounts of mineral oil, emulsifier and water at room temperature to make 5 mL samples.

Samples were homogenized after combining the various constituents using an impeller-type homogenizer (Omni-Mixer, London Scientific, London, ON). Samples were pre-blended for one minute at 5100 rpm and then homogenized at 39000 rpm for two minutes. Following emulsification, samples were immediately pipetted into NMR tubes (OD = 1 cm), capped and quench-cooled in a circulating water bath at 5°C. Six such samples were prepared at each concentration of wax (three each for sedimentation analysis and droplet size analysis).

Samples were also prepared via a post-crystallization regime. With this method, samples were homogenized at 60°C, with all of the components being in the liquid state. A mixture of 4% (w/w) paraffin wax in mineral oil was melted at 100°C then held in a water bath with the other components at 60°C. At this temperature and level of dilution in the mineral oil, the paraffin wax did not crystallize. As with the pre-crystallization regime, appropriate quantities of water, mineral oil, emulsifier and paraffin wax in mineral oil were measured into homogenization cells. Homogenization was carried out at 60° by immersing the cell in a water bath. The time and shear rate conditions were the same as for the pre-crystallization regime. Immediately following homogenization, a sample of the emulsion was pipetted into an NMR tube, capped and placed in a circulating water bath at 5°C.

The type of emulsion formed was confirmed by observing what happened when a drop of the emulsion was added to either mineral oil or water. Being W/O, when the emulsion was added to oil, it dispersed. Conversely, when placed in water, the emulsion remained as drops on the water's surface. All emulsions were stored for a minimum of 10 days at 5°C.

Reproduced with permission of the copyright owner. Further reproduction prohibited without permission.

2.2.4 Determination of Sedimentation Stability

As a means of assessing sedimentation behaviour, 4 mL aliquots of emulsion were pipetted into NMR tubes to a height of approximately 6 cm and stored at 5°C. The height of the total system and the height of the lower opaque phase (dispersed water droplets and wax crystals) were measured to determine the volume fraction of the sediment. This volume fraction was then measured daily over the course of 10 days. Other studies have monitored the degree of water separation as a function of time (Johansson *et al.*, 1995d), but this phenomenon was not visually apparent in any of samples prepared in this study.

2.2.5 Determination of Droplet Size Distributions (DSD)

Following homogenization, aliquots of 0.6 mL were pipetted into NMR tubes to obtain a column height of 1 cm. Droplet size distribution analyses of the W/O emulsions were carried out using a Bruker Minispec Mq20 Pulsed Nuclear Magnetic Resonance (pNMR) unit (Bruker Canada, Milton, ON) equipped with a pulsed gradient unit that allows unimodal characterization of the emulsion droplet size distribution in the W/O emulsions. The principle is based on the restricted diffusion of water molecules (Tanner & Stejskal, 1968; Fourel *et al.*, 1994, 1995). The instrument was calibrated and operated according to the manufacturer's instruction manual (Bruker, 2000). All analyses were performed at 5°C (maintained by a refrigerated circulating waterbath). Each droplet size distribution measurement took 15 minutes to perform. Initial (t=0) measurements were completed within 30 minutes of emulsification and quenching. The instrument is able to differentiate between water and oil, wax or solid fat molecules due to their different respective proton relaxation times. The instrument calculates the volume-weighted average

droplet size (d_{33}), the geometric mean droplet diameter ($d_{(0)}$) and the standard deviation of the log normal distribution of the droplet diameters. The relationship between these parameters is defined as:

$$d_{33} = d_{(0)} e^{3\sigma^2} \quad (6)$$

Droplet size distributions were measured at intervals of 0, 6, 12, 24, 48, 96, 144 and 240 hours.

2.2.6 Microscopy

Polarized light microscopy (PLM) was used to examine the morphology of the W/O emulsions after 10 days of storage. Emulsions were sampled with a Pasteur pipette and placed on viewing slides (Fisher Scientific, Nepean, ON), upon which a cover slip (Fisher Scientific, Nepean, ON) was gently placed. A Zeiss Axioplan-2 light microscope (Zeiss Instruments, Toronto, ON) with a 63x Achroplan water immersion objective was used and images were captured with a Q-Imaging CCD camera and analysed using Northern Eclipse software (version 6.0, Empix Imaging, Mississauga, ON). As a minimum, three slides were prepared for each treatment and each photomicrograph represents a typical field.

2.2.7 Statistics

Triplicate analyses were performed on all droplet size measurements and sedimentation experiments. Statistical analyses were performed with SPSS Statistical Package v8.0.1 using ANOVA and Tukey analysis (SPSS, Chicago, IL, USA). Differences were considered significant at $p < 0.05$.

Reproduced with permission of the copyright owner. Further reproduction prohibited without permission.

2.3 Results and Discussion

2.3.1 Sedimentation of Emulsions

Figure 3 shows the visual appearance of all emulsions after 24 days of storage at 5°C. All samples made with pre-crystallized wax flocculated to some degree, as evidenced by visible channels, whereas the samples prepared with post-crystallized wax were more uniform in their appearance, and no sedimentation or flocculation was observed at 1.0 or 2.0% wax. Addition of as little as 0.125% wax provided notable stabilization to either type of emulsion ($p<0.05$) as compared to samples containing no wax. This difference in emulsion stability may be attributed to differences in the crystal properties when prepared via the different regimes, as discussed in section 2.3.5.

The height of the dispersed phase was measured in relation to the total height of the emulsion over 10 days (Figure 4). Addition of 0.125% wax had a profound effect on the stability of the emulsions to sedimentation over the duration of 10 days compared to samples containing no wax. However, the visual method of analysis used did not allow for the measurement of the mid-column separation, or channeling that occurred with the pre-crystallized samples as seen in Figure 3. As such, the quantitative data is limited in how accurately it describes the sedimentation behaviour of the samples over time, and should be considered in conjunction with the photographic evidence.

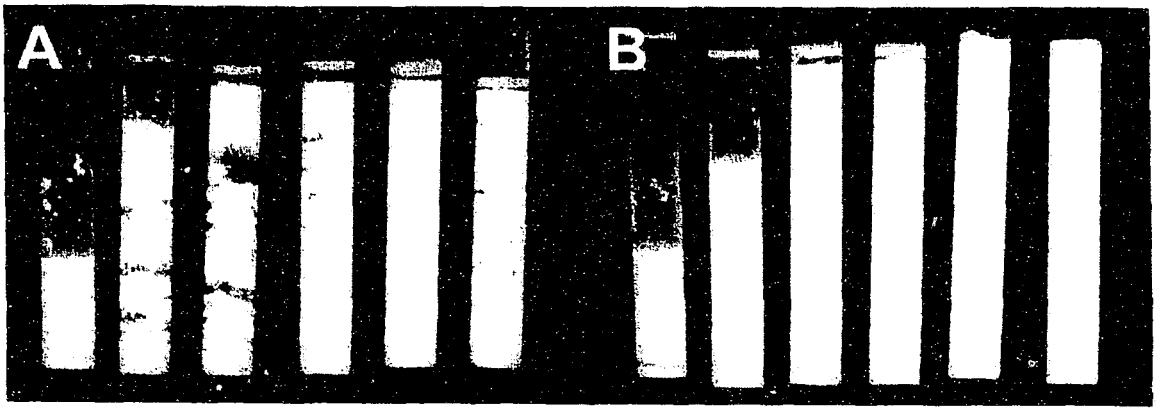

Figure 3: Sedimentation of water in oil emulsions after 24 days. Figure 1A shows samples prepared with pre-crystallized wax; B shows samples prepared with wax crystallized following emulsification. For both sets, emulsions shown contain 0.0, 0.125, 0.25, 0.50, 1.0 and 2.0% wax (from left to right).

Reproduced with permission of the copyright owner. Further reproduction prohibited without permission.

2.3.2 Coalescence Behaviour of Emulsions

Droplet size determination via pNMR has a number of distinct advantages over light scattering methods. They are *in-situ*, non-destructive, and allow the repeated analysis of individual samples over time. Secondly, the method measures individual droplets although they may in fact be flocculated in a cluster. Light scattering techniques are based on the theory whereby droplets are assumed to be isolated from each other, and as such, light scattered by flocculated droplets is not properly interpreted (McClements, 1999; Fourel *et al.*, 1995).

As shown in Figure 5, initial volume-weighted average droplet diameter (d_{33}) of the emulsions' dispersed phase decreased with increasing amounts of wax for both the pre-crystallized (Figure 5A) and post-crystallized systems (Figure 5B). An increase in d_{33} values over time indicates coalescence of water droplets has occurred. With emulsions containing pre-crystallized wax, there is a very rapid initial increase in d_{33} over the first two days, and then the values remain fairly constant for the remaining observed time. With the post-crystallized emulsions, there is no similar abrupt increase in the initial d_{33} values.

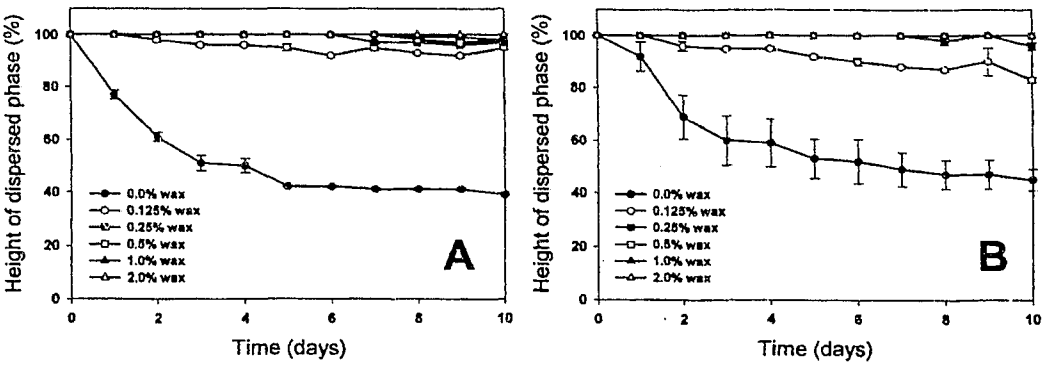

Figure 4: Height of the dispersed phase (expressed as a percent of total liquid height of emulsion in tube) for water in light mineral oil emulsions stabilized with various levels of paraffin wax. A: with pre-crystallized wax; B: with wax crystallized following emulsification.

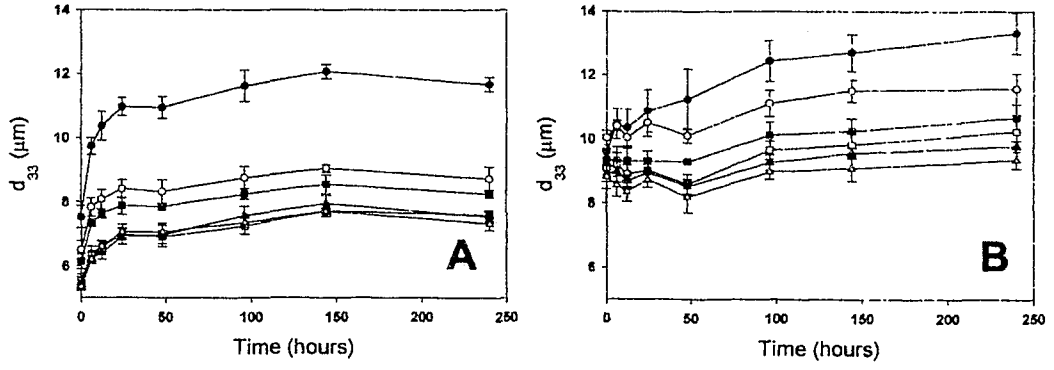

Figure 5: Volume-weighted average droplet diameter (d_{33}) of 20% (v/v) water in mineral emulsions stored at 5°C. Emulsions prepared with A: precrystallized wax; B: wax crystallized following emulsification at levels of (●) 0%, (○) 0.125%, (■) 0.25%, (□) 0.50%, (▲) 1.0%, (Δ) 2.0%.

Reproduced with permission of the copyright owner. Further reproduction prohibited without permission.

The percent changes in droplet size from the initial measurements to those taken at 10 days are compared in Figure 6. A lower percent change is indicative of enhanced stability of the emulsion against coalescence. Interpreted this way, there is a significant decrease ($p<0.05$) in the amount of droplet coalescence between 0 and 0.125% solid wax addition in both the pre-crystallized and the post-crystallized systems. The post-crystallized system, however, exhibited a consistently higher degree of stability against droplet coalescence over the pre-crystallized system with the addition of the same amount of wax ($p<0.05$). This is clearly illustrated in Figure 7. Figures 7A and B show the change in droplet size distribution (recorded at 0 and 10 days) for samples prepared with 0% and 2.0% pre-crystallized wax, respectively. This is in comparison to samples prepared via the post-crystallization method as shown in Figures 7C and D, again for samples with 0% and 2.0% wax, respectively. These concentrations were chosen as they clearly illustrate the different shapes of the droplet size distributions. Emulsions containing 2.0% post-crystallized wax (Figure 7D) show the smallest change in droplet size distribution shape as shown by the similarity between the curves representing the droplet size distributions at 0 and 10 days. This sample also had the smallest breadth of the distribution indicating a reduction in coalescence of both smaller and larger droplets than their pre-crystallized counterpards. Samples containing no wax (Figure 7A and C) showed a large increase in the average droplet size and the breadth of the droplet size distribution. By rapidly crystallizing the wax in the emulsion following homogenization, the degree of droplet coalescence can be markedly reduced.

Reproduced with permission of the copyright owner. Further reproduction prohibited without permission.

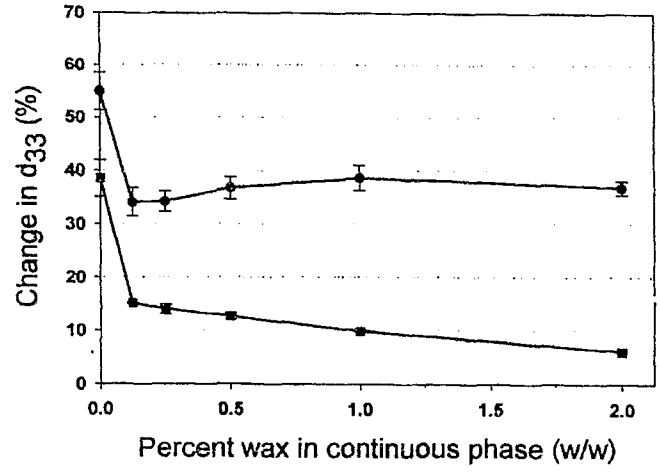

Figure 6: Percent increase in volume average droplet diameter from 0 hrs to 240 hours for 20% (v/v) water in oil emulsions stabilized with increasing amounts of paraffin wax (w/w in oil phase). Wax crystallized before (●) and after (■) emulsification.

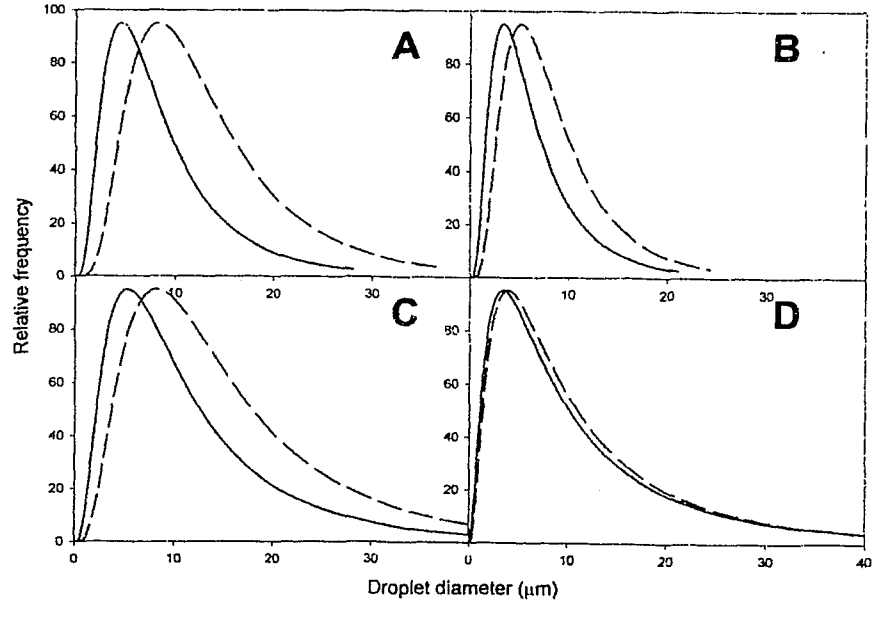

Figure 7: Water droplet size distribution for 20% (v/v) water-in-oil emulsions 0 days (——); 10 days (------). Plots A and B represent emulsions containing 0% and 2.0% (w/w) wax, respectively, prepared via the pre-crystallization method. Plots C and D are for emulsions containing 0% and 2.0% wax, respectively, prepared via the post-crystallization method.

Reproduced with permission of the copyright owner. Further reproduction prohibited without permission.

2.3.3 Microscopy

Photomicrographs of emulsions after 10 days at 5°C showed that emulsions containing no wax had a high degree of larger diameter droplets (Figures 8A and B), not observed for emulsions containing 2% wax (Figsures 8C and D). Also depicted in Figures 8C and D are features visualized by PLM and overlaid on the images of the droplets. Of note is the location of the wax crystals which were always in association with water droplets and were not seen isolated in the bulk continuous phase, suggesting an affinity of the crystals to the oil-water interface - one of the main criteria for stabilization of emulsions due to fine particles. This affinity of the crystals to the interface is facilitated by the added surfactant. The surface of the wax crystals becomes increasingly polar due to adsorption of the surfactant (Johansson and Bergenståhl, 1995c). As a result of this increased polarity it becomes more thermodynamically favourable for the crystals to reside at the oil/water interface. This surface activity was seen in samples prepared by both methods.

Reproduced with permission of the copyright owner. Further reproduction prohibited without permission.

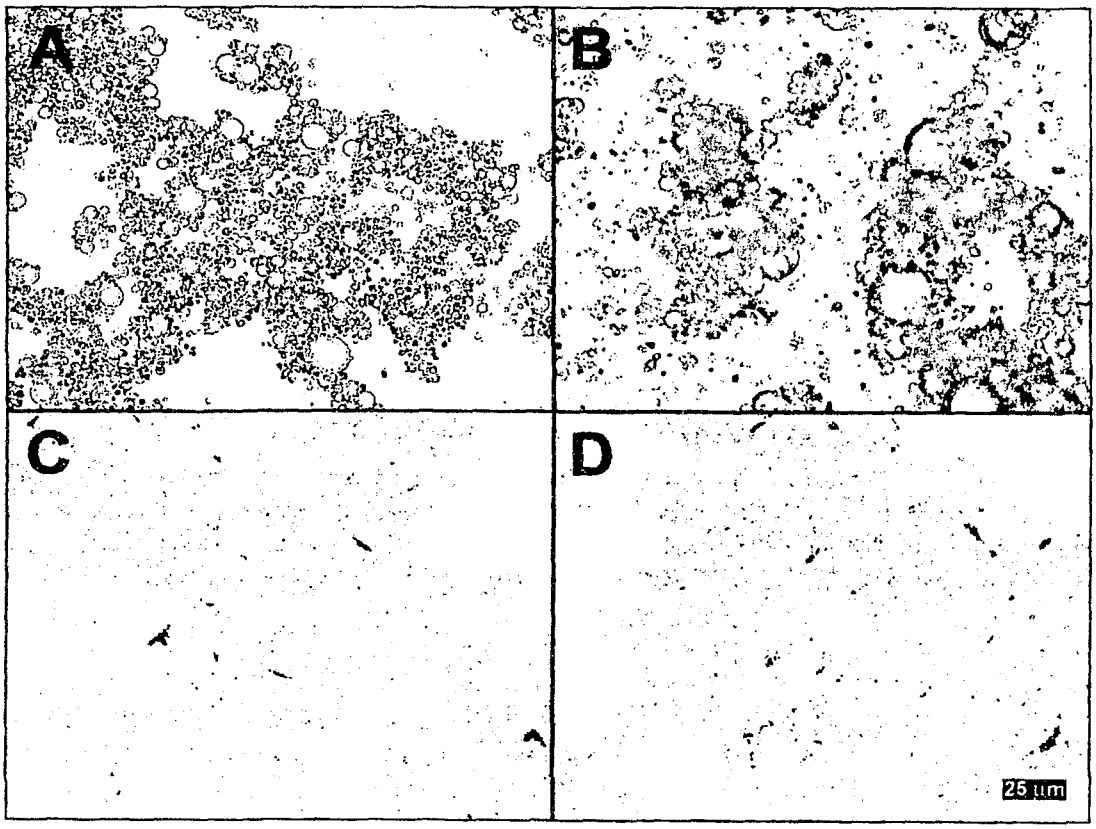

Figure 8: Photomicrographs of 20% (v/v) W/O emulsions after 10 days at 5°C. Images A and B are of samples containing no wax prepared by the pre-crystallization and post-crystallization methods, respectively. Images C and D are of samples containing 2% wax prepared by the same methods, respectively. Dark regions in C and D are features resolved via polarized light microscopy.

Reproduced with permission of the copyright owner. Further reproduction prohibited without permission.

2.3.4 Mechanisms

As emulsions are thermodynamically unstable, given sufficient time, small droplets will form larger ones and eventually phase-separate. Coalescence requires four steps – flocculation, thin film drainage, film rupture and merging of droplets (Johansson *et al.*, 1995d). As described above, W/O emulsions were less stable at lower solids content as there was an insufficient solid mass to surround the droplets and sterically stabilize the aqueous droplets. In samples with higher levels of solids, flocculation and coalescence was decreased. Lucassen-Reynders (1962) explained that the energy content of the bonds in a fat crystal network could be deemed an energy barrier against the free diffusion of crystals away from the network and towards an interface. Once formed, this network keeps droplets separate from one another due to the presence of interstitial crystals thus reducing the rate of flocculation.

When droplets do flocculate, mechanisms of thin film drainage and film rupture become important. A highly viscous and rigid interfacial film laden with crystals, some of which may be surface-active, will retard coalescence by slowing the rate of film drainage and eventual rupture thereby promoting the kinetic stability of the emulsion. Given that the systems investigated contained a constant level of non-crystalline emulsifier, the crystal-free rheology of the interface should be the same for all samples. Thus, the number, shape and size of the crystals located at the interface will dictate differences in film drainage and rupture. Particle removal from an interface is also a necessary precursor to coalescence. Energy requirements for the lateral movement of crystals will depend on the composition and rheology of the interface. Complete displacement of the crystal from the interface will depend on

these two factors as well as the wettability of the crystals at the interface. In this investigation, given the compositions of the liquid phases were constant, wettability of the crystals would also be expected to be the same in all cases. Thus, the factors that can account for the observed differences in flocculation and coalescence stability are a result of differences in the nature of self-association or network formation between the crystals and crystal size, morphology, abundance, and location at the interface.

2.3.5 Structure of the solid wax phase

Thompson et al. (1985) found that the stability of crude oil emulsions was dependent on the temperature history of the oil prior to emulsification. Oil that had been rapidly cooled resulted in the formation of small wax crystals, while the slow cooling of oil resulted in larger crystals. Subsequently, emulsions produced from the oil containing the small crystals were more stable to demulsification. With the methods of sample preparation employed here, the wax was crystallized according to two temperature regimes. The wax in the samples made with pre-crystallized wax was crystallized by cooling at a slower rate than the samples crystallized following emulsification. The expected result would be the creation of larger crystals, and fewer small crystals compared to the quench-cooling crystallization employed in the preparation of the post-crystallized samples. It is possible that the high shear conditions of homogenization broke up and disrupted some of the larger crystals predominant in the pre-crystallized system, but it is unlikely that this changed the relative proportions of very small crystals present in either system. That is, after homogenization there would be still be more smaller crystals in the post-crystallized

Reproduced with permission of the copyright owner. Further reproduction prohibited without permission.

emulsions compared to the pre-crystallized emulsions with the same percent of added wax.

Smaller crystals are able to provide more complete coverage of emulsion droplets. Crystallization of wax at a time when an interface is already present would allow the formed crystals to create a very close-fitting crystalline shell about the droplet and provide effective steric hindrance to coalescence. Such crystallization behaviour has been observed in butter by Buchheim and Dejmek (1997) and it is likely that a similar structure is formed in the post-crystallization method where wax is crystallized from the melt in the presence of water droplets. The presence of these small crystals was not resolvable using PLM. This coating on the water droplets would provide effective resistance to droplet coalescence, but doesn't necessarily explain the resistance of the post-crystallized emulsions to flocculation and sedimentation. To explain this phenomenon it is necessary to consider the rheological properties of the continuous phase as it relates to the nature of the wax crystals contained therein.

The presence of a crystal network would account for the different flocculation behaviour observed in the two methods. Droplet sizes were comparable in either case, so the differences in flocculation are not attributable to differences in sedimentation rates based on droplet size. Rapid crystallization of the wax followed by static storage of the emulsion in the case of the post-crystallized samples would favour the formation of a solid wax network of fine crystals, evenly distributed through the continuous phase. Given sufficient inter-particle bonds this would provide a framework, or structure to restrict the movement of water droplets, thus reducing coalescence, but most noticeably by reducing flocculation and

sedimentation. On the other hand, emulsions containing pre-crystallized wax would not have this refined network structure. There would be fewer small crystals and more large ones owing to the crystallization kinetics. This would result in a less homogeneous crystal network. Secondly, any gel-like structure created during the crystallization of the wax is destroyed upon emulsification resulting in a non-continuous network. Consequently, the water droplets and the crystals themselves are freer to migrate and the result is the uneven, channelled emulsion observed.

2.3.6 Conclusions

In conclusion, rapid crystallization of solid, continuous phase particles in an emulsion following homogenization results in a system which is more stable to both coalescence and flocculation than is achieved by pre-crystallization of the solid phase. Refinement of this technique and application to food-based systems may allow the development of increasingly functional or novel products.

Reproduced with permission of the copyright owner. Further reproduction prohibited without permission.

3 Stabilization of a Water in Canola Oil Emulsion using Crystals of High Melting Fat

3.1 Introduction

Experience from the analysis of the model system was applied to a study of emulsions composed of food ingredients. In order to remain appealing for consumers, food emulsions must remain stable over long periods of storage. Being thermodynamically unstable systems, they must be stabilized by improvement of their kinetic stability. It is known that in many emulsified foods solid particles are necessary for emulsions stabilization (e.g. egg yolk particles in mayonnaise). However, surprisingly little study has been made into the specific characteristics of solid particles that will optimize their performance in a given emulsion system. It is in this chapter that a margarine-type W/O system is employed to study the effects that fat crystal morphology, surface interactions (liquid-liquid and liquid-solid), and emulsion preparation technique have on the stability of this emulsion system. Methods from the wax and mineral oil study were altered as described to suit the different materials.

3.2 Materials and Methods

3.2.1 Characterization of Base Materials

Base materials used in this study included bleached, deodorized canola oil (CO) containing no additives (as the continuous phase), fully hydrogenated canola stearine (HCO) and fully hydrogenated cottonseed stearine (HCSO) as the crystal phases. These materials were donated by Bunge Foods (Toronto, ON). The canola oil was stored under nitrogen blanket at 5°C to reduce oxidation. Polyglycerol polyricinoleate (PgPr) is a lipophilic emulsifier (HLB<5) and was provided by

Nealanders International Inc. (Mississauga, ON). In Canada, PgPr is currently approved for use in chocolate at up to 0.50% where it lowers viscosity during conching and moulding operations. The allowable daily intake of PgPr as set by the European Community is 7.5 mg/kg body weigh. PgPr is commercially made by the interesterification of castor oil fatty acids and polyglycerol (Wilson *et al.*, 1998).

3.2.2 Triglyceride (TAG) Profile

The triglyceride composition of the canola oil, canola stearine and cottonseed stearine were determined by Gas Liquid Chromatography. AOCS Method Ce 5-86 (AOCS, 1997) was used as follows: Oven temperature at injection was 70°C followed immediately by ramping to 170°C at 20°C per minute. The ramp rate was then decreased to 15°C per minute and heating continued through to 350°C. The injector temperature was maintained at 5°C above the oven temperature. All TAGs were eluted by the time 350°C was reached. A 4m x 0.53 mm (ID) Supelco Petrocol column (Supelco, Oakville, ON) was used with on-column injection in a Perkin Elmer AutoSystem XL GC (Woodbridge, ON).

3.2.3 Fatty Acid Content

The fatty acid content of the HCO, HCSO and canola oil was determined according to AOCS Method Ca 5a-40 (AOCS, 1997).

3.2.4 Melting Point and Solubility of Solid Fats

The melting behaviour of the HCSO and HCO were determined by two methods. The capillary method (AOCS Method Cc 1-25, (AOCS, 1997)) was used to determine the point of complete melting. The melting points of the fats are important, as fats should be heated to 30° higher than their melting point prior to recrystallization to erase any crystal memory (Walstra, 2003). Also, the solid fat

Reproduced with permission of the copyright owner. Further reproduction prohibited without permission.

content (SFC) as a function of temperature was determined using low resolution NMR spectroscopy (AOCS Method Cd 16b-93 (AOCS, 1997)).

The solubility of the solid fats in canola oil was determined by turbidometric analysis, as described in section 2.2.2. The sample with the minimum concentration of solid fat showing absorption was interpreted as the maximum solubility of the solid fat in canola oil at 5°C.

3.2.5 X-Ray Diffraction

A Rigaku Geigerflex (Danvers, MA) X-ray diffraction (XRD) unit (λ=1.79 Å) was used to determine the powder diffractograms of the solid fats used in the study (HCO and HCSO). Emulsions and crystal-in-oil suspensions were vacuum filtered and analyzed at room temperature (21-24°C). Scans from 1.5 to 35° 2-θ were performed to evaluate short and long spacings.

3.2.6 Interfacial Tension Measurements

Measurements of interfacial tension between water and canola oil were determined at room temperature using the equipment described in Section 2.2.1. In this case, the density of the canola oil was 0.912 g/ml. Other correction factors were the same.

3.2.7 Contact Angle Measurements

HCSO and HCO were heated to 90°C and 100°C respectively and crystallized at room temperature in aluminum weigh boats. Solidified disks of hard fat from the weigh boats were then cut into approximately 1 cm squares and placed with the smooth bottom side up in a cuvette. Cuvettes were then filled with 2 ml of either canola oil or canola oil with 0.125% (w/w) PgPr (the concentration used in emulsion formation). A small droplet (1-2 mm diameter) of water was then injected

Reproduced with permission of the copyright owner. Further reproduction prohibited without permission.

onto the surface of the solid fat using a micro-syringe and stored for 24 hours. Images of the water droplet were captured with a Teli CCD camera with macro lens assembly and IDS Falcon/Eagle Framegrabber. Image analysis to determine the contact angle of the water droplet against the crystal surface was performed using SCA 20 version 2.1.5 build 16 (DataPhysics Instrument GmbH, Germany).

3.2.8 Microscopic Analysis of Emulsions

Polarized light microscopy and confocal laser scanning microscopy were used to examine the emulsions and the stabilizing role of the crystals, if any. The same microscope was used as in Section 2.2.6. This time image capture was accomplished using a LSM 510 confocal module and the associated software (LSM 510, version 3.2, Zeiss Instruments, Toronto, ON). A temperature-controlled stage (TS-60 stage, Instec Inc., Boulder, CO) was employed to maintain samples at 5°C. Emulsion samples were prepared in the usual manner, except that fluorescent dyes Fluorol Yellow 088 (Sigma-Aldrich, Oakville, ON) and Rhodamine B (Acros, Ottawa, ON) were added as stains to the oil and water phases, respectively, at 0.01% (w/w). Fluorol Yellow 088 dye present in the oil phase was imaged through excitation at 488 nm and detection via an LP 505 filter on the CLSM. Rhodamine B dye was excited at 543 nm with the emitted light passing through an LP 560 filter for detection.

A controlled test was performed to determine if either dye had any effect on the droplet size distribution of the emulsions at the time of formation, or over the course of 7 days. To do this, four sets of post-crystallized emulsions were prepared (each in triplicate) containing 1% HCO (see Section 3.2.9 for method). Each set contained a different combination of dyed and un-dyed liquid phases. Where 'X'

Reproduced with permission of the copyright owner. Further reproduction prohibited without permission.

denotes no dye added, and 'D' denotes dye added, and the first letter indicates the discontinuous (water) phase and the second letter the continuous (oil) phase, the combinations of emulsions were thus: X/X, X/D, D/X and D/D. (e.g. X/D emulsion would contain non-dyed water dispersed in oil dyed with Fluorol Yellow 088.) Droplet size distributions were measured at 6 hours and at 7 days using PFG-NMR (see Section 2.2.5) and microscopy. To determine droplet size distributions a minimum of three image fields were captured and the droplets traced and measured using Northern Eclipse 6.0 image analysis software (Northern Eclipse, Oakville, ON). No difference was found between the four treatments. Results are presented in Appendix A.

3.2.9 Preparation of Emulsions

Various protocols were developed to prepare emulsions using the food-type materials. As with the investigation using mineral oil, emulsions were prepared using pre and post-crystallization regimes but the conditions employed were altered to suit the change in materials (see below). The goal, as with the model emulsions, was also to produce initial emulsion droplet size distributions that were comparable between the pre and post-crystallization processes. The pre-crystallization protocol involved the following steps. A fat crystal stock solution consisting of 100 g of 4% (w/w) hard fat in canola oil was heated to 30°C above the melting point of the pure fat in a 250 mL beaker. The mixture was then cooled at room temperature under conditions of mild shear (240 RPM) using a LabMaster TS2010 (Lightnin, Etobicoke, ON) fitted with a Rushton-type impeller (6 vanes, 12 mm x 10 mm, overall diameter 50 mm). The mixture was stirred for 6 hours and then placed in the refrigerator at 5°C. Emulsions containing this crystal stock were made within the next 18 to 24 hours.

RYERSON UNIVERSITY LIBRARY

All final emulsions were 20% (v/v) water with 0.125% (w/w) PgPr in the oil phase. Appropriate volumes of water, oil, crystallized fat oil stock and oil with 0.5% (w/w) PgPr were measured at 5°C into homogenizer cups. Emulsions were immersed in an ice water bath to maintain the temperature near 5°C during the homogenization process. For these pre-crystallized samples, the homogenizer was operated at 4500-5700 RPM for one minute to pre-blend, followed by two minutes at 24000-30000 RPM to homogenize. Samples for sedimentation analysis were prepared as per section 2.2.4. Samples for droplet size analysis were prepared as per section 2.2.5.

A variation to the pre-crystallized method was also performed, whereby the solid fat was crystallized from the melt in the presence of 0.125% (w/w) PgPr.

With the post-crystallized samples, it was essential to homogenize the sample while the high melting fat was still liquid and then, immediately following emulsification, to quickly cool the sample to form the stearine crystals. A 4% (w/w) solution of the high melting fat in canola oil was heated to 30°C above the melting point of the pure fat and then maintained at 45°C to prevent recrystallization. This was the lowest temperature found at which re-crystallization of the solid fat did not occur. Other components used in the preparation of the emulsion were also maintained, combined and homogenized at this temperature, through the use of a 45°C water bath. After the mixing and homogenization operations noted earlier, the homogenization cell was immersed in an ice-water bath and the speed of the homogenizer reduced to the mixing speed of 4500-5700 rpm. Mixing was carried out for 6 minutes, which was determined to reduce the temperature of the contents to 5°C. The emulsion was then immediately pipetted into NMR tubes for DSD and

Reproduced with permission of the copyright owner. Further reproduction prohibited without permission.

sedimentation analysis. DSD measurements for t=0 were completed within 30 minutes of cessation of the cooling/mixing step.

3.2.10 Water droplet size distribution

Droplet size distributions were determined using Pulsed Field Gradient NMR, as described in Section 2.2.4.

3.3 Results and Discussion

3.3.1 Base Material Characterization

The triglyceride (TAG) composition of the base materials, as determined by gas liquid chromatography are presented in Table 1.

Table 1: Triglyceride composition (weight percent) of raw materials determined by gas liquid chromatography.

Aliphatic Çarbons	Canola Oil	Canola Stearine	Cottonseed Stearine
24	0.13		0.01
26	0.13		
28	0.84		
34		0.08	0.07
36		0.15	
38		0.97	1.12
46	0.68	0.57	
48		1.48	1.38
50	0.70	3.23	16.35
52	11.59	13.26	42.51
54	78.49	73.64	34.83
56	6.23	5.00	2.56
58	1.06	0.83	0.18
60	0.07	0.66	0.11
62	0.10	0.12	0.05

The predominant triglycerides in CO and HCO were of 54 aliphatic carbons (C54). The most prevalent TAG species in CO were C52 (11.6), C54 (78.5) and C56 (6.2%). In HCO the predominant triglycerides were also C52 (13.2), C54 (73.6) and C56 (5.0%). In HCSO, the key TAGs were C50 (16.4%), C52 (42.5%) and C54

Reproduced with permission of the copyright owner. Further reproduction prohibited without permission.

(34.8%). HCO and HCSO are manufactured via the complete hydrogenation of canola and cottonseed oil, respectively (IV=1). As such, the TAG species present in the HCSO were 2-stearyldipalmitin (PSP) (C50), 1-palmityldistearin (PSS) (C52) and tristearin (SSS) (C54) (Chang *et a.*,. 1990; Timms, 1984). In the canola oil, the primary TAGS were composed of the unsaturated oleic and linoleic fatty acids. Being a completely hydrogenated product, the canola stearine was composed primarily of the fully saturated tristearine (SSS) (C54) TAG.

The base materials were also analyzed for their free fatty acid content. The results, expressed as a percent based on oleic acid (AOCS, 1997) are presented in Table 2.

Table 2: Free fatty acid content, capillary melting point and solubility of base materials.

Material	Free fatty acids as oleic, %	Capillary Melting Point (°C)	Solubility (% w/w) at 5°C	
			Pure oil	Oil + 0.125% PgPr
CO	0.017 ± 0.002	-	-	-
HCO	0.018 ± 0.003	69.5 ± 0.2	<0.02%	<0.02%
HCSO	0.050 ± 0.002	62.5 ± 0.2	<0.02%	<0.02%

CO and HCO contained similar levels of free fatty acids. HCSO contained nearly three times as much, by comparison. While HCSO melted at a temperature 7° lower than HCO the solubility at the temperature of emulsion storage was the same.

The hydrogenated fats were both found to exhibit sharp melting profiles, but at slightly different temperatures (see Figure 9). Both were mostly solid below 50°C and completely liquid at around 65°C for HCSO and 75°C for HCO. The discrepancy between the melting points determined by the two methods is explained by the limited temperature intervals of SFC determination employed in the pNMR

Reproduced with permission of the copyright owner. Further reproduction prohibited without permission.

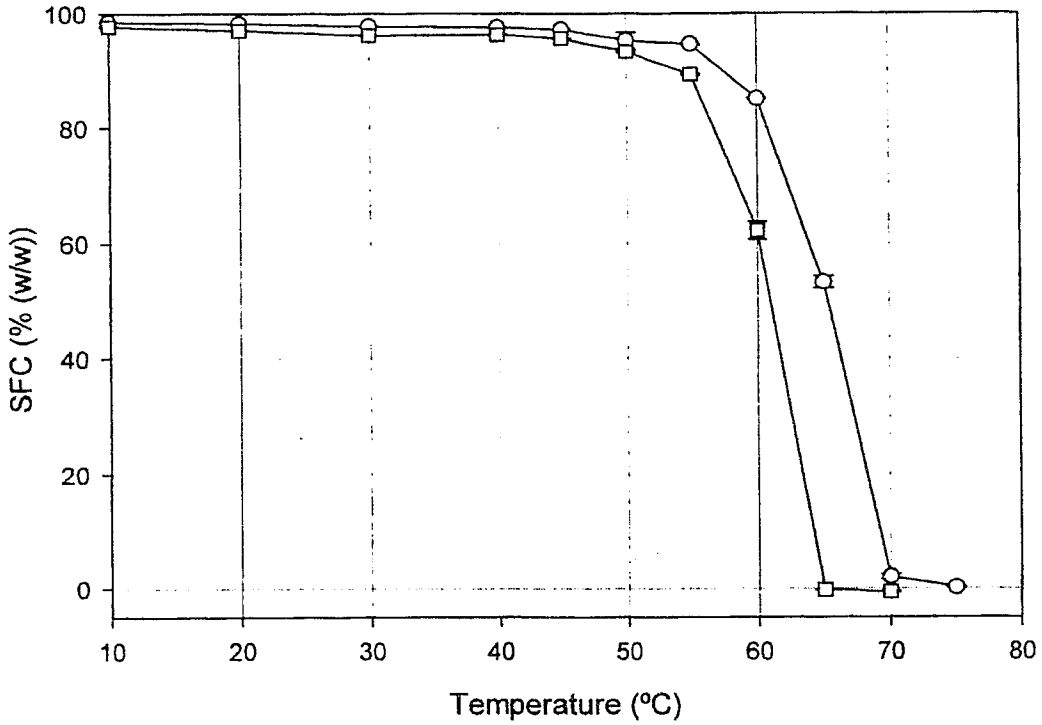

Figure 9: Melting profiles of fully hydrogenated canola oil (○) and fully hydrogenated cottonseed stearine (□) as evaluated with pulsed NMR.

Reproduced with permission of the copyright owner. Further reproduction prohibited without permission.

method, as well as the limited resolution of the NMR at low SFC levels. The most important information from the melting point studies is the temperature of complete melting, such that the solid fat is heated to no less than 30°C above this temperature to erase any crystal memory. At 5°C the solubilities of both fats in CO were less than 0.02% as shown in Table 2. As such, in the description of the prepared emulsions, the percent stearine added and percent solid fat present are used interchangeably.

3.3.2 Surface Phenomena

In this section the relationship between the interfacial tension of the oil and water phases, and the contact angles that are made between this interface and flat solid surfaces of HCO and HCSO are evaluated. The behaviour of micron-sized fat crystal particles at droplet interfaces will be directly related to these macroscopic observations.

The interfacial tension between water and canola oil at room temperature was 28.8 mN m^{-1}. The interfacial tension decreased through the addition of the emulsifier PgPr as shown in Figure 10. The concentration of PgPr selected for the study was 0.125%. The interfacial tension between canola oil and water at this concentration of PgPr was 13.4 mN m^{-1} at room temperature. At this concentration, the resulting emulsions (with 0% solid fat) exhibited clearly measurable changes in droplet size over a period of 10 days storage at 5°C (Figure 11).

Reproduced with permission of the copyright owner. Further reproduction prohibited without permission.

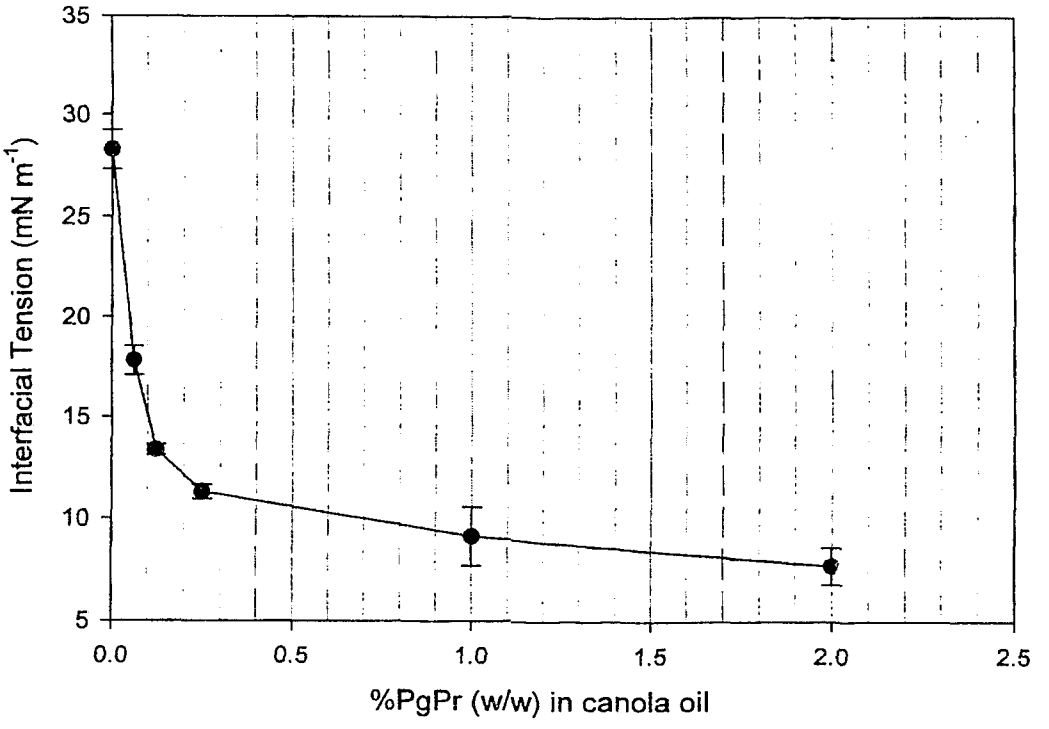

Figure 10: Interfacial tension between water and canola oil with increasing concentrations of PgPr.

Reproduced with permission of the copyright owner. Further reproduction prohibited without permission.

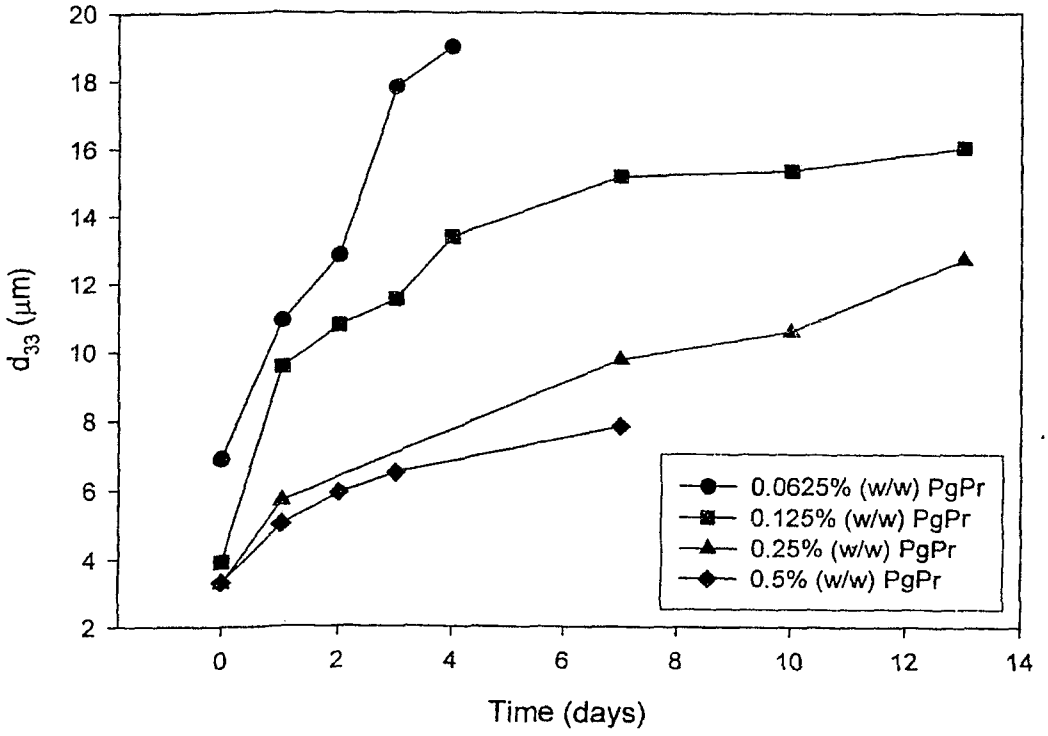

Figure 11: Volume weighted mean droplet diameter (d_{33}) for 20% (v/v) W/O emulsions containing various concentrations of PgPr in canola oil.

Reproduced with permission of the copyright owner. Further reproduction prohibited without permission.

Emulsions made with higher levels of PgPr were increasingly stable against coalescence. Commercially practical emulsions could be manufactured at such higher levels, however, to suit this study, a metastable emulsion system was desired so the effect of added fat crystals could be clearly observed within a reasonable time frame.

The interfacial tension between two liquid phases will influence the contact angle of a particle adsorbed at this interface. As discussed earlier, for particles to effectively stabilize an emulsion, the particles should ideally be located at the interface, but more so within the continuous phase. Thus in the case of a water in oil emulsion system, the contact angle of the water against the solid body would be greater than 90°. Typical images of sessile water droplets are shown in Figure 12. A smaller contact angle is seen for water droplets in the presence of emulsifier compared to those residing within pure oil. The small 'hills' upon which the droplets appear to sit (Fig. 12A and C) are shadows of the droplet cast on the solid fat surface. Baselines are drawn where these hills meet the droplet base. Average contact angles (measured through the water phase) for water droplets resting on HCO and HCSO in the presence of CO and CO with PgPr are reported in Table 3.

Table 3: Contact angle measurements for sessile water drops.

Solid Phase	Continuous Phase	Contact Angle
canola stearine	Canola oil	164.9 ± 0.2°
canola stearine	Canola oil with 0.125% PgPr	157.1 ± 0.3°
cottonseed stearine	Canola oil	172.4 ± 0.8°
cottonseed stearine	Canola oil with 0.125% PgPr	161.5 ± 0.9°

Reproduced with permission of the copyright owner. Further reproduction prohibited without permission.

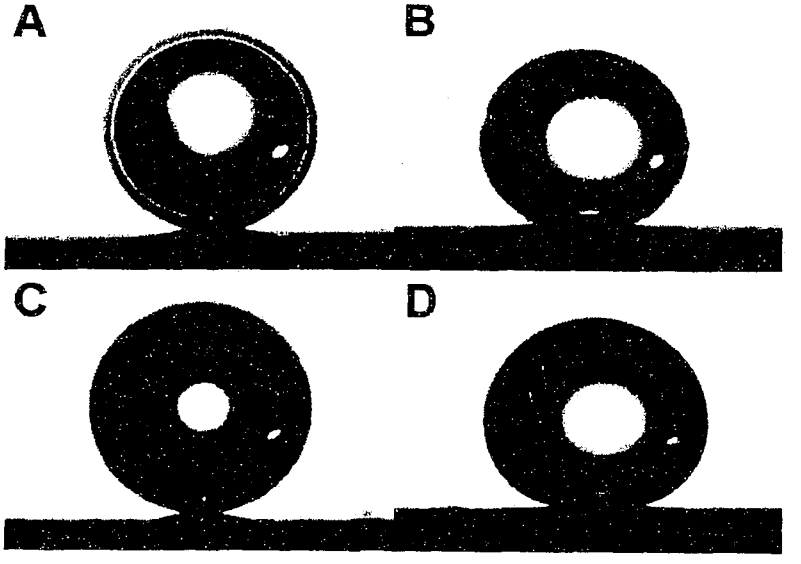

Figure 12: Typical images of water droplets used to determine contact angle. Substrate is solid canola stearine in A and B; continuous phase is canola oil without (A) and with (B) PgPr at 0.125% (w/w). Substrate is solid cottonseed stearine in C and D; continuous phase is canola oil without (C) and with (D) PgPr at 0.125% (w/w) (D).

Reproduced with permission of the copyright owner. Further reproduction prohibited without permission.

It is recalled from Section 1.1.1 that a fat crystal will be wetted by both the water and oil phases if the following condition is true:

$$\gamma_{ow} > \gamma_{os} - \gamma_{sw} \tag{4}$$

The resolution of the forces at the junction point is described by Young's Equation (Young, 1855),

$$\gamma_{ow}\cos\theta = -\gamma_{ow}\cos(180-\theta) = \gamma_{so} - \gamma_{sw} \tag{7}$$

where θ is the contact angle as measured through the water phase. The interfacial tension between the water and oil can be modified through the addition of surfactants and is measured as the force required to deform the interface. However, the solid surface cannot be deformed, so neither γ_{sw} nor γ_{so} can be measured directly. To determine the solid/water or solid/oil interfacial tensions a semi-empirical equation of state (Good, 1979) may be used:

$$\cos\theta_Y = \frac{(0.015\gamma_{sw} - 2.00)(\gamma_{ow}\gamma_{sw})^{1/2} + \gamma_{ow}}{\gamma_{ow}[0.015(\gamma_{ow}\gamma_{sw})^{1/2} - 1]} \tag{8}$$

where $\cos\theta_Y$ is the Young's angle. The Young's angle is the contact angle made by a liquid on a smooth, homogeneous surface of a specified composition and structure, and where this contact angle changes according to Young's equation. In the current investigation, given the somewhat impure nature of the raw materials, it is unlikely that the contact angles observed are in fact Young's. Using the contact angle data presented in Table 4 and Young's equation (7), Table 4 lists the values of the solid/water, solid/oil interfacial tensions. We can then use this information to determine the energy required (E_{disp}) to displace sub-micron sized fat particles from droplet interfaces with the same interfacial tensions.

Reproduced with permission of the copyright owner. Further reproduction prohibited without permission.

Table 4: Calculated interfacial tensions and displacement energy for a spherical particle of radius 0.1 μm (see text for details).

Solid Phase	Continuous Phase	γ_{sw} (mN m^{-1})	γ_{so} (mN m^{-1})	E_{disp} (kT)
Canola stearine	Canola oil	104.3	76.5	262
Canola stearine	Canola oil with 0.125% PgPr	119.2	106.9	636
Cottonseed stearine	Canola oil	104.5	75.9	17
Cottonseed stearine	Canola oil with 0.125% PgPr	119.5	106.8	273

If we consider spherical solid fat particles of radius r, the energy associated with this particle when it resides in the continuous oil phase would be

$$4\pi r^2 \gamma_{os} \tag{9}$$

As described by Levine *et al.* (1989), when a sperical particle is positioned at the oil-water interface the energy attributed to it will be

$$\pi r^2 \left[2\gamma_{os}(1-\cos\theta)+2\gamma_{ws}(1+\cos\theta)-\left(\gamma_{ow}\sin^2\theta\right)\right] \tag{10}$$

The third term represents the area of water/oil interface that is lost due to the spherical particle's presence at the interface. The difference in the energies associated with these two physical locations of the particle will describe the energy required to displace such a particle of a given size from the interface into the continuous phase. A droplet covered in particles that require larger inputs of energy to displace them will be more stable against coalescence. If we assume particles of radius 0.1 μm, then the energy required to displace particles from the interface would be as listed in Table 4 A particle of canola stearine in the presence of emulsifier would require 2.3 times as much energy to displace it from the interface as would a cottonseed stearine particle under the same conditions. When no PgPr is added to

Reproduced with permission of the copyright owner. Further reproduction prohibited without permission.

the canola oil, the energy of displacement is less than in the situation where PgPr is present. Thus, the addition of surfactant aids in the stabilizing effect of the particles.

3.3.3 Destabilization of Emulsions

Destabilization of emulsions results mainly from four processes, namely: sedimentation (or creaming), flocculation, coalescence and Ostwald ripening (Bergenståhl, 1994).

3.3.3.1 Sedimentation of Emulsions

Figure 13hows the visual appearance of post-crystallized emulsions after 10 days of storage at 5°C. The white section of the sample is the dispersed phase (water droplets and solid fat, if present). The clear layer visible on top is canola oil. The cloudy white material visible in a few tubes is small amounts of water droplets or solid fat that has adhered to the side of the tub. At lower solids levels (i.e. 0.125% and 0.25%) samples made with canola stearine were slightly more resistant to sedimentation than those containing cottonseed stearine. No samples containing HCO were completely stable against sedimentation. However, less than 5% supernatant oil was achieved through the addition of a minimum of 0.25% canola stearine or 0.50% cottonseed stearine.

Typical samples of emulsions prepared with pre-crystallized fats are shown in Figure 14 As seen, most samples sedimented in a very similar fashion, with the exception of cottonseed samples containing 1 and 2% solid fat that exhibited both sedimentation and a form of creaming, perhaps due to entrapped air bubbles. After 10 days, samples with no solid fat resulted in a sediment volume of approximately 45% of the original emulsion volume. Addition of solid fat up to 2% increased the

Reproduced with permission of the copyright owner. Further reproduction prohibited without permission.

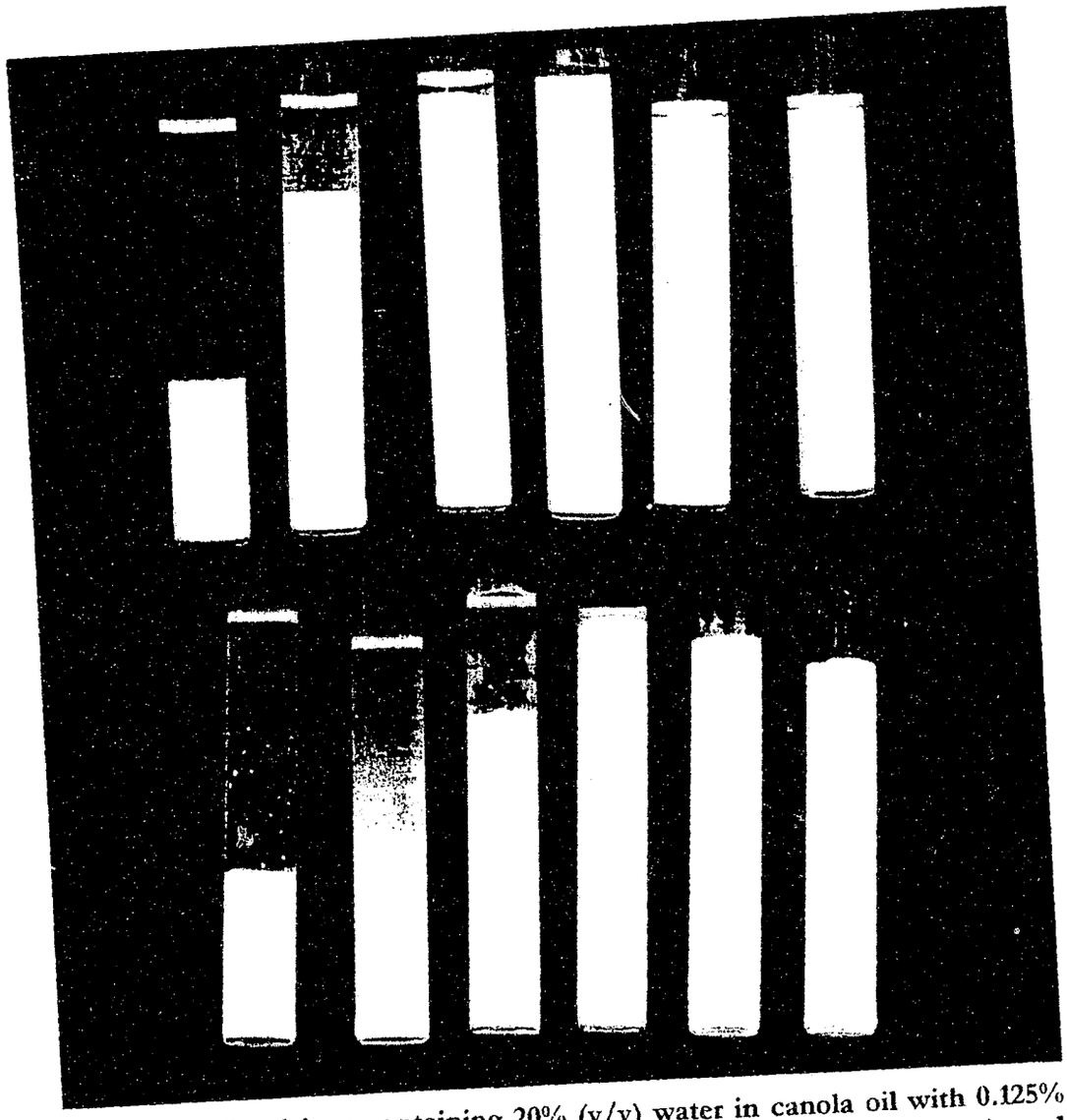

Figure 13: Emulsions containing 20% (v/v) water in canola oil with 0.125% (w/w) PgPr (emulsifier) and post-crystallized canola stearine (top) and cottonseed stearine (bottom) stored for 10 days at 5°C. Left to right, 0%, 0.125%, 0.25%, 0.50%, 1.0%, 2.0% solid fat (w/w) in oil phase.

Reproduced with permission of the copyright owner. Further reproduction prohibited without permission.

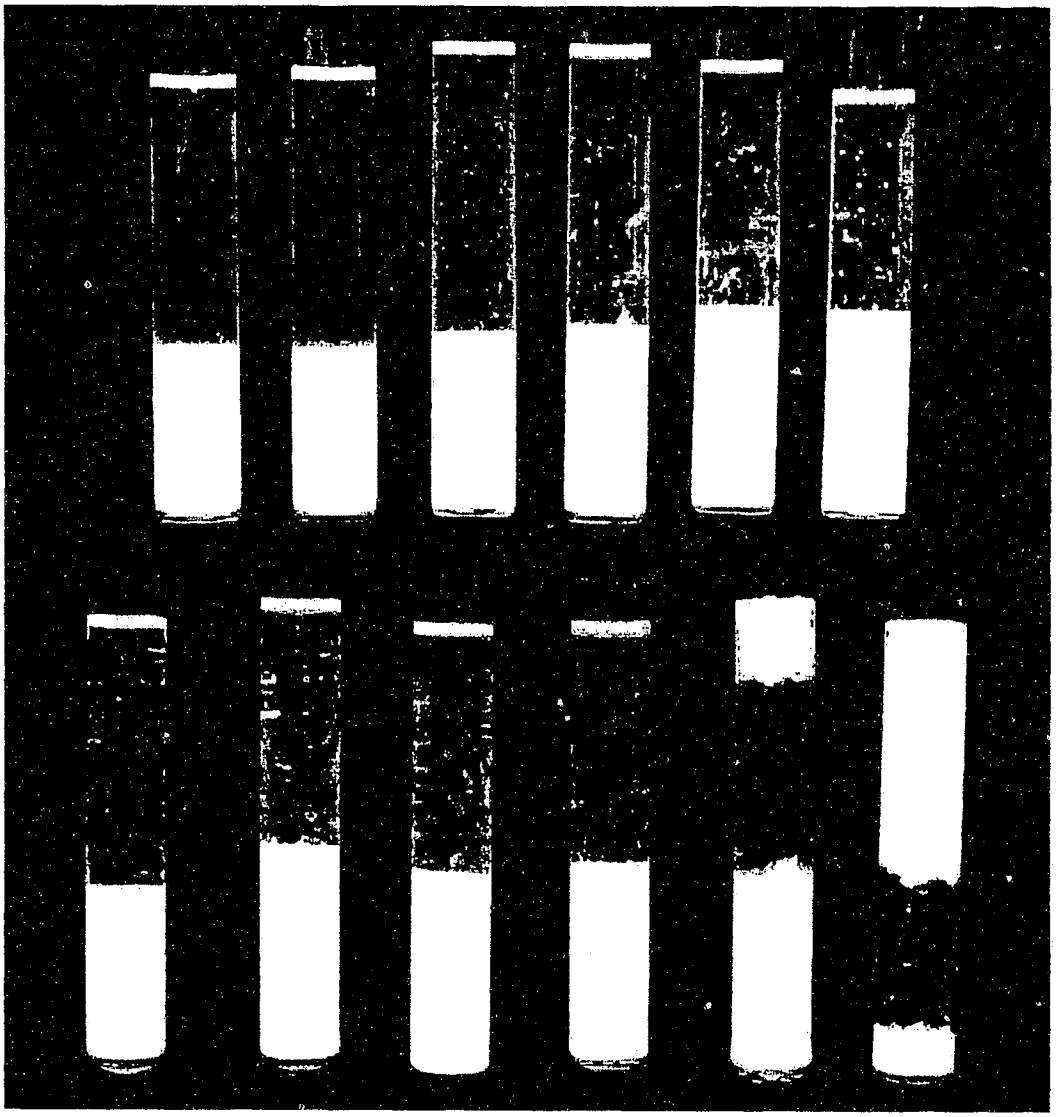

Figure 14: Emulsions containing 20% (v/v) water in canola oil with 0.125% (w/w) PgPr (emulsifier) and pre-crystallized canola stearine (top) and cottonseed stearine (bottom) stored for 10 days at 5°C. Left to right, 0%, 0.125%, 0.25%, 0.50%, 1.0%, 2.0% solid fat (w/w) in oil phase.

Reproduced with permission of the copyright owner. Further reproduction prohibited without permission.

sediment volume for canola stearine samples to 52%, while cottonseed stearine resulted in a dispersed phase volume (sedimented and creamed) of 68%.

The stability of the emulsions was greatly improved through the addition of solid fat when it was crystallized following emulsification. Conversely, the addition of fat crystallized prior to emulsification had little effect on the sedimentation stability of those emulsions.

3.3.3.2 Evolution of Water Droplet Size Distribution

Droplet size distribution data for each treatment are presented in Appendix B Regardless of the method of preparation, the initial d_{33} values are approximately 4 μm, decreasing with added solid fat. Over the course of 10 days the d_{33} values increased by varying degrees depending on the addition of hard fat. The initial $d_{(0)}$ values were approximately 4μm for the pre-crystallized samples, whereas the initial values for the post-crystallized sample centred at ~2 μm. Again, these initial mean diameter values decreased with the addition of solids.

3.3.3.2.1 Post-crystallization Regime

To assess the influence of solid fat addition on coalescence the percent change in $d_{(0)}$ (Figure 15A) and d_{33} (Figure 15 from day 0 to day 10 is plotted as a function of percent solid fat in the canola oil phase. With the post-crystallized HCO and HCSO a noticeable improvement in stabilization over ten days was seen for both materials between 0 and 0.50%. Further addition of solid fat has little effect, for either HCO or HCSO. This stabilization against coalescence coincides with what was observed for the stabilization of the post-crystallized emulsions against sedimentation. Thus, the stabilization against coalescence is likely linked to the decreased sedimentation caused by the added solid fat. Figures 16 and 17 show

Reproduced with permission of the copyright owner. Further reproduction prohibited without permission.

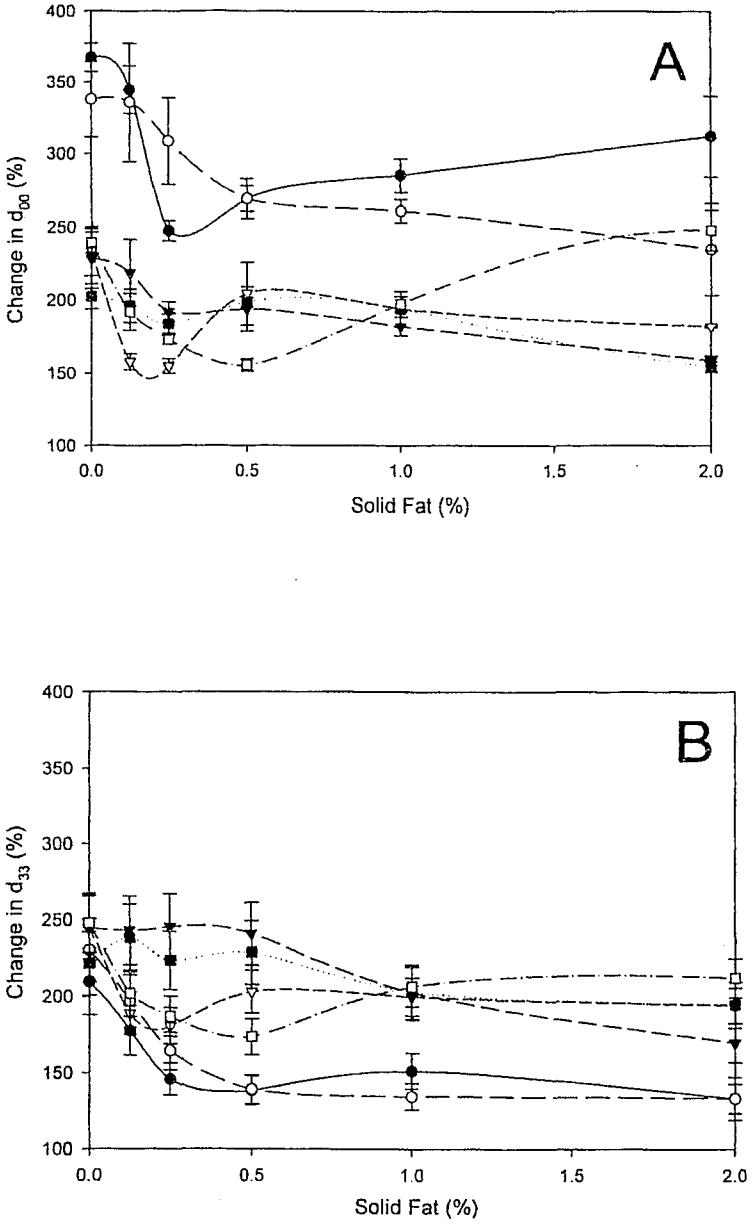

Figure 15: Percent change in (A) d_{00} and (B) d_{33} from day 0 to day 10. Canola post-crystallized (●), Cottonseed post-crystallized (○), Canola pre-crystallized without PgPr (▼), Cottonseed pre-crystallized without PgPr (▽), Canola pre-crystallized with PgPr (■), Cottonseed pre-crystallized with PgPr (❐).

Reproduced with permission of the copyright owner. Further reproduction prohibited without permission.

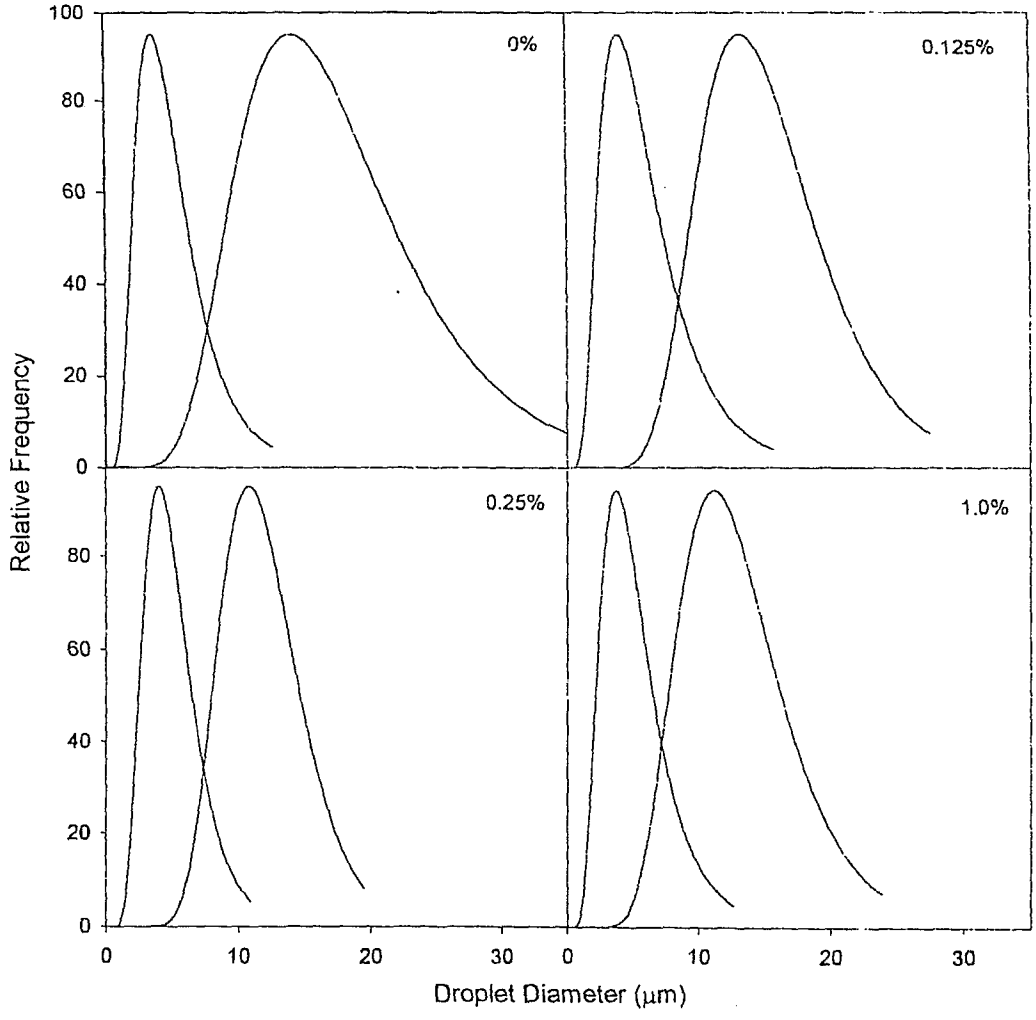

Figure 16: Typical water droplet size distribution curves for post-crystallized samples containing the indicated amounts of solid canola stearine in the oil phase. In all cases, left-most curve is for 0 days and right-most curve represents the distribution for 10 days.

Reproduced with permission of the copyright owner. Further reproduction prohibited without permission.

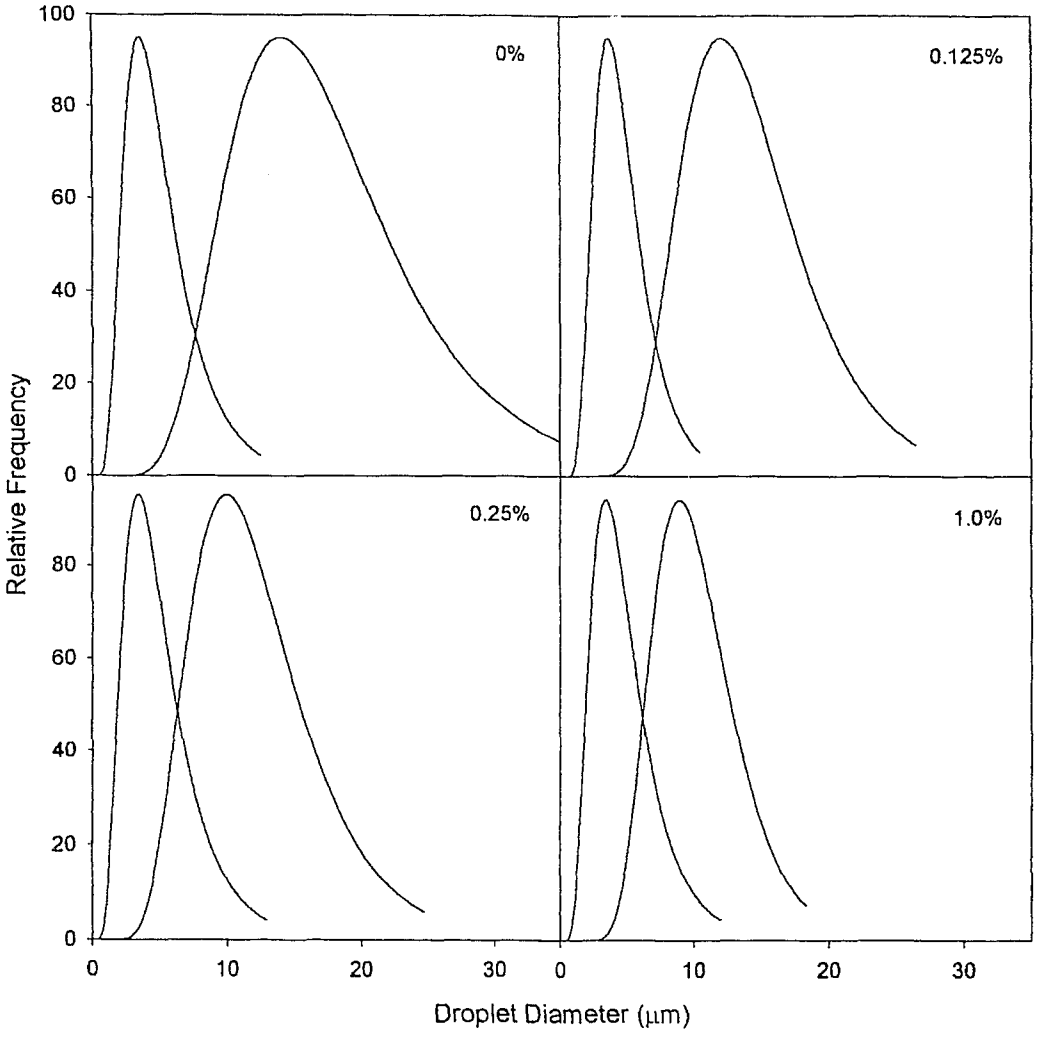

Figure 17: Typical water droplet size distribution curves for post-crystallized samples containing the indicated amounts of solid cottonseed stearine in the oil phase. In all cases, left-most curve is for 0 days and right-most curve represents the distribution for 10 days.

Reproduced with permission of the copyright owner. Further reproduction prohibited without permission.

typical water droplet size distribution curves for post-crystallized HCO and HCSO samples, respectively.

3.3.3.2.2 Pre-crystallization Regime

Two variations on the pre-crystallization regime were examined: One variation involved crystallizing the fat in the presence of PgPr (as would occur with the post-crystallization regime), while the other variation had the fat crystallize in pure oil. Little difference was seen between these two variations. Raw data is presented in Appendix B. The effect on coalescence is again, more easily interpreted by referring to the graphs of percent change in $d_{[0]}$ and d_{33} over 10 days (Figures 15A and B). Both variations are closely paired for each type of solid fat. At 1% and 2% both materials behaved similarly, however, at lower concentrations, the cottonseed stearine was more effective at decreasing droplet coalescence over ten days. Given that the sedimentation behaviour was similar for both solid fats and at all solid fat concentrations, (with the exception of the HCSO that creamed at 1 and 2%) an explanation must be sought for the enhanced stabilization against coalescence resulting from the HCSO. Evidence from examination of the emulsions using microscopy, as discussed in the next section, assists with this explanation.

Reproduced with permission of the copyright owner. Further reproduction prohibited without permission.

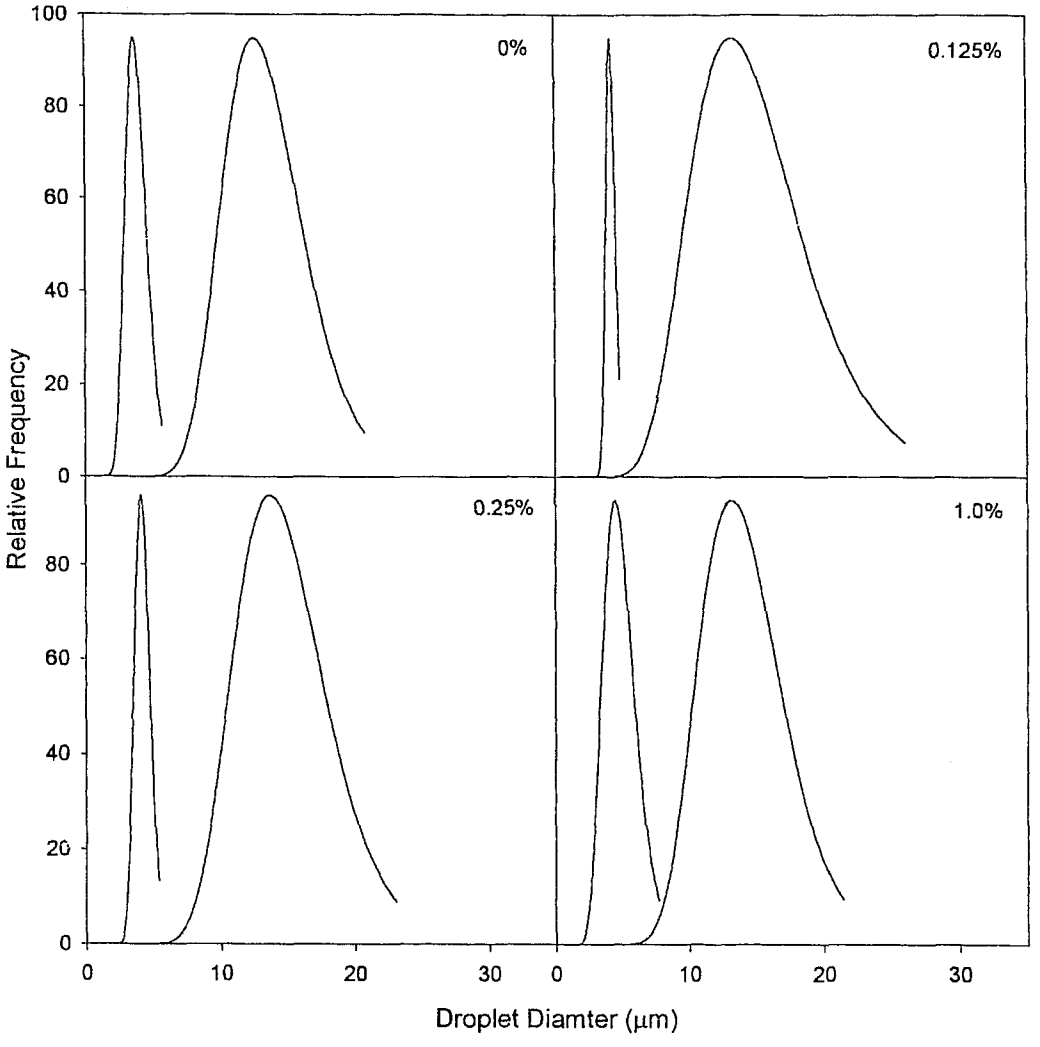

Figure 18: Typical droplet size distribution curves for pre-crystallized samples containing the indicated amounts of solid canola stearine in the oil phase. In all cases, left-most curve is for 0 days and right-most curve represents the distribution for 10 days.

Reproduced with permission of the copyright owner. Further reproduction prohibited without permission.

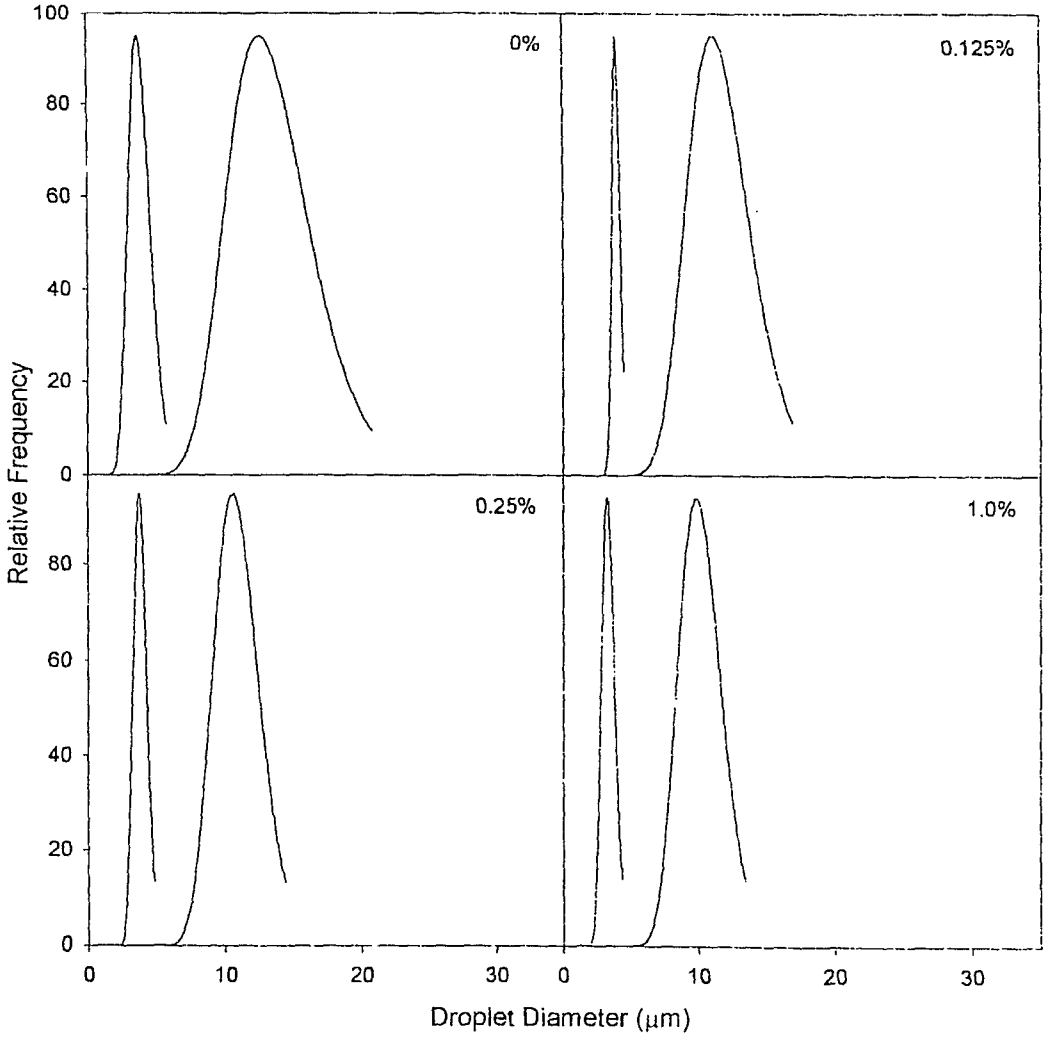

Figure 19: Typical droplet size distribution curves for pre-crystallized samples containing the indicated amounts of solid cottonseed stearine in the oil phase. In all cases, left-most curve is for 0 days and right-most curve represents the distribution for 10 days.

Reproduced with permission of the copyright owner. Further reproduction prohibited without permission.

3.3.4 Microscopy

Rhodamine B dye was observed to produce a halo effect when used to stain emulsion droplets (see Fig. 20). That is, when imaged using the laser scanning confocal microscope, the edges of the observed droplets were brighter than the middle of the drops. No such similar effect was observed with Fluorol Yellow 088 stain. An investigation using a planar (non-droplet) interface between stained water and oil showed a gradual intensification (within approximately 1 hour) of the fluorescence signal in the region immediately adjacent the interface, suggesting a migration and accumulation of the dye at or near the interface. The controlled test performed to determine the effect, if any, of the dyes on droplet size distributions showed no effect. See Appendix A for results.

Figures 20 through 23 show micrographs of emulsions at 0 and 10 days, at key concentrations of solid fat. Corresponding negative PLM images of the 10-day samples are also shown. With the post-crystallized samples (Figs. 20 and 21), crystalline fat is not readily discernable at the lower concentrations against the interference produced by droplet interfaces. However, at 2% fat, small crystal masses can be readily seen. Emulsion droplets show an increase in size over 10 days, at all concentrations, however, a greater number of smaller droplets are observed at higher solid fat concentrations. The droplets are also less flocculated at higher solid fat concentrations. The network of crystals observable at 2% solid fat appears to be responsible for this observation.

With the pre-crystallized samples (Figures 22 and 23), fat crystals are observed at lower concentrations, but many of these crystals are large with respect to the size of the water droplets and of little consequence for droplet stabilization.

Reproduced with permission of the copyright owner. Further reproduction prohibited without permission.

However, with the pre-crystallized cottonseed stearine (Figure 23), smaller crystals are also observed, being especially evident in the sample containing 2% solid fat.

To observe the structure of the crystal phase without interference caused by water droplets, samples were prepared with CO, emulsifier (0.125% (w/w)) and 2% (w/w) of either HCSO or HCO. The sample preparation protocol was the same as used in the preparation of emulsions, but no water was added. Figure 24 shows PLM images of pre and post-crystallized systems made with both HCO and HCSO. With respect to the post-crystallized fats, both solid fats were very similar in their appearance. Crystals are approximately 10 μm in length and are evenly distributed throughout the continuous oil phase. XRD analysis revealed that the cottonseed stearine was in the β polymorph when crystallized in this manner, while it is normally a β'-stable fat. Images C and D show samples containing pre-crystallized HCO and HCSO. In this case the spherulites were of strikingly different morphology, with the HCO being present in sharp β spherulites and the HCSO crystal agglomerations having a more randomly oriented structure. XRD analysis confirmed that the cottonseed was in this case present in its typical β' polymorph, while the canola was in the β polymorph. Also of note was the presence of small crystal shards in the cottonseed sample. These smaller crystals may be responsible for the enhanced stabilization provided to the pre-crystallized samples made with cottonseed stearine, where the percent change in d_{001} and d_{33} over ten days was more notably decreased by the addition of cottonseed stearine than by the same amounts of canola stearine.

Reproduced with permission of the copyright owner. Further reproduction prohibited without permission.

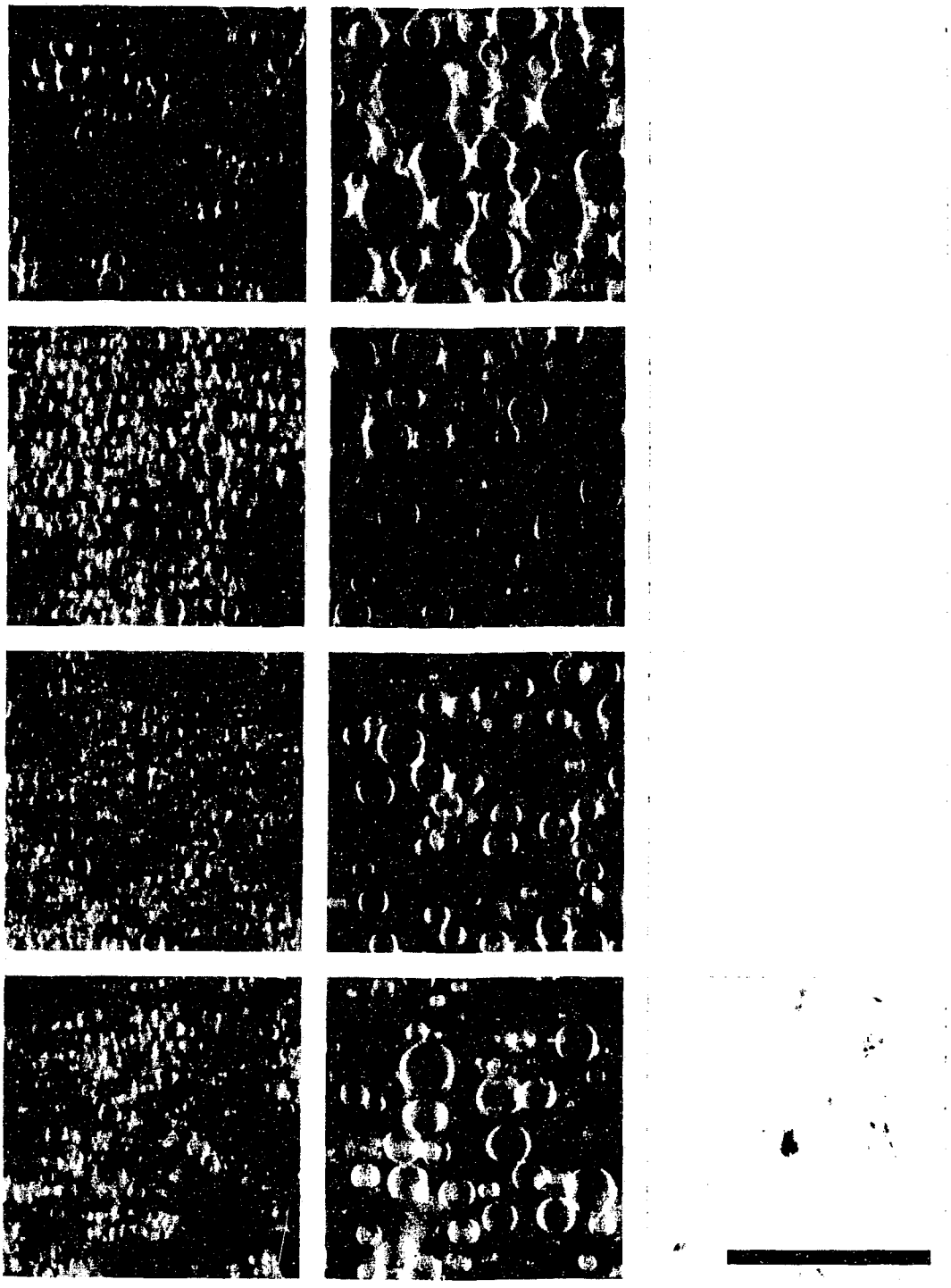

Figure 20: Emulsions containing post-crystallized canola stearine at 0% (top row), 0.125% (second row), 0.25% (third row) and 2.0% (bottom row), at 6 hrs (first coloumn) and 10 days (second column). PLM negative images (third column) correspond to 10 days images. Scale bar represents 50 μm.

Reproduced with permission of the copyright owner. Further reproduction prohibited without permission.

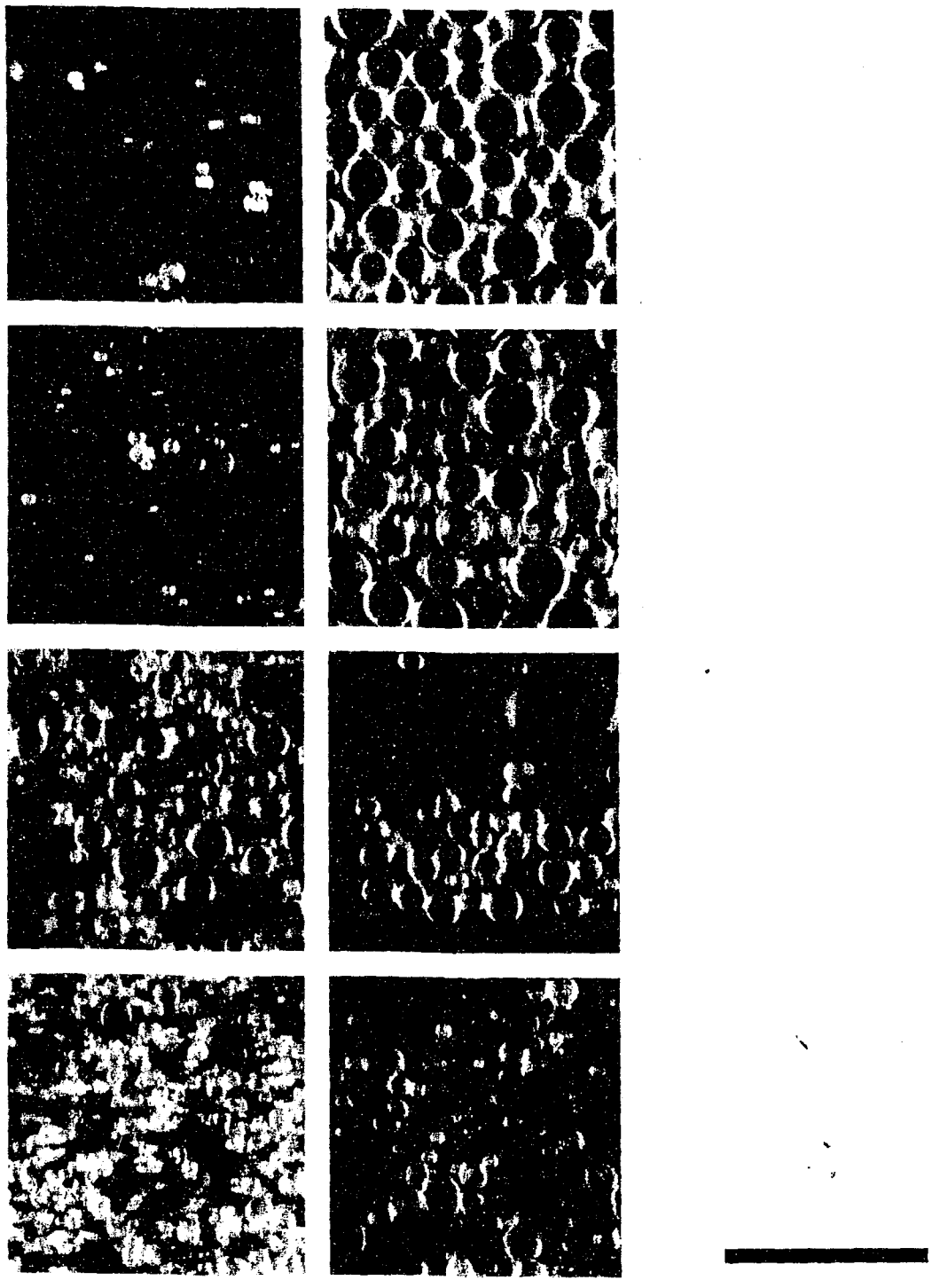

Figure 21: Emulsions containing post-crystallized cottonseed stearine at 0% (top row), 0.125% (second row), 0.25% (third row) and 2.0% (bottom row), at 6 hrs (first coloumn) and 10 days (second column). PLM negative images (third column) correspond to 10 days images. Scale bar represents 50 μm.

Reproduced with permission of the copyright owner. Further reproduction prohibited without permission.

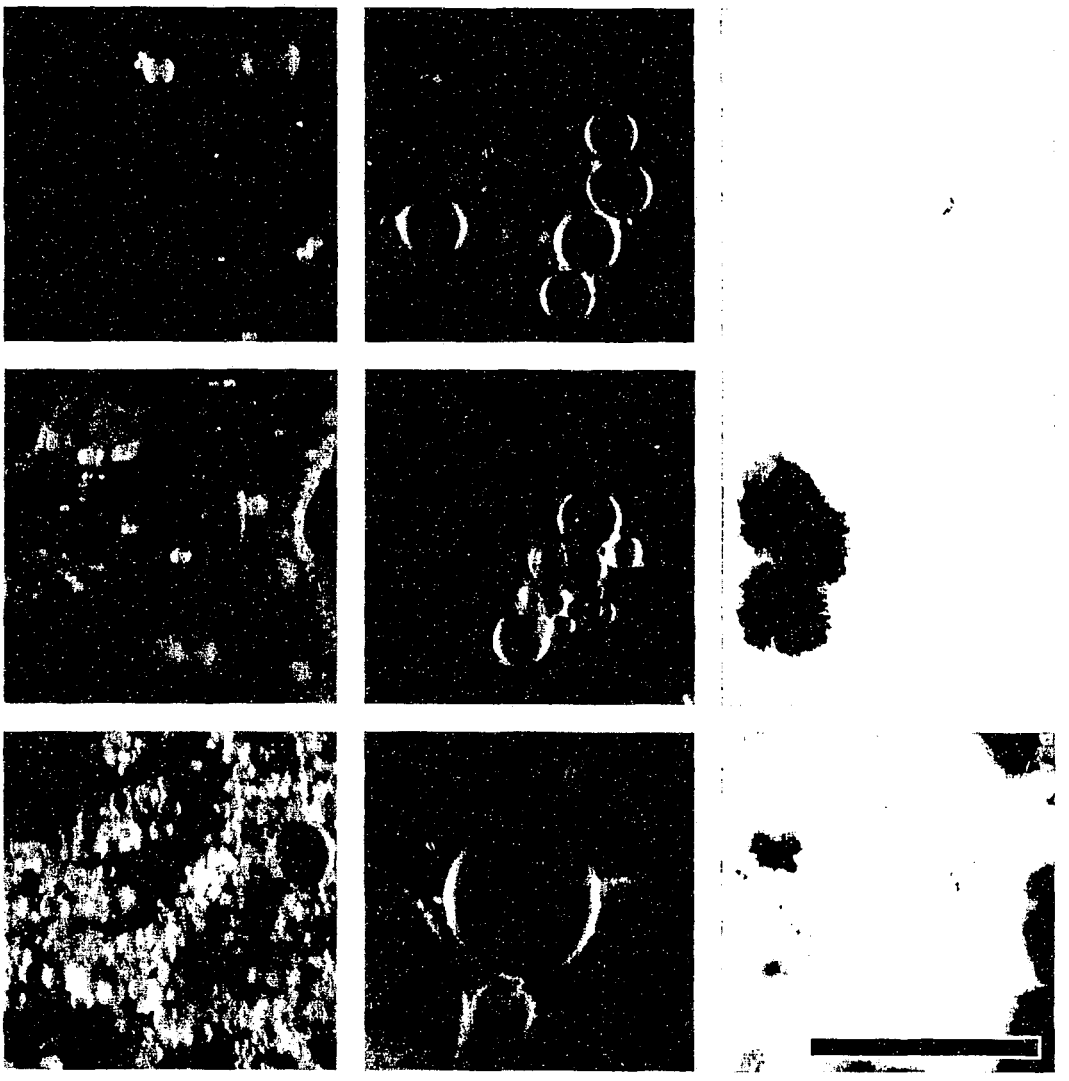

Figure 22: Emulsions containing pre-crystallized canola stearine at 0% (top row), 0.125% (second row), and 2.0% (bottom row), at 6 hrs (first coloumn) and 10 days (second column). PLM negative images (third column) correspond to 10 days images. Scale bar represents 50 μm.

Reproduced with permission of the copyright owner. Further reproduction prohibited without permission.

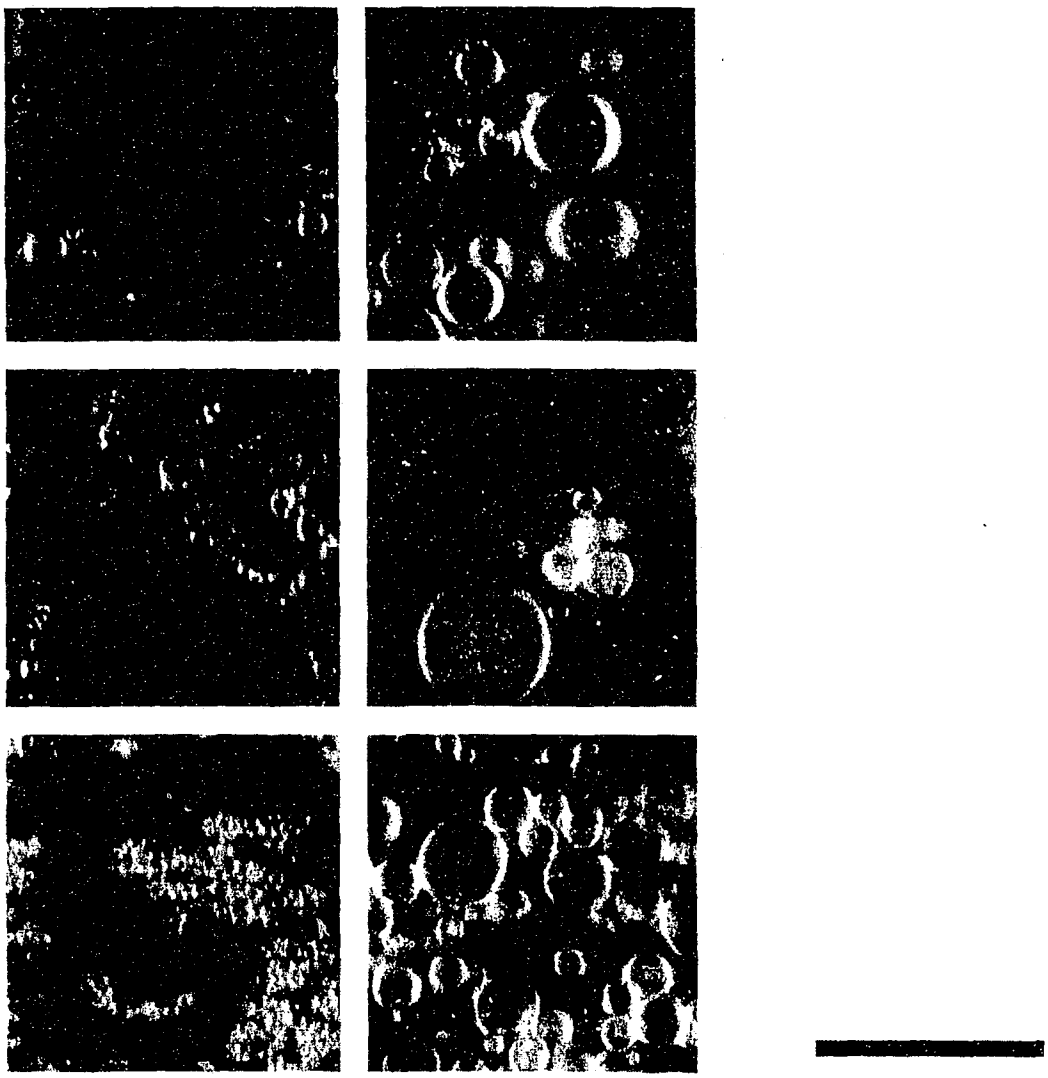

Figure 23: Emulsions containing pre-crystallized cottonseed stearine at 0% (top row), 0.125% (second row), and 2.0% (bottom row), at 6 hrs (first coloumn) and 10 days (second column). PLM negative images (third column) correspond to 10 days images. Scale bar represents 50 μm.

Reproduced with permission of the copyright owner. Further reproduction prohibited without permission.

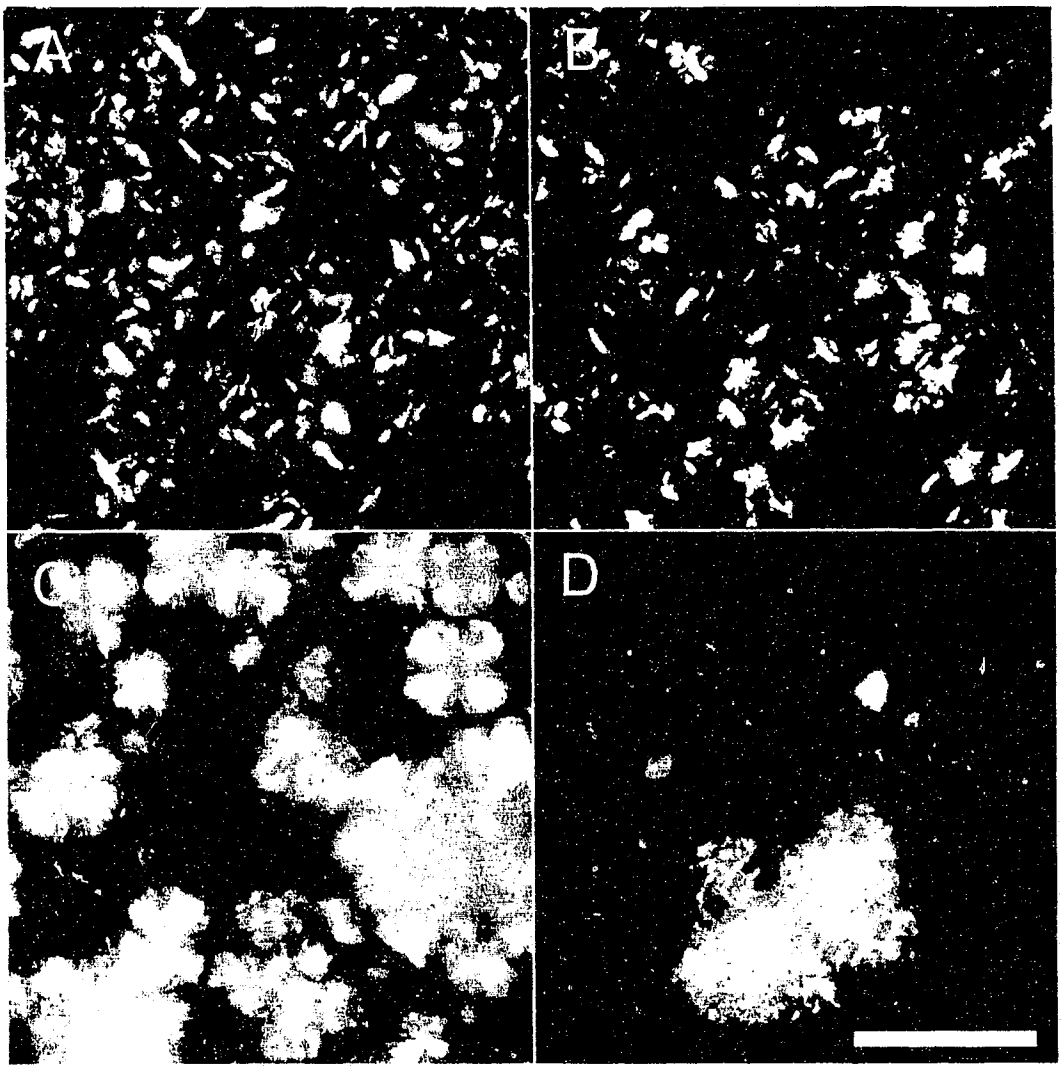

Figure 24: 2% (w/w) crystal suspensions. (A) HCO post-crystallized; (B) HCSO post-crystallized; (C) HCO pre-crystallized; (D) HCSO pre-crystallized . Scale bar represents 50μm.

Reproduced with permission of the copyright owner. Further reproduction prohibited without permission.

These smaller crystals would be better suited to provide an adsorbed layer surrounding the droplets. This adsorbed layer would effectively increase the elasticity and viscosity of the interface reducing the rate of droplet coalescence (Tambe & Sharma, 1993, Johansson *et al.*, 1995d).

3.3.5 Discussion

The relationship between the d_{33} and d_{10} value describes the polydispersity of the emulsion droplets, with their quotient providing the degree of polydispersity. The post-crystallization regime resulted in emulsions with broader size distributions than did the pre-crystallization regime. This difference was also observed in samples with no added solid fat, indicating it was not likely related to any action of solid fat particles. Water in oil emulsions are formed via a combination of turbulent and viscous forces. Had the Reynolds number of the flow of the continuous phase been greater than 2500, the approximate droplet diameter of the dispersed phase could have been approximated by

$$d = \frac{\gamma}{\varepsilon^{1/2}\eta_C^{1/2}} \qquad (11)$$

where γ is the interfacial tension, ε the amount of mechanical energy applied to the system (power density), and η_C the viscosity of the continuous phase (Walstra, 2003). Thus, it was likely that increased temperatures, as were employed in the post-crystallization regime would result in decreased O-W interfacial tensions, which subsequently allowed for the creation of smaller droplets in a system with a given energy input.

Figures 25 and 26 show the ratio of d_{33}/d_{10} for all post-crystallized canola and cottonseed samples during 10 days of storage. In both cases the ratio is initially quite high, decreasing rapidly over the first 48 hour, levelling off at approximately

Reproduced with permission of the copyright owner. Further reproduction prohibited without permission.

1.4. This indicates that when the emulsions are prepared in this manner there are, initially, a large number of very small droplets that disappear over the first day. Conversely, Figures 27 and 28 show the ratio of d_{33} to d_{00} for pre-crystallized emulsions. The ratios are lower than with the post-crystallized systems, with the cottonseed system being less polydisperse. With the post-crystallized samples, the disappearance of the small droplets is likely due to Ostwald ripening (Walstra, 2003). The conditions required for Ostwald ripening to occur, i.e. partial solubility of the dispersed phase in the continuous phase, moderate interfacial tension and low osmotic pressure in the dispersed phase, are all met. Ostwald ripening is not normally of consequence in food system emulsions as the droplets are usually larger than those found in this study, and hence have a decreased Laplace pressure. As well, salt is usually present in the aqueous droplets of most food emulsions which results in an osmotic resistance to droplet water loss (Walstra, 2003). In this study no salt was added to the aqueous phase, so this impediment was not present.

As in the previous study involving paraffin components, the presence of a crystal network here too would help to account for the different sedimentation behaviour observed in the two methods. Rapid crystallization of the solid fat followed by static storage of the emulsion in the case of the post-crystallized samples favours the formation of a network of fine solid fat crystals, evenly distributed through the continuous phase. Given sufficient inter-particle bonds this would provide a framework, or structure to restrict the movement of water droplets, by reducing sedimentation, flocculation and thus coalescence. On the other hand, emulsions made with pre-crystallized stearines would not have this refined network structure. Owing to the crystallization kinetics, more large crystals and fewer small

Reproduced with permission of the copyright owner. Further reproduction prohibited without permission.

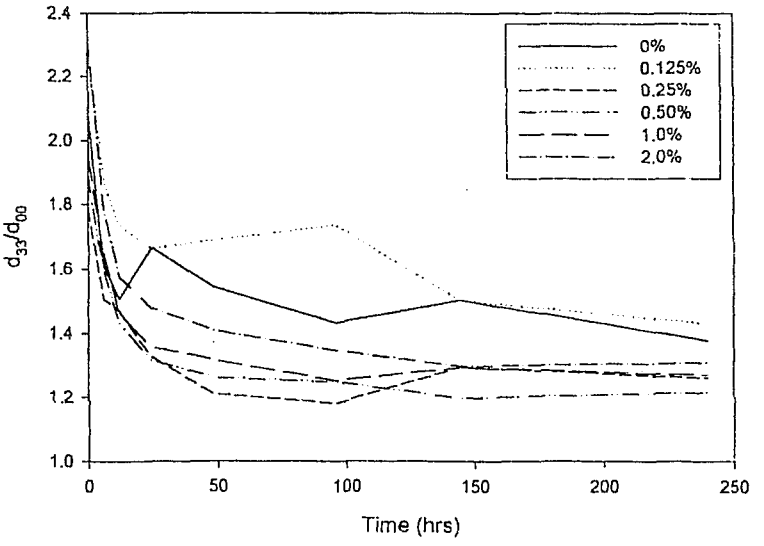

Figure 25: Ratio of d_{33} to d_{00} for W/O emulsions made with between 0 and 2.0% canola stearine, crystallized following emulsification.

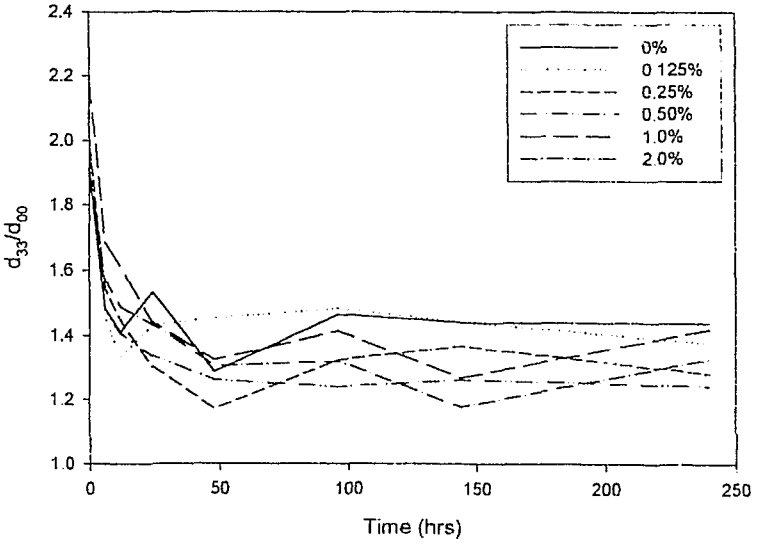

Figure 26: Ratio of d_{33} to d_{00} for W/O emulsions made with between 0 and 2.0% cottonseed stearine, crystallized following emulsification.

Reproduced with permission of the copyright owner. Further reproduction prohibited without permission.

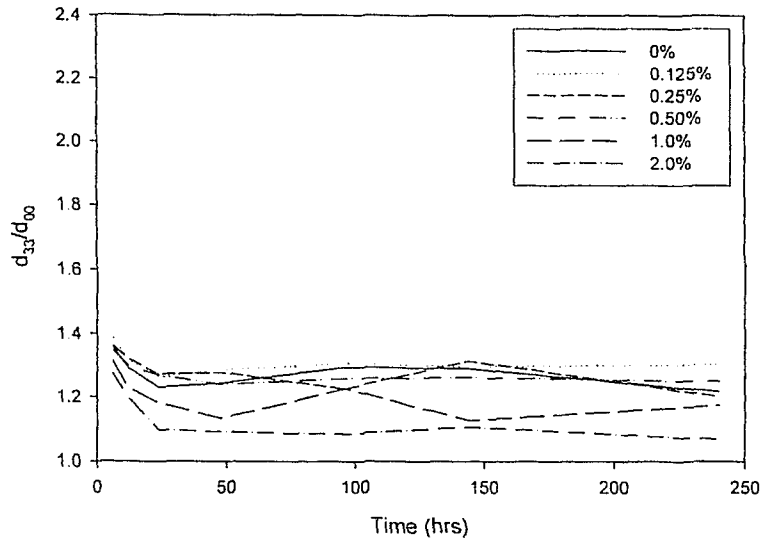

Figure 27: Ratio of d_{33} to d_{00} for W/O emulsions made with between 0 and 2.0% canola stearine, crystallized prior to emulsification.

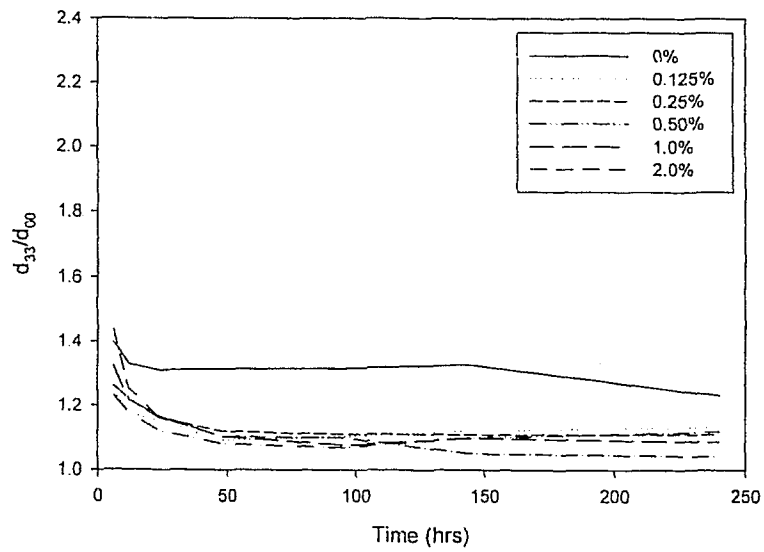

Figure 28: Ratio of d_{33} to d_{00} for W/O emulsions made with between 0 and 2.0% cottonseed stearine, crystallized prior to emulsification.

Reproduced with permission of the copyright owner. Further reproduction prohibited without permission.

ones were formed. This resulted in a less homogeneous crystal network. Consequently, the water droplets and the crystals themselves were freer to migrate and the result was the compact sediment observed.

Reproduced with permission of the copyright owner. Further reproduction prohibited without permission.

4 Polymorphic Behaviour of Hydrogenated Cottonseed Stearine

4.1 Introduction

The solidification of lipids from the melt is influenced by many factors. These factors include the composition of the lipids themselves, the tempering regime employed, the presence of other lipids or additives and the mechanical conditions to which the system is subjected (e.g. shear, agitation, etc.). In the industrial production of food lipid products these factors are controlled in order to achieve desired polymorphic and morphological properties. In the production of margarine, for example, to achieve a smooth texture and suitable spreadability, the β' polymorph must be the predominant crystal species. To accomplish this, fats that are naturally β'-stable may be used, or β-stable fats may be blended with non-β-tending fats. Additives, such as emulsifiers may also be used in the 0.1 to 0.5% (w/w) range to hinder the β' to β transition. Typical emulsifiers used for this purpose include monoacyglycerols and sorbitan tristearate. In chocolate products the polymorphic form of the continuous cocoa butter phase is critical to the products' organoleptic properties. Careful tempering is used to promote the production of the metastable β-V crystal form.

In lipid systems, kinetics will favour the formation of a metastable polymorph (i.e. often, but not exclusively, the α-form), while thermodynamics will favour the formation of more stable forms (such as β', but more often β). In accordance with the convention of Ostwald's law of stages, nucleation and growth of the metastable form will predominate initially. The majority of our understanding into these polymorphic transitions observed in fat systems has been based on observations of model systems composed of single triacylglycerols or simple

Reproduced with permission of the copyright owner. Further reproduction prohibited without permission.

mixtures. With respect to natural fats and natural fat blends many questions remain to be answered.

In the previous section, solid fat crystals were studied with regards to their effect on the kinetic stabilization of emulsions. One of the fats used for this purpose, namely hydrogenated cottonseed oil (HCSO), was found to behave in an unexpected manner with regards to its polymorphism. This section is the result of further investigations into this material. HCSO is commonly used as a β'-tending fat in margarine and shortening production. In this section it is shown that the final, (stable) polymorphic form and morphology can be dramatically modified through dilution, tempering, addition of polyglycerol polyricinoleate (PgPr) and conditions of static or dynamic crystallization.

4.2 Materials and Methods

Fully hydrogenated cottonseed oil (HCSO) and canola oil (CO) were as those used and characterized previously in Section 3.3.1. Both were used without further purification. The lipophilic emulsifier, Polyglycerol polyricinoleate (PgPr) was also used and described previously. PgPr is used in margarine production to stabilize fats in the β' polymorph. Solutions of 4% (w/w) HCSO in CO were crystallized from the melt to either 5°C or 25°C. Figure 29 shows typical cooling curves for HCSO crystallized under static conditions to each of the final temperatures. Cooling conditions were very similar for all samples whether crystallized with or without stirring or with or without the addition of PgPr. Stirring was achieved using a Rushton-type impellor at 240 rpm. PgPr was added at 0.25% (w/w).

Reproduced with permission of the copyright owner. Further reproduction prohibited without permission.

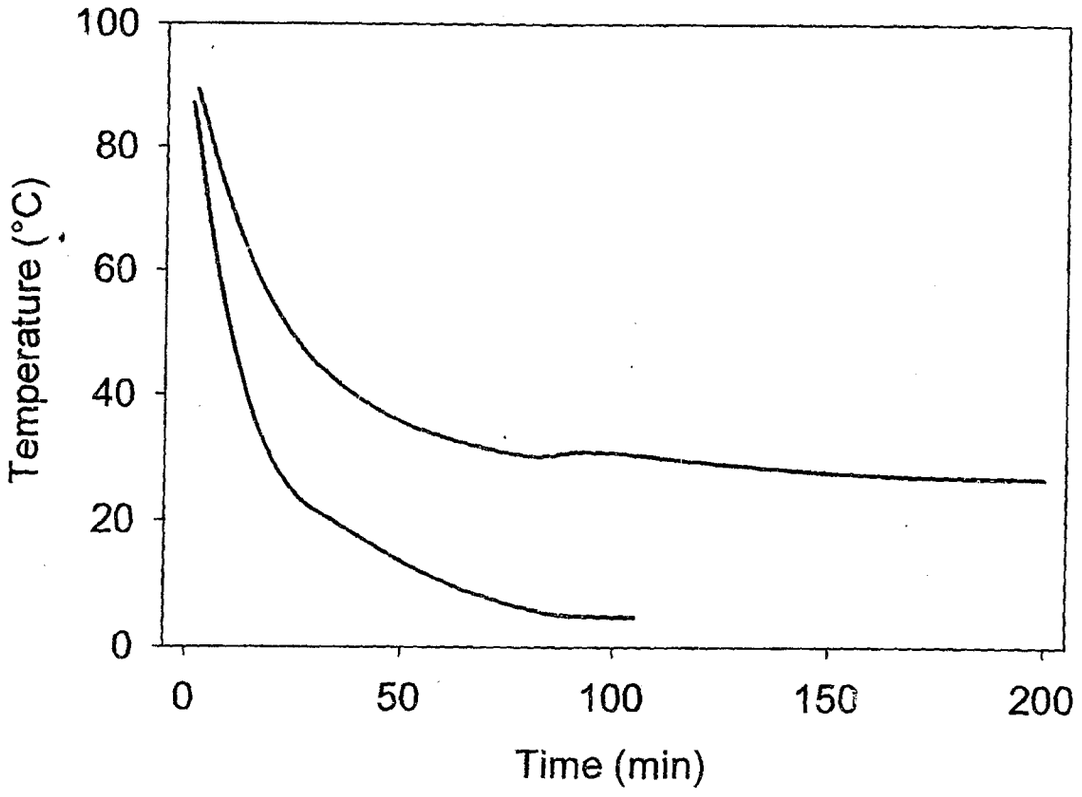

Figure 29: Cooling curves for 4% (w/w) HCSO from melt to 25°C (upper curve) and melt to 5°C (lower curve).

Reproduced with permission of the copyright owner. Further reproduction prohibited without permission.

Calorimetric data was obtained with a TA Instruments Q100 differential scanning calorimeter (DSC) (TA Instruments-Water LCC, New Castle, DE) equipped with a refrigerated cooling system. The instrument was calibrated using a gallium standard (Sigma-Aldrich Co., St. Louis, MO, 99.999%) and flushed with nitrogen at 15 mL/min. Thermal analysis was performed on 3 different sample types: 100% HCSO, 4% (w/w) HCSO in CO, and 4% (w/w) HCSO in CO with 0.125% (w/w) PgPr. Samples of approximately 4-5 mg were hermetically sealed in aluminum pans. An empty pan was used as a reference. Thermal cycles closely mimicking the cooling regimes shown in Figure 29 were performed. [1] Melt to 25°C: Samples were heated to 93°C, held for 5 min then cooled to 35°C at 1.25°C/min. Subsequently, they were cooled to 25°C at 0.07°C/min where they were held isothermally for 15 min. [2] Melt to 5°C: Samples were heated to 93°C and held for 5 min, were cooled to 25°C at 2.8°C/min then to 5°C at 0.25°C/min, where they were held isothermally for 60 min. Data were analyzed using the instrument software. All samples for each thermal cycle were measured in duplicate.

Polarized light microscopy (PLM) was used to examine the morphology of HCSO crystallized in CO. The equipment and methodology employed were as per Section 3.2.8.

Powder diffractograms were determined as per Section 3.2.5

4.3 Results and Discussion

4.3.1 Characterization of Base Materials

See Section 3.2.1 for TAG composition of the CO and HCSO used in this study. The SFC of 100% HCSO is described in Section 3.3.1. Further to this work, the crystallization and polymorphic behaviour of this material was determined. X-

Reproduced with permission of the copyright owner. Further reproduction prohibited without permission.

ray diffraction analysis of the polymorphism of the flake HCSO showed a very strong long spacing at 44.6Å, with corresponding medium and weak reflections at 14.98 and 9.01Å, respectively. The diffraction pattern also showed strong short spacings (Figure 30) of 3.79Å, 4.21Å and a doublet at 4.33Å/4.34Å. These results indicated that the flake HCSO existed as a double layer in the β'-form (β'-2) (Timms, 1984). The crystallization thermogram of 100% HCSO, obtained using DSC, showed a single peak at 48.21 +/- 0.04C with a corresponding enthalpy of 99.36 +/- 2.33 J/g (Figure 31). DSC results also showed a small shoulder peak, possibly corresponding to the crystallization of a second fraction, or a minor polymorphic transition. However, no β-form crystals were detected as a result of either cooling regime. HCSO Crystallization Behaviour

4.3.1.1 Cooling to 25°C.

Under this cooling profile, the crystallization of HCSO was affected very little by either agitation or the addition of PgPr. Table 5 shows that all short spacings were identical. Further, all 25°C samples existed in the β'-2 form and exhibited very strong reflections at 43.2Å. Lutton et al. (1948) showed that the first order reflection of PSP occurred at 42.8Å, whereas the first order reflection of β'-form SSS and PSS occurred at 46.8Å and 45.1Å. The observed β' diffraction pattern of diluted HCSO was dominated by PSP, not SSS and PSS.

Reproduced with permission of the copyright owner. Further reproduction prohibited without permission.

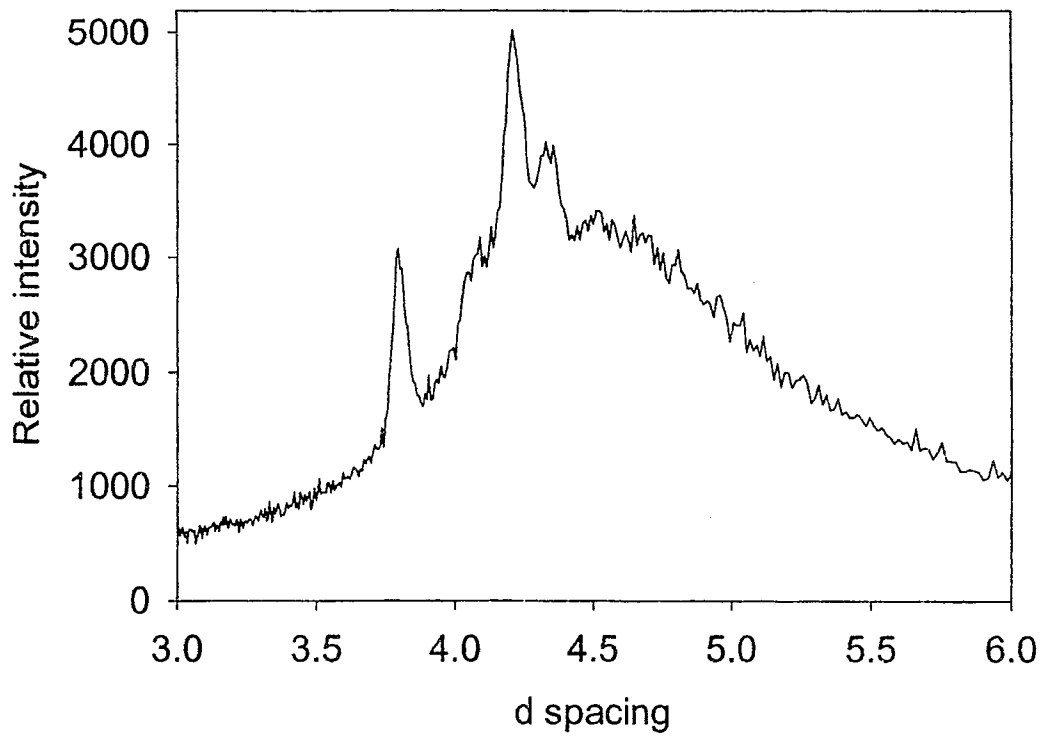

Figure 30: Short spacings of flake HCSO as evaluated by powder XRD.

Reproduced with permission of the copyright owner. Further reproduction prohibited without permission.

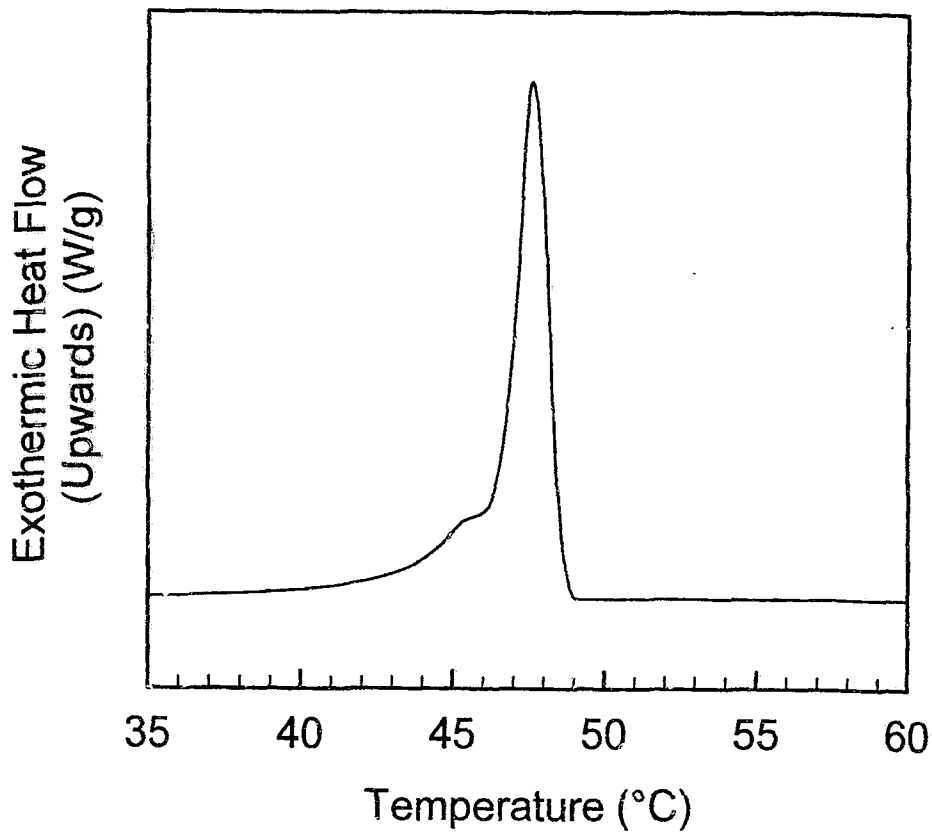

Figure 31: DSC thermogram showing cooling profile of 100% HCSO.

Reproduced with permission of the copyright owner. Further reproduction prohibited without permission.

Table 5: Long and short spacings for all samples crystallized from the melt to 25°C. (Legend: V: very; S: strong; M: medium; W: weak)

Long spacings	Short spacings
d(001) = 43.2VS	3.78S
d(003) =14.93M	4.06M
d(004) = 11.28VW	4.19VS
d(005) = 8.97W	4.33M

Polarized light microscopy (PLM) (Figure 32) showed that all samples crystallized to 25°C consisted of agglomerated crystal masses, varying with changes in the crystallization conditions. Figure 32A shows statically crystallized HCSO structures. These structures averaged about 50 μm in diameter and ranged in diameter from 15-150μm. Crystallization under agitation resulted in structures averaging approximately 100μm in diameter (Figure 32B). The borders of these structures were smoother than those of their statically crystallized counterparts. A similar effect was observed by Van Putte and Bakker (1987) with palm oil, where agitation resulted in the growth of smoother spherulites than those produced under static conditions. Samples crystallized under agitation exhibited a wide range in crystal sizes. Likely, this was a result of small crystals breaking off larger agglomerates and resulting in secondary growth (Timms, 1995). HCSO crystallized statically in the presence of PgPr (Figure 32C) resulted in agglomerates averaging about 40 μm in diameter, with well-defined edges. Combining agitation and PgPr (Figure 32D) resulted in large agglomerates approximately 100 μm in diameter, as well as smaller crystals resulting from agitation as mentioned earlier.

Reproduced with permission of the copyright owner. Further reproduction prohibited without permission.

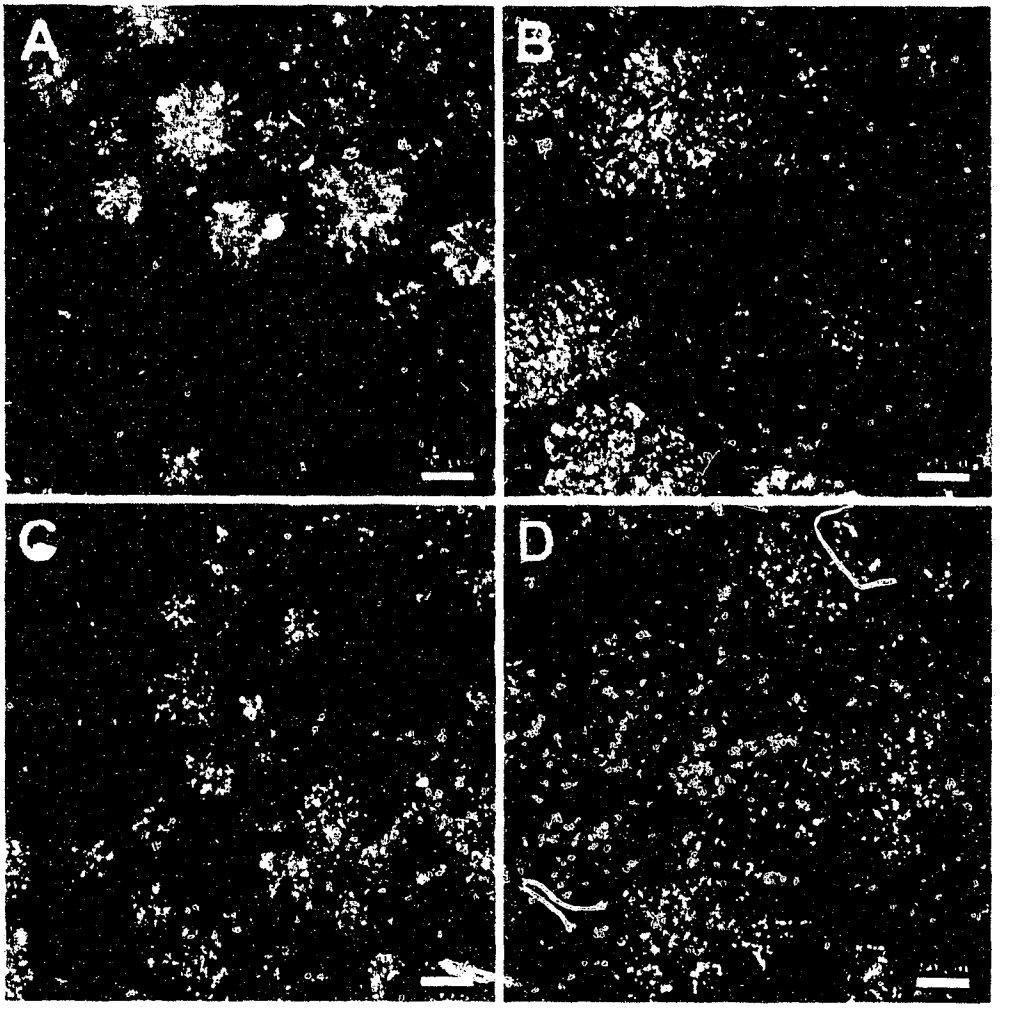

Figure 32: PLM images of 4% (w/w) HCSO in canola oil crystallized at 25°C. A) Static crystallization; B) Crystallization with agitation; C) Static crystallization with PgPr; D) Crystallization with agitation and PgPr.

Reproduced with permission of the copyright owner. Further reproduction prohibited without permission.

4.3.1.2 Cooling to 5°C

Cooling samples to 5°C resulted in substantial differences in polymorphic behaviour and crystal morphology. In all cases, the crystals generated under these conditions of greater supercooling were smaller and of increased number compared those formed at 25°C.

The long spacings for HCSO crystallized to 5°C with and without agitation (no PgPr added) had d(001) reflections that were approximately 1Å (Table 6) larger than their 25°C counterparts.

Table 6: Long spacings for samples crystallized from the melt to 5°C. Abbreviations as per Table 1.

	Static crystallization	Sheared crystallization
No PgPr	d(001) = 44.60VS d(003) =14.77M d(005) = 8.86W d(006) = 7.34VW	d(001)= 44.60VS d(003) =14.77M d(005) = 8.71VW
PgPr	d(001) = 43.65VS d(003) =14.77M d(004) = 10.81VW d(005) = 8.78W d(006) = 7.29W	d(001) = 41.87VS d(003) =14.56M d(005) = 8.82W d(006) = 7.27VW

Crystallization under static conditions with PgPr produced crystals with a 1Å decrease in the d(001) reflection. The combination of agitation and PgPr resulted in a ~3Å decrease in lamellar thickness compared to the HCSO crystallized under static conditions, free of PgPr. According to Lutton et al. (1948), the first order reflection of SSS occurred at 45.15Å, while the first order reflection of PSS occurred at 44.7Å. Thus, the β-indicative diffraction pattern of the diluted HCSO was dominated by these two TAG species and not PSP.

Reproduced with permission of the copyright owner. Further reproduction prohibited without permission.

The short spacings observed provided much information about the crystallization behaviour of HCSO (Figure 33). When HCSO was statically crystallized, with and without PgPr, the results were similar and indicated strong β-crystal spacings at 3.69, 3.86 and 4.59Å. There was also a peak in the 5.25-5.35Å region. Lutton et al. (1948) showed that SSS when in the β-form was partly characterized by a peak of medium intensity at 5.24Å, while PSS when present in the β-form demonstrated a reflection at 5.34Å. Thus it appears that these short spacing represent a combined effect of SSS and PSS. When crystallized with agitation the HCSO spectrum was similar in form but with a reduced intensity possibly suggesting a "destructuring" of the crystal structure. The combination of both PgPr and agitation during crystallization produced dramatic changes in the short spacings. The reflection at 3.69Å disappeared, and the peaks at 3.86 and 4.59 Å shifted to peaks at 3.82Å and 4.55Å. There was also a large hump observed in the 4.02-4.40Å region. These observations suggest the simultaneous existence of alpha, β' and β forms. The short spacings for HCSO crystallized at 25°C are shown for comparison.

Polarized light microscopy of samples crystallized at 5°C (Figure 34) showed spherulitic crystal morphology for all samples. These spherulites were smaller than those produced via cooling to 25°C being about 15-20 μm in size. Spherulites crystallized with agitation and PgPr appeared denser than those produced via other treatments.

Reproduced with permission of the copyright owner. Further reproduction prohibited without permission.

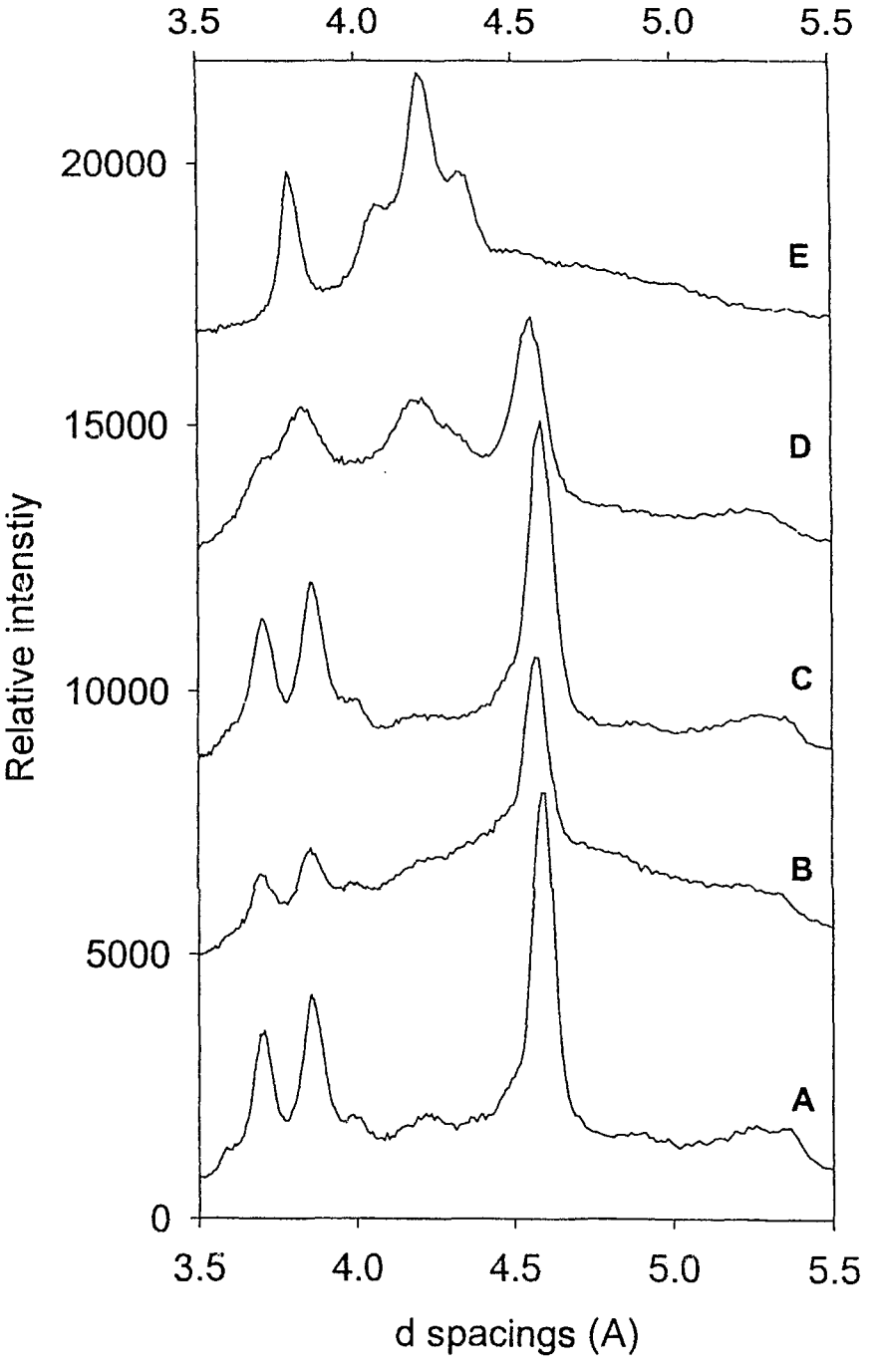

Figure 33: Short spacings of 4% (w/w) HCSO crystallized to 5°C. A) Static crystallization; B) Crystallization with agitation; C) Static crystallization with PgPr; D) Crystallization with agitation and PgPr; E) Putative results from 25°C crystallization.

Reproduced with permission of the copyright owner. Further reproduction prohibited without permission.

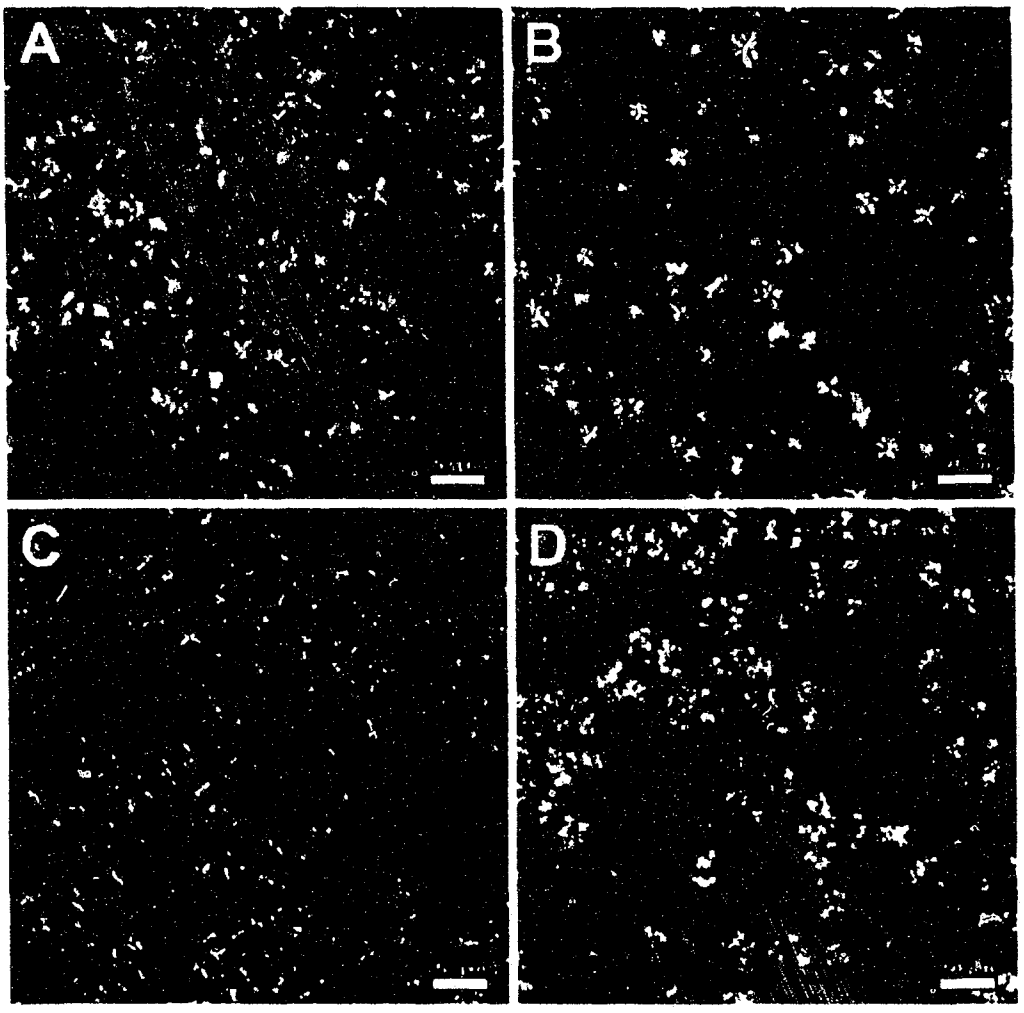

Figure 34: PLM images of 4% (w/w) HCSO in canola oil crystallized at 5°C. A) Static crystallization; B) Crystallization with agitation; C) Static crystallization with PgPr; D) Crystallization with agitation and PgPr.

Reproduced with permission of the copyright owner. Further reproduction prohibited without permission.

4.3.2 Mechanistic Considerations

Often in processed foods a fat will be mixed with an oil to obtain specific physical and rheological properties. Upon dilution many naturally occurring fats are kinetically driven to their most stable polymorphic form (deMan *et al.*, 1995; Gray, 1976; Rousseau *et al.*, 1996). When allowed to do so, crystals will normally adopt their most thermodynamically stable state. With the diluted HCSO, it would have been expected that the lipid molecules would adopt the more favourable β-form. As shown earlier, 100% HCSO is stable in the β' form, however, upon dilution in canola oil, it can be crystallized into stable β' or β-form crystals. It is thus left to determine how dilution influences this β' to β transition. One possibility would be that the canola oil is introduced into the crystal lattice, however, this is unlikely. Norton *et al.* (1985) showed that triolein (OOO) oil does not incorporate itself into the lattice of tripalmitan (PPP) when it is diluted in the latter and crystallized. This incompatibility may be explained, at least in part, by the curved *cis* bonds present in the oleic hydrocarbon chains of OOO that would not fit into the lattice of the crystallizing TAGs (Elisabettini, 1995). All the same, dilution should allow TAGs of HCSO to more freely rotate and adopt a lower energy thus enabling a β' to β polymorphic transition. With 100% HCSO irregularities in chain length create an energy barrier against crystallization that is larger than that encountered in pure TAGs (Larsson, 1971). HCSO is composed of both PSP (β'-stable) and SSS/PSS (β-stable), and as such there may be segregation of these two TAG classes explaining the broad first order long spacings (Hernqvist, 1988). The results also suggested rotational freedom is very limited in the 100% HCSO where the PSP, which is β'-stable, prevents the β' to β transformation. Conversely, in the diluted system, where the total SFC is

Reproduced with permission of the copyright owner. Further reproduction prohibited without permission.

limited to 4%, the PSP was not able to prevent this β' to β transition and the SSS and PSS species could therefore phase separate and crystallize in their most thermodynamically favourable conformation, the β-form.

The cooling regime, in addition to the dilution effect, played a significant role in determining the polymorphic pathway. Neither cooling regime represented quench-cooling, as the rates were far too slow for this designation. However, cooling to 25°C would nonetheless have presented conditions of lower supersaturation than the 5°C regime. With lower degrees of supersaturation TAGs should have more time to find a stable crystal configuration. Generally, under conditions of higher supercooling molecules attach themselves more quickly and more irreversibly, resulting in less perfect and less stable crystals.

Undiluted HCSO was found to be β'-stable regardless of cooling regime. It would be expected that cooling slowly to 25°C would result in a more stable polymorph, while cooling more quickly to 5°C might result in a metastable polymorph that would then undergo a solid state transformation to a more stable form.

However, when diluted and cooled more quickly to 5°C, HCSO formed a β-stable polymorph, while cooling more slowly resulted in the formation of a β'-stable form. DSC of the crystallization of diluted HCSO shows that a β' to β transition is not visible at 25°C (Figure 35A), but is observed when cooling to 5°C (Figure 35B). In this case it is seen to occur as a solid-state transformation. The enthalpy of crystallization was 4.3-5.2 J/g for all events. No α-form crystallization was observed in either scenario, indicating that crystallization occurred directly into the β' form. In a study of numerous hydrogenated fats, Riiner (1970) noted a similar phenomenon.

Reproduced with permission of the copyright owner. Further reproduction prohibited without permission.

Gibon et al. (1986) found in a study on the intersolubility of PSP, POP and SSS, that when the β' form was crystallized via the α-form it was less stable than when crystallized directly from the melt. This was attributed to crystal perfection. In the present study, cooling to 25°C resulted in the formation of a highly ordered β' form, whereas cooling more quickly to 5°C resulted in a poorly formed β' that quickly transformed to β.

PgPr and agitation had little effect on HCSO crystallization. When cooling to 25°C, HCSO crystal dimensions were not affected by agitation or PgPr, though agitation did promote larger crystal agglomerates. As PgPr addition did not affect short or long spacings, it was likely not incorporated into the lattice. Similar results were obtained when cooling to 5°C, with the exception of agitation combined with PgPr. It is possible that PgPr incorporation slowed the alpha to β' to β transformation. Agitation may allow PgPr to be incorporated by means of nanoscopic inclusions (being indiscernible by PLM) into the forming crystals.

Reproduced with permission of the copyright owner. Further reproduction prohibited without permission.

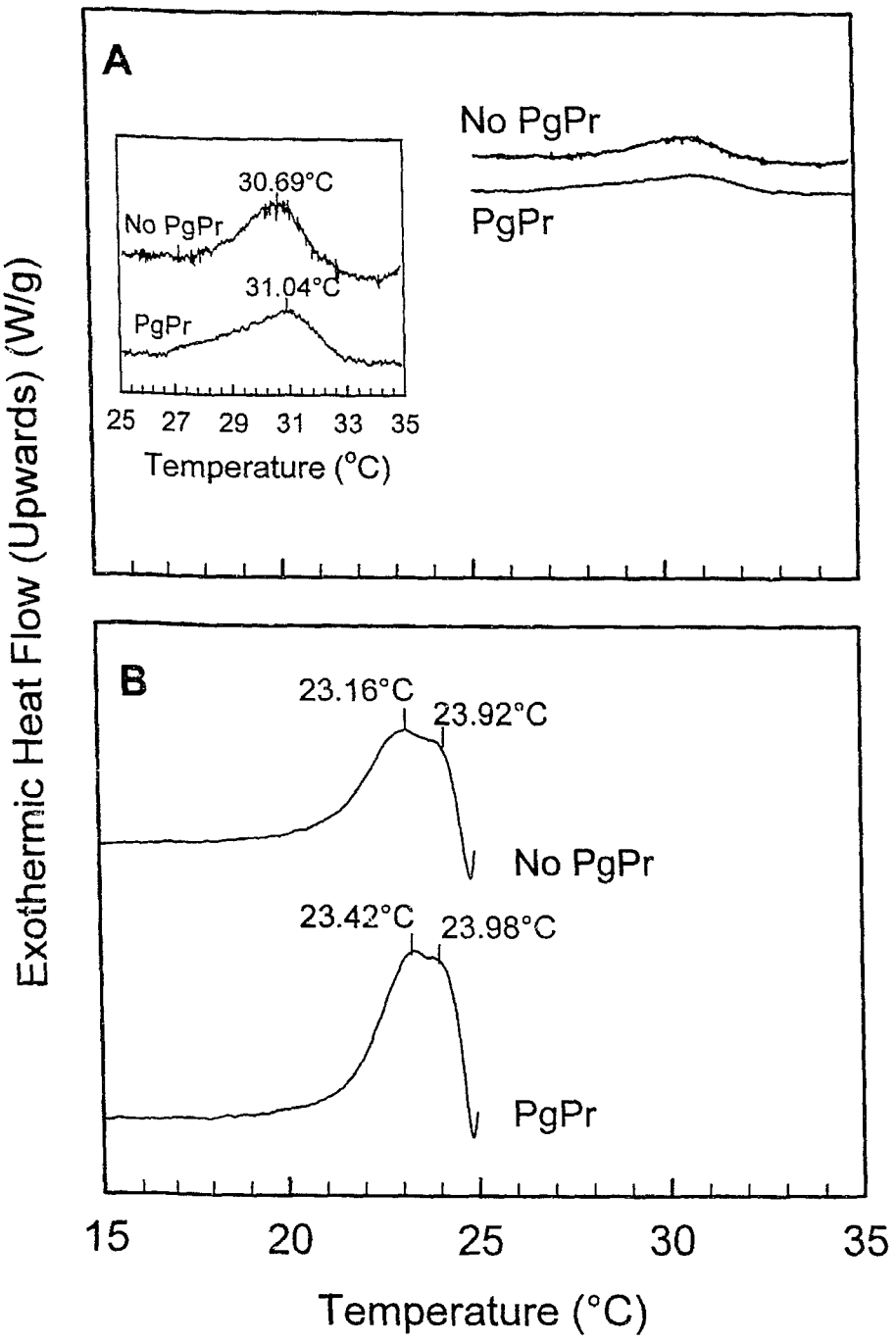

Figure 35: DSC thermograms of 4% (w/w) HCSO with and without addition of PgPr. A) melt to 25°C; B) melt to 5°C.

Reproduced with permission of the copyright owner. Further reproduction prohibited without permission.

5 Conclusions

This study investigated the stabilization of water in oil emulsions through the addition of solid phase crystals of wax or fat. Stability was assessed based on sedimentation, flocculation and coalescence behaviour. It was demonstrated that small quantities of solid particles were able to effectively stabilize these emulsions. Two main types of systems were considered; a basic, model system, and a real world, or applied system. The factors affecting the ability of these crystals to stabilize emulsions were the crystal structure of the solid wax or fat phase, the wetting behaviour of the solid and the concentration of the solid phase. These findings are relevant to the disciplines of food, pharmaceutical and crude oil sciences.

Reproduced with permission of the copyright owner. Further reproduction prohibited without permission.

6 References

AOCS. Official Methods and Recommended Practices of the American Oil Chemists' Society, 5th ed.; AOCS, Champaign, IL, 1997.

Atkins, P.W. Changes of state: physical transformation of pure substances. *Physical Chemistry;* 4th ed.; W.H. Freeman and Company: New York, NY, 1990; Chapter 6, 147-148.

Bergenståhl, B. Topics in Food Emulsions. Ph.D. Thesis. Institute for Surface Chemistry, Stockholm, Sweden, and Department of Food Technology, Lund University, Lund, Sweden, 1994.

Bruker Analytische Messtechnik Gmbh. Instruction manual: droplet size analysis in water-in-oil emulsions using nuclear magnetic resonance (NMR). 2000 Karlsruhe.

Bucheim, W.; Dejmek, P. Milk and dairy-type emulsions. In *Food Emulsions,* 3rd ed.; Friberg S.E.; Larsson, K. Eds.; Marcel Dekker: New York, NY, 1997; pp. 235-278.

Chang, M.-K.; Abraham, G.; John, V.T. Production of cocoa butter-like fat from interesterification of vegetable oils. *J. Am. Oil Chem. Soc.* **1990,** *67,* 832-834.

Darling, D.F. Recent advances in the destabilization of dairy emulsions. *J. Dairy Res.* **1982,** *49,* 695-712.

deMan, L.; deMan, J.M.; Blackman, B. Effect of tempering on the texture and polymorphic behaviour of margarine fats. *Fat Sci. Technol.* **1995,** *97,* 55-60.

Dickinson, E. Structure and composition of adsorbed protein layers and the relationship to emulsion stability. *J. Chem. Soc., Faraday Trans.* **1992,** *88,* 2973-2983.

Reproduced with permission of the copyright owner. Further reproduction prohibited without permission.

Edwards, D.A.; Wasan, D.T. A micromechanical model of linear surface rheological behavior. *Chem. Eng. Sci.* **1991**, *46*, 1247-1257.

Elisabettini, P.; Desmedt, A.; Gibon, V.; Durant, F. Effect of sorbitan tristearate on the thermal and structural properties of monoacid triglycerides – influence of a "cis" or "trans" double bond. *Fat. Sci. Technol.* **1995**, *97*, 65-69.

Fourel, I.; Guillement, J.P.; Le Botlan, D. Determination of water droplet size distributions by low resolution PFG-NMR: I. "Liquid" emulsions. *J. Colloid Interface Sci.* **1994**, *164*, 48-53.

Fourel, I.; Guillement, J.P.; Le Botlan, D. Determination of water droplet size distributions by low resolution PFG-NMR: II. "Solid" emulsions. *J. Colloid Interface Sci.* **1995**, *169*, 119-125.

Friberg, S.E. Emulsion stability. In *Food Emulsions*, 3rd ed.; Friberg S.E.; Larsson, K. Eds.; Marcel Dekker: New York, NY, 1997; pp 1-56.

Garti, N.; Aserin, A.; Tiunova, I.; Benyamin, H. Double emulsions of W/O/W stabilized by fat microcrystals. Part I. Selection of emulsifiers and fat microcrystalline particles. *J. Am. Oil Chem. Soc.* **1999** *76* (3), 383-389.

Gibon, V.; Durant, F.; Deroanne, C. Polymorphism and intersolubility of some palmitic, stearic and oleic triglycerides: PPP, PSP and POP. *J. Am. Oil Chem. Soc.* **1986**, *63*, 1047-1055.

Gray, M.S.; Lovegren N.V.; Feuge, R.O. Effect of 2-oleodipalmitin and 2-elaidopalmitin on polymorphic behavior of cocoa butter. *J. Am. Oil Chem. Soc.* **1976**, *53*, 727-731.

Reproduced with permission of the copyright owner. Further reproduction prohibited without permission.

Good, R.J.; Contact angles and the surface free energy of solids. In *Surface and Colloid Science*, Vol. 2.; Good, R.J.; Stromberg, R.R. Eds.; Plenum Press, New York, NY, 1979, pp 1-30.

Hernqvist, L. On the crystal structure of the β_1'-form of triglycerides and the mechanism behind the $\beta_1' \rightarrow \beta$ transition of fats. *Fat Sci. Technol.* **1988**, *90*, 451-454.

Hodge, S.M.; Rousseau, D. Flocculation and Coalescence in Water-in-Oil Emulsions Stabilized by Paraffin Wax Crystals. *Food Research International*, **2003**, *36* (7), 695-702.

Johansson, D.; Bergenståhl, B. Lecithins in oil-continuous emulsions. Fat crystal wetting and interfacial tension. *J. Am. Oil Chem. Soc.* **1995a**, *72* (2), 205-211.

Johansson, D.; Bergenståhl, B. Wetting of fat crystals by triglyceride oils and water. 1. The effect of additives. *J. Am. Oil Chem. Soc.* **1995b**, *72* (8), 921-930.

Johansson, D.; Bergenståhl, B. Wetting of fat crystals by triglyceride oil and water. 2. Adhesion to the oil/water interface. *J. Am. Oil Chem. Soc.* **1995c**, *72* (8), 933-938.

Johansson, D.; Bergenståhl, B.; Lundgren, E. Water-in-triglyceride oil emulsions. Effect of fat crystals on stability. *J. Am. Oil Chem. Soc.* **1995d**, *72* (8), 939-950.

Johansson, D. Weak gels of fat crystals in oils at low temperatures and their fractal nature. *J. Am. Oil Chem. Soc.* **1995e**, *72* (10), 1235-1237.

Krog, N.; Larsson, K. Crystallization at interfaces in food emulsions – a general phenomenon. *Fat Sci. Technol.* **1992**, *94*, 55-57.

Larsson, K. Hydrocarbon chain conformation in fats. *Chemica Scripta* **1971**, *1*, 21-23.

Reproduced with permission of the copyright owner. Further reproduction prohibited without permission.

Lee, R. F. Agents which promote and stabilize water-in-oil emulsions. *Spill Science and Technology Bulletin* **1999,** *5* (2), 117-126.

Levine, S., Bowen, B.D.; Partridge, S.J. Stabilization of emulsions by fine particles I. Partitioning of particles between continuous phase and oil/water interface. *Colloids Surf.* **1989,** *38,* 325-343.

Lucassen-Reynders, E.H. Stabilization of water in oil emulsions by solid particles. Ph.D. Thesis, Wageningen Agricultural University, The Netherlands, 1962.

Lucassen-Reynders, E.H.; van den Tempel, M. Stabilization of water-in-oil emulsions by solid particles. *J. Phys. Chem.* **1963,** *67,* 731-734

Lucassen-Reynders, E.H. Interfacial viscoelasticity in emulsions and foams. *Food Structure* **1993,** *12,* 1-12.

Lutton, E.S.; Jackson, F.L.; Quimby, O.T. The polymorphism of the mixed triglycerides of palmitic and stearic acids. *J. Am. Chem. Soc.* **1948,** *70,* 2441-2445.

McClements, D.J. Emulsion Stability. In *Food Emulsions: Principles, Practice, and Techniques;* McClements, D.J.; Ed.; CRC Press: New York, NY, 1999; pp 185-234.

McClements, D.J.; Demetriades, K.J. An Integrated Approach to the Development of Reduced-Fat Food Emulsions. *Crit. Rev. Food Sci. Nutr.* **1998,** *38* (6), 511-536.

Norton, I.T.; Lee-Tuffnell, C.D.; Ablett S.; Bociek, S.M. A calorimetric, NMR and X-ray diffraction study of the melting behavior of tripalmitin and tristearin and their mixing behavior with triolein. *J. Am. Oil Chem. Soc.* **1985,** *62,* 1237-1244.

Reproduced with permission of the copyright owner. Further reproduction prohibited without permission.

Ogden L.G.; Rosenthal, A.J. Interactions between fat crystal networks and sodium caseinate at the sunflower oil-water interface. *J. Am. Oil Chem. Soc.* **1998,** *75*, 1841-1847.

Pickering, S.U. Emulsions. *J. of the Am. Chem. Soc.* **1907,** *91*, 2001-2021.

Reinders, W. Die verteilung eines suspendieiten pulvers oder eines eines kolloid gelösten Stoffes Zwischen Zwe. *Lösungmitteln*, **1913**.

Riiner, U. Investigation of the polymorphism of fats and oils by temperature programmed X-ray diffraction. *Lebenss.-Wiss. Technol.* **1970,** *3*, 101-106.

Rousseau, D.; Forestière, K.; Hill, A.R.; Marangoni, A.G. Restructuring butter fat through blending and chemical interesterification. 1. Melting behavior and triacylglycerol modifications. *J. Am. Oil Chem. Soc.* **1996,** *73*, 963-972.

Rousseau, D. Fat crystals and emulsion stability – a review. *Food Research International*, **2000,** *33*, 3-14.

Schulman, J.H.; Leja, J. Control of contact angles at the oil-water-solid interfaces. Emulsions stabilized by solid particles (BaSO4). *Trans. Faraday Soc.* **1954,** *18*, 598-605.

Swaisgood, H.E. Characteristics of milk. In *Food chemistry;* 3rd ed.; Fennema, O.R., Ed.; Marcel Dekker: New York, NY, 1996.

Tambe, D.E.; Sharma, M.M. Factors controlling the stability of colloid-stabilized emulsions. I. An experimental investigation. *J. Colloid Interface Sci.* **1993,** *157*, 244-253.

Tanner, J.E.; Stejskal, E.O. Restricted self-diffusion of protons in colloidal systems by the pulsed-gradient, spin-echo method. *J. Chem. Phys.* **1968,** *49* (4), 1768-1777.

Reproduced with permission of the copyright owner. Further reproduction prohibited without permission.

Thompson, D.G.; Taylor, A.S.; Graham, D.E. Emulsification and demulsification related to crude oil production. *Colloids Surf.* **1985,** *15*, 175-189.

Timms, R.E. Phase behavior of fats and their mixtures. *Prog. Lipid Res.* **1984,** *23*, 1-38.

Timms, R.E. Crystallization of Fats. In *Developments in Fats and Oils;* Hamilton, R.J. Ed.; Blackie Academic and Professional: New York, NY, 1995; pp 204-223.

Van Boekel, M.A.J.S. Influence of fat crystals in the oil phase on stability of oil-in-water emulsions. Ph.D. Thesis, Wageningen Agricultural University, The Netherlands, 1980.

Van Putte, K.P.A.M.; Bakker, B.H. Crystallization kinetics of palm oil. *J. Am. Oil Chem. Soc.* **1987,** *64*, 1138-1143.

Walstra, P. Dispersed systems: Basic consideration. In *Food Chemistry;* 3rd ed., Fennema, O.R., Ed.; Marcel Dekker: New York, NY, 1996; Chapter 3.

Walstra, P. *Physical Chemistry of Foods;* Marcel Dekker: New York, NY, 2003.

Wilson, R.; Van Schie, B. J.; Howes D. Overview of the preparation, use and biological studies on polyglycerol polyricinoleate (PGPR). *Food Chem. Toxicol.* **1998,** *36*, 711-718.

Young, T. (1855). In Peacock, G. (ed.). Miscellaneous works. London: Murray. [In Menon, V.B. & Wasan, D.T. (1988). Characterization of oil-water interfaces containing finely divided solids with applications to the coalescence of water-in-oil emulsions: a review. *Colloids Surf., 29*:7-27.]

Reproduced with permission of the copyright owner. Further reproduction prohibited without permission.

7 Appendices

7.1 Appendix A

Reproduced with permission of the copyright owner. Further reproduction prohibited without permission.

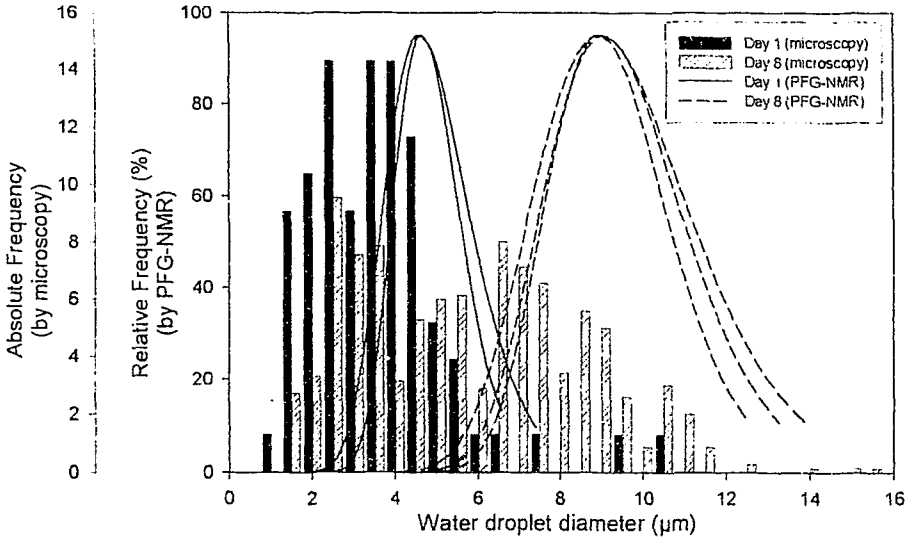

Figure A1: Comparison of W/O emulsion droplet size distributions obtained from PFG-NMR and drop counting of microscope images. Both water and oil phases unstained (i.e. X/X).

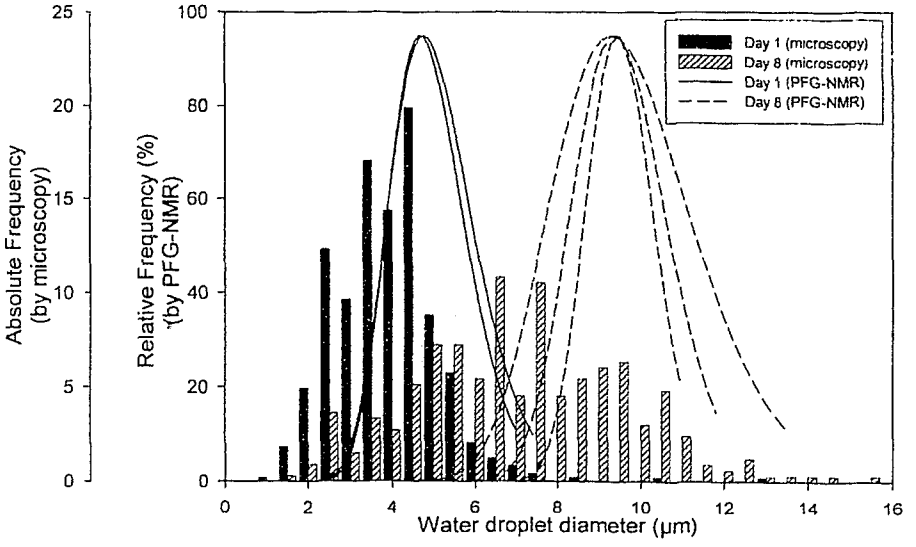

Figure A2: Comparison of W/O emulsion droplet size distributions obtained from PFG-NMR and drop counting of microscope images. Water phase stained with 0.01% Rhodamine B dye; Oil phase unstained (i.e. D/X).

Reproduced with permission of the copyright owner. Further reproduction prohibited without permission.

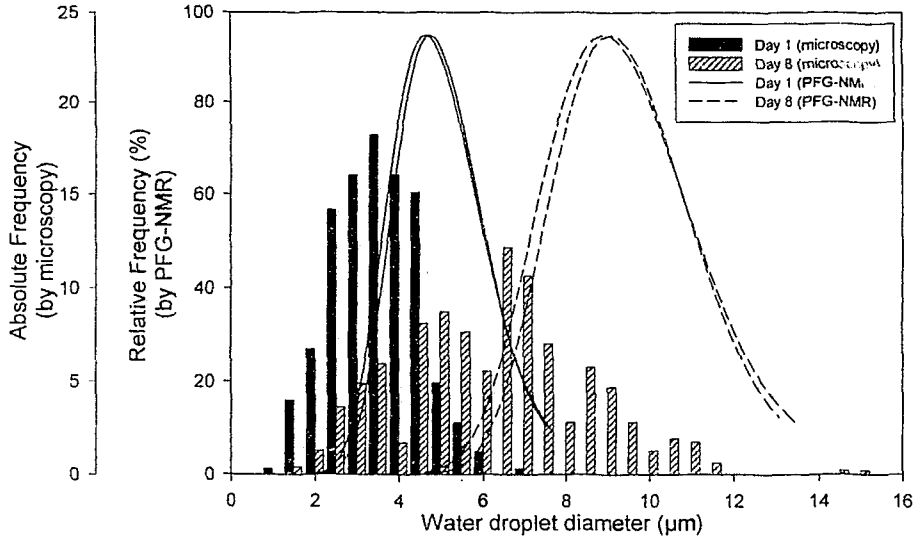

Figure A3: Comparison of W/O emulsion droplet size distributions obtained from PFG-NMR and drop counting of microscope images. Water phase unstained; Oil phase stained with 0.01% Fluorol Yellow 088 (i.e. X/D).

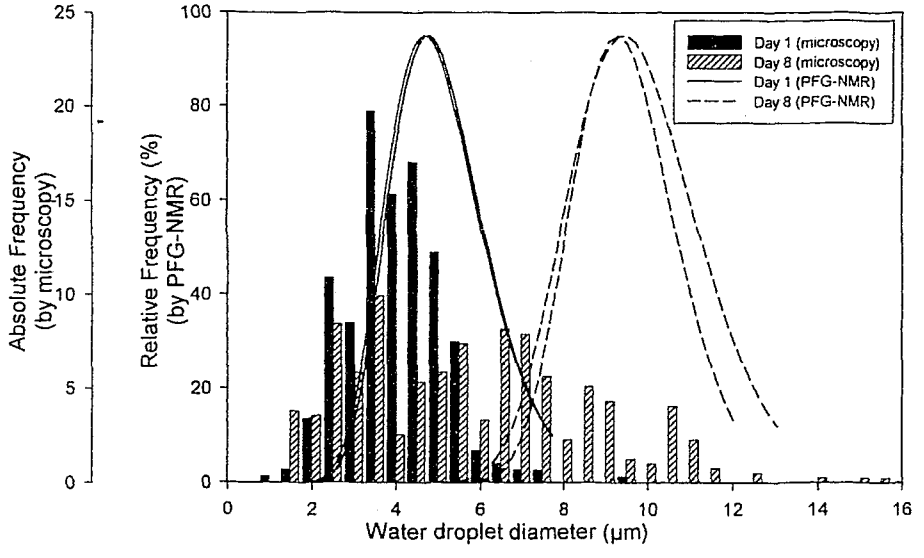

Figure A4: Comparison of W/O emulsion droplet size distributions obtained from PFG-NMR and drop counting of microscope images. Water phase stained with 0.01% Rhodamine B dye; Oil phase stained with 0.01% Fluorol Yellow 088 (i.e. D/D).

Reproduced with permission of the copyright owner. Further reproduction prohibited without permission.

7.2 Appendix B

Reproduced with permission of the copyright owner. Further reproduction prohibited without permission.

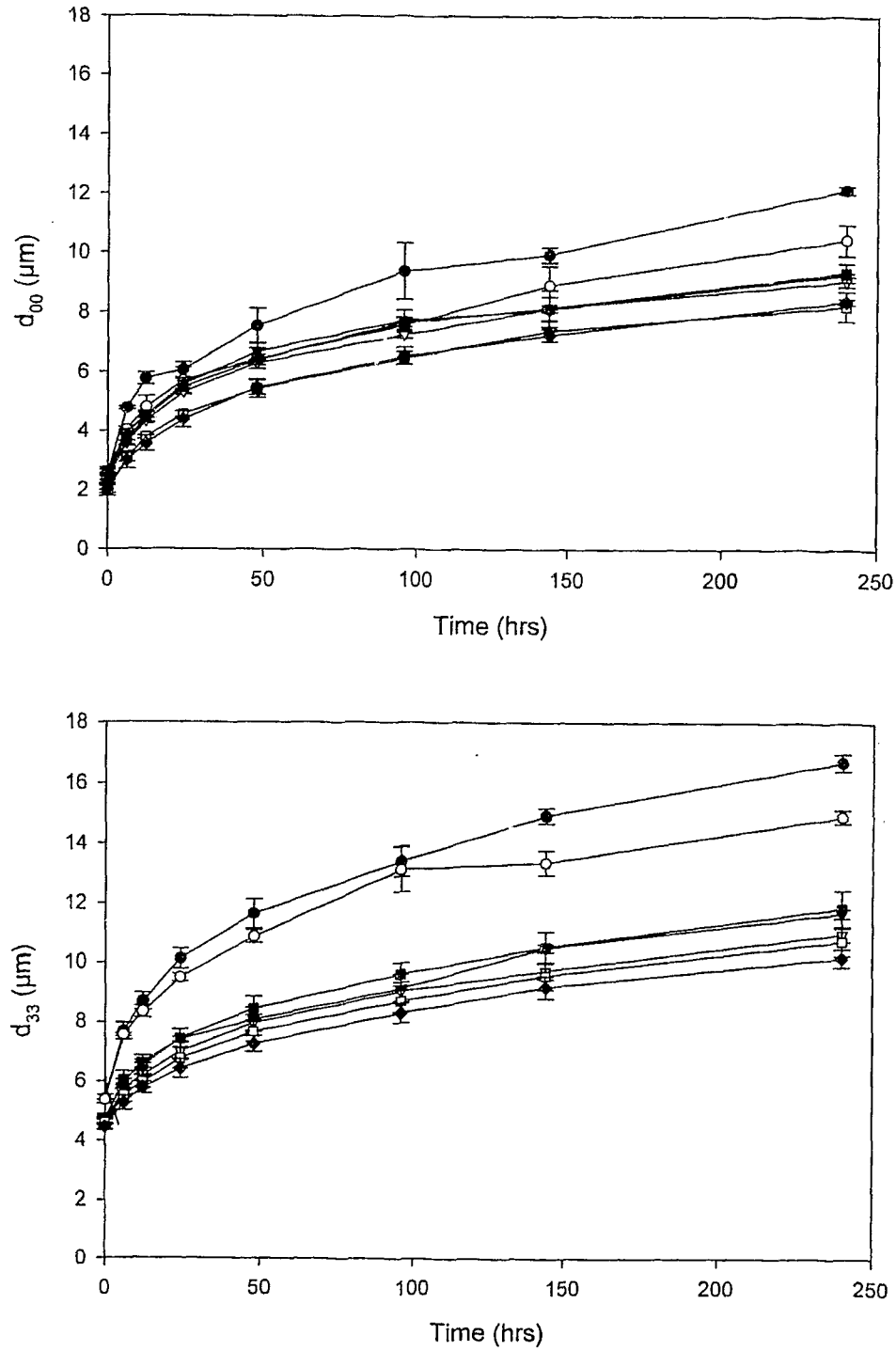

Figure B1: Evolution of droplet coalescence as measured by d_{00} (top) and d_{33} (lower) for samples containing canola stearine. Solid fat crystallized following emulsification. 0% solid fat (●), 0.125% (○), 0.25% (▼), 0.50% (▽), 1.0% (■), 2.0% (□).

Reproduced with permission of the copyright owner. Further reproduction prohibited without permission.

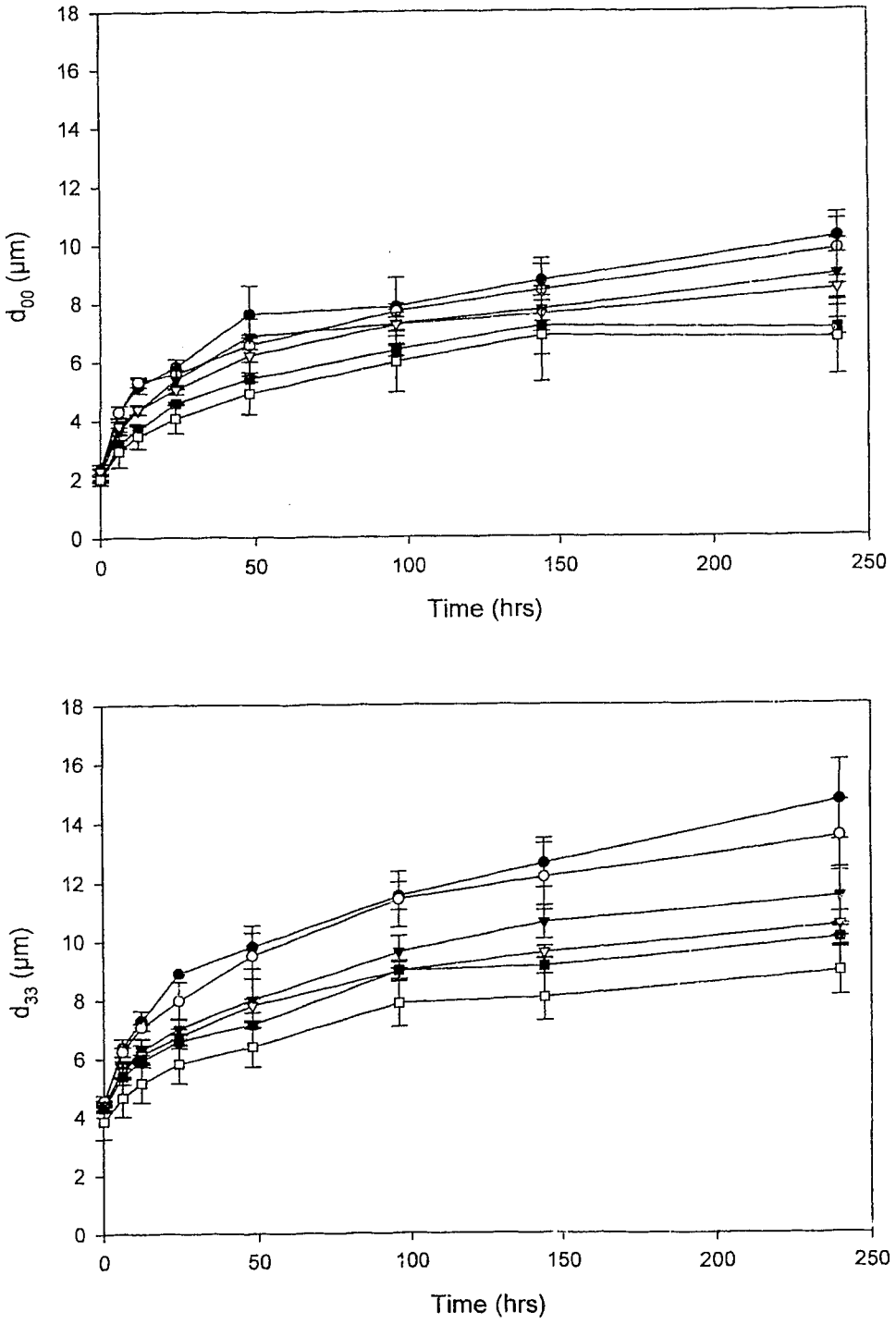

Figure B2: Evolution of droplet coalescence as measured by d_{00} (top) and d_{33} (lower) for samples containing cottonseed stearine. Solid fat crystallized following emulsification. 0% solid fat (●), 0.125% (○), 0.25% (▼), 0.50% (▽), 1.0% (■), 2.0% (□).

Reproduced with permission of the copyright owner. Further reproduction prohibited without permission.

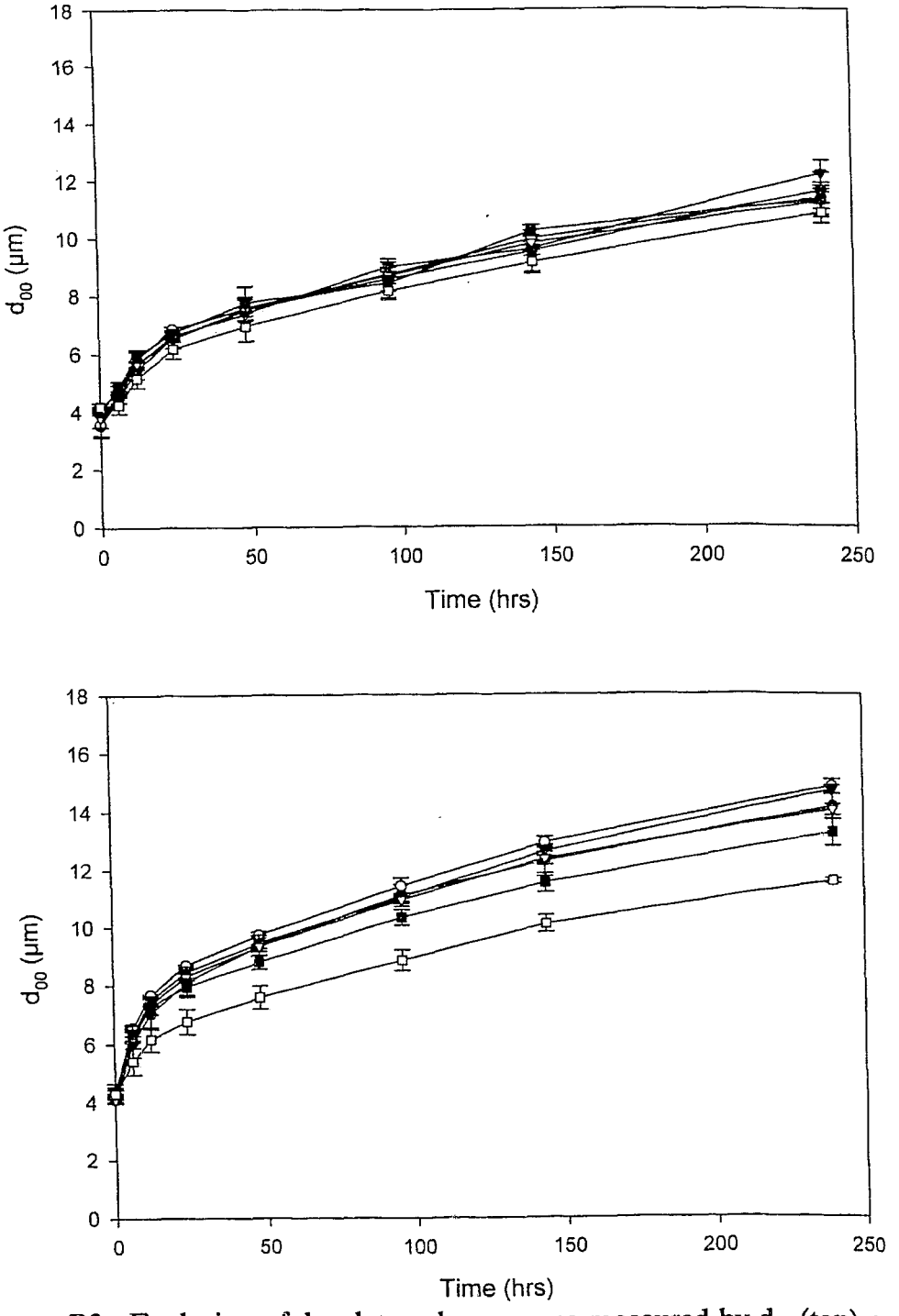

Figure B3: Evolution of droplet coalescence as measured by d_{00} (top) and d_{33} (lower) for samples containing canola stearine. Solid fat crystallized prior to emulsification in the absence of PgPr. 0% solid fat (●), 0.125% (○), 0.25% (▼), 0.50% (○), 1.0% (■), 2.0% (□).

Reproduced with permission of the copyright owner. Further reproduction prohibited without permission.

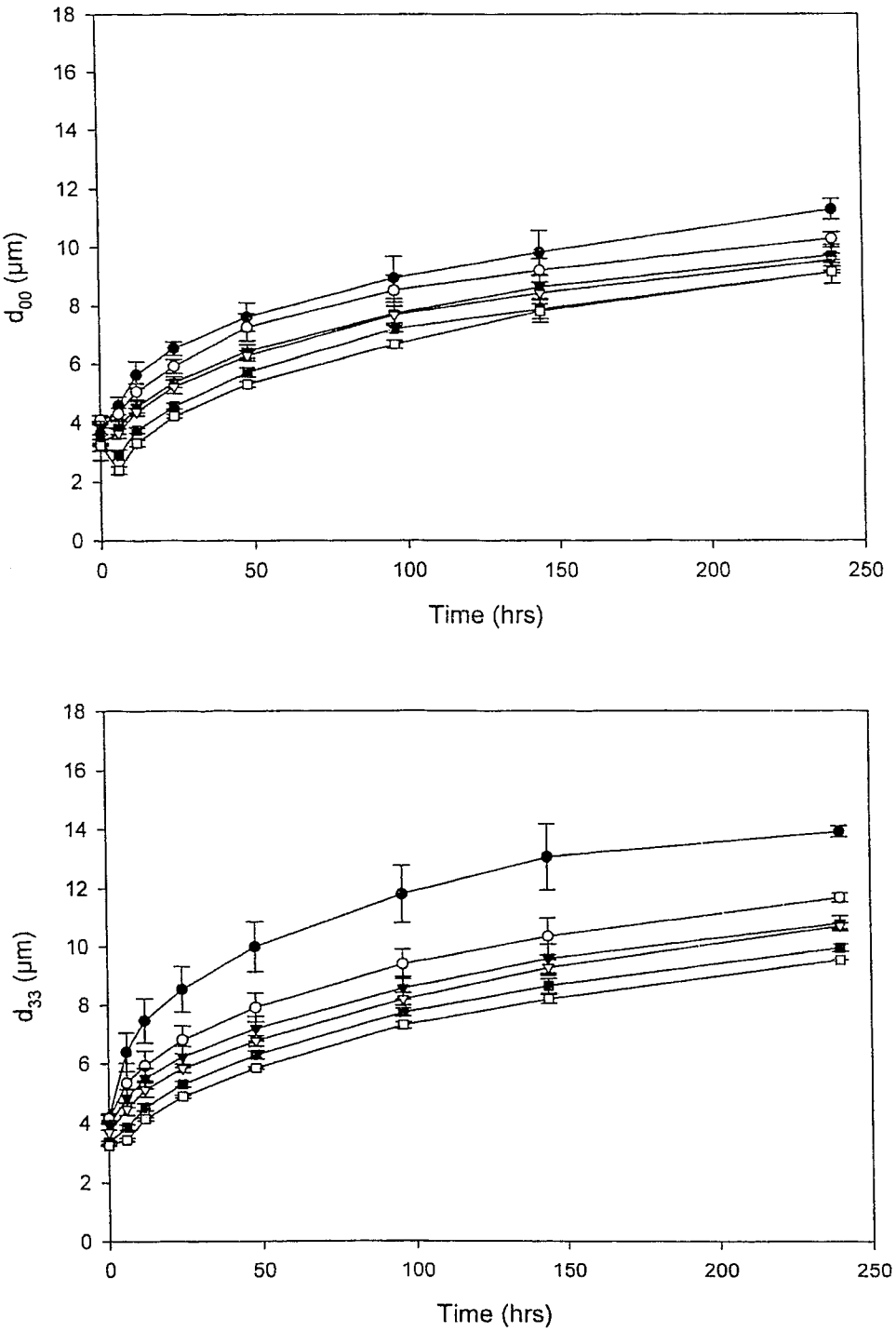

Figure B4: Evolution of droplet coalescence as measured by d_{00} (top) and d_{33} (lower) for samples containing cottonseed stearine. Solid fat crystallized prior to emulsification in the absence of PgPr. 0% solid fat (●), 0.125% (○), 0.25% (▼), 0.50% (▽), 1.0% (■), 2.0% (□).

Reproduced with permission of the copyright owner. Further reproduction prohibited without permission.

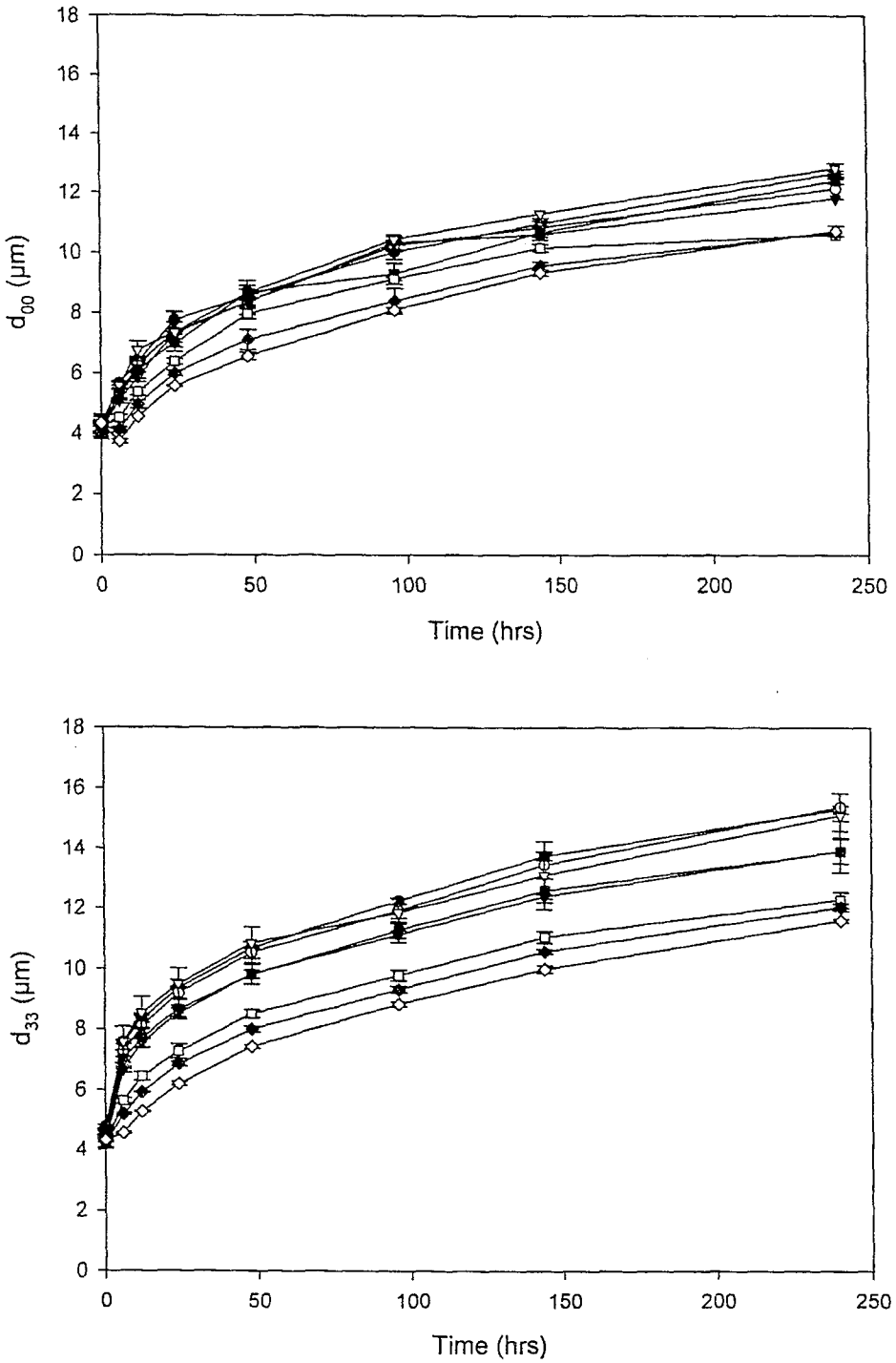

Figure B5: Evolution of droplet coalescence as measured by d_{00} (top) and d_{33} (lower) for samples containing canola stearine. Solid fat crystallized prior to emulsification in the presence of 0.125% PgPr. 0% solid fat (●), 0.125% (○), 0.25% (▼), 0.50% (▽), 1.0% (■), 2.0% (□).

Reproduced with permission of the copyright owner. Further reproduction prohibited without permission.

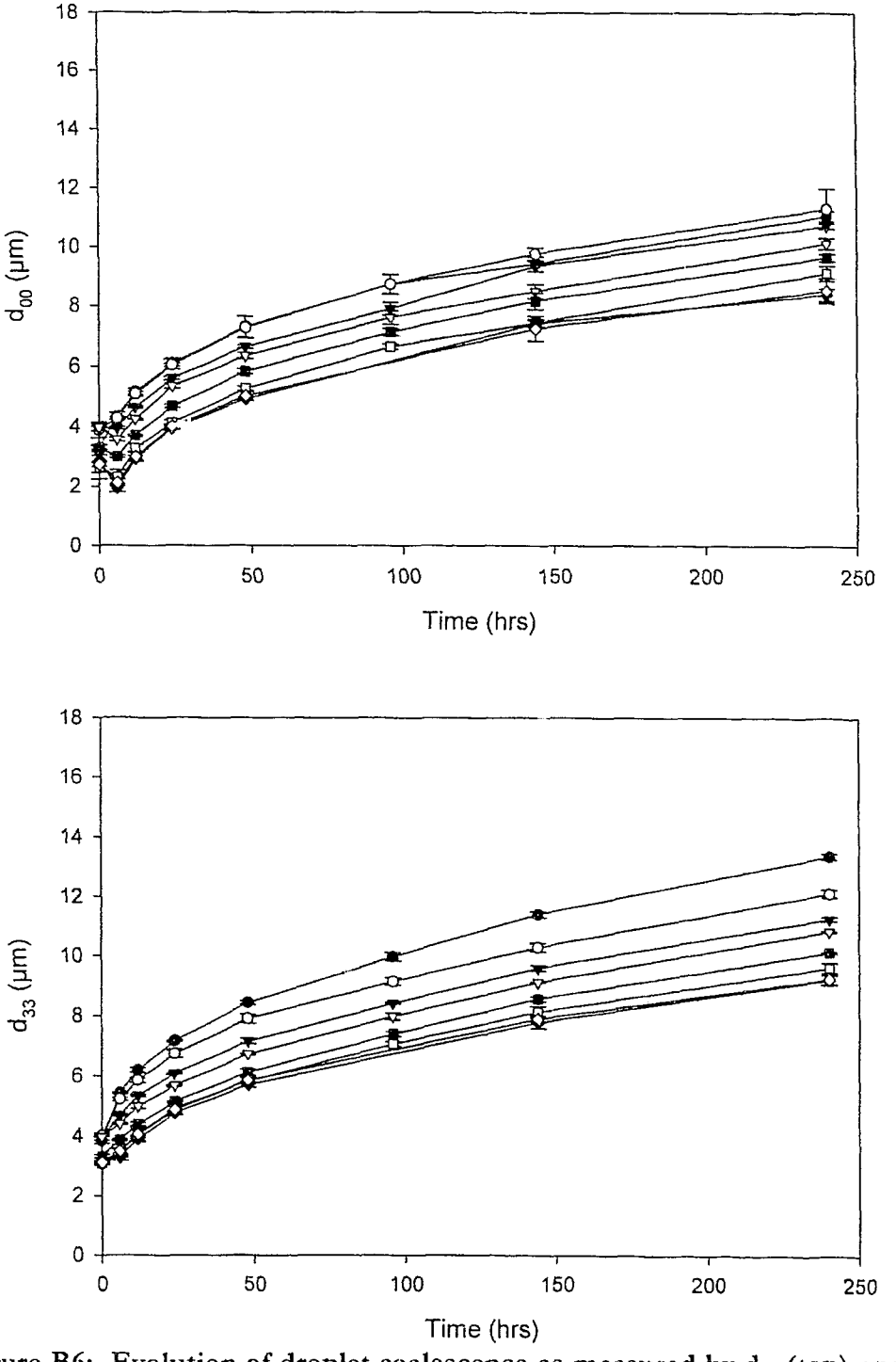

Figure B6: Evolution of droplet coalescence as measured by d_{00} (top) and d_{33} (lower) for samples containing cottonseed stearine. Solid fat crystallized prior to emulsification in the presence of 0.125% PgPr. 0% solid fat (●), 0.125% (○), 0.25% (▼), 0.50% (▽), 1.0% (■), 2.0% (□).

Reproduced with permission of the copyright owner. Further reproduction prohibited without permission.